24 DESIGN PHASE OPTICAL TESTS

24.1 INTRODUCTION

24.1.1 Uses. Optical testing methods are widely used in all branches of scientific and technical work. The basic techniques, or modifications thereof, enable some of the most sensitive and precise measurements man has ever known. Gage blocks may be measured to better than 0.0000001" with relatively simple interferometric apparatus while velocities of satellites hundreds or thousands of miles away may be measured with the Doppler shift techniques common to older astrophysics problems.

24.1.2 Related fields. It will be noted that from time to time reference will be made to work that has been done in the field of microwave antennas. This has been done in the belief that it will be very instructive to become acquainted with design techniques involving wavelengths that are frequently approaching a tenth of the radiating aperture. Further, the use of aberrations, interference, diffraction, and control of aperture illumination are discussed and demonstrated in a way frequently difficult at light optics frequencies. The very recent achievements in light optics where the aberrations are all reduced (save color) to the diffraction-limited stage is many years old in the microwave-antenna field. Microwave antenna designers borrowed heavily from older optical techniques and it is quite possible that a study of their efforts will be highly rewarding to the light-optics designer.

24.1.3 Methods and problems pertinent to optics.

24.1.3.1 While these methods cover a wide gamut, discussion in this section will be confined to a small sampling of the methods particularly suitable to the design, construction, and evaluation of visual optical systems. A few words regarding the origin of the testing problems which will be encountered will be in order.

24.1.3.2 The design of an optical instrument is obviously predicated on a need having been established. Sometimes the nature of this need is such that electrical and mechanical considerations may dictate, to a considerable extent, the physical shape of the optical system. However, even after this has been determined there still remains the problem of translating the customer's purely optical requirements into a form that is significant to the lens designer. Field of view, curvature of field, transmission over a given spectral band, distortion, etc. can be specified rather accurately and unambiguously. Questions, however, as to image quality and what figure of merit is to be used in deciding whether this or that design will most closely give the customer the information he seeks when he uses the instrument, raise problems that have yet to be solved completely. There seems to be more and more evidence of late that to phrase the problem in this way--viz. that the optical instrument be an "information handling system" -- is preferable to the more vague requirement that it be a system that forms a good image. Agreed, the former actually sounds more vague, but current effort indicates the above sentence is probably correct.

24.1.3.3 The postulating of a figure of merit implies that one must test proposed designs to see if they meet the assumed theoretical criterion. Once the design is firm, the optician takes over and now he must perform tests to see that his construction faithfully follows the prescription given to him by the lens designer. Here we must point out that there is another testing step necessary. The optician's job may be considered complete and accurate when the radii, edge thicknesses, center thicknesses, spacings, indices, etc. agree with the specifications handed down by the lens designer. The fact that the optician's work is presumably accurate does not, however, serve as a complete check on the usability of the system. It must be remembered that the designer used some theoretical criterion such as amount of energy in a point image, phase front or Seidel aberrations. The next step therefore is to see how well the constructed system lives up to his predictions in one or more of these respects.

24.1.3.4 There is little doubt that the ultimate test of any system is a field test under the original conditions imposed in the customer's specifications. A system can conceivably be excellent in the laboratory and yet be so sensitive to vibration that it is useless in the field. Further laboratory testing under simulated field conditions is therefore indicated; installation in field equipment being attempted only after the prototype has been tested thoroughly in the laboratory.

24.1.3.5 Here is another point that should be strongly raised. Granted that field tests are the ultimate in one sense, we should not lose sight of the fact that the nature of field tests frequently is such as to cloud the performance of the optical system by the introduction of parameters not basically a part of the problem. The writer clearly recalls airborne cameras yielding several hundred lines per minute resolution in the laboratory and only 20-30 lines per minute in the air. The trouble was definitely not with the camera or optical system but rather with the mechanical mounting in the plane. Some more or less absolute standard of perfection based on the customer's optical requirements is therefore mandatory. Tests in this category are extremely valuable. Resolving power, sine-wave tests, etc. fall into this category.

24.1.4 The testing program.

24.1.4.1 A consideration of the principles outlined above indicates that the complete testing program rather naturally falls into the following categories. It should be pointed out that many more types of tests are known in each category, but space permits only this limited sampling.

24.1.4.2 Testing during the design phase.

(1) Calculation of the Seidel Aberrations

(2) Calculation of the Spot Diagrams

(3) Determination of the phase front and perhaps the predicted diffraction by knowing the phase front and amplitude distribution over the aperture.

24.1.4.3 Testing during the manufacturing phase.

(1) Foucault Test

(2) Star Test

(3) Ronchi Test

(4) Interferometric Tests and/or determination of phase front.

(5) Measurements of curvature of field, astigmatism, transmission, field of view, front and back focal lengths etc.

24.1.4.4 Testing during the evaluation phase.

(1) Any or all of the tests in 24.1.4.3 above.

(2) Measurement of the resolving power.

(3) Measurement of the sine-wave response.

We will now proceed to discuss each of these tests.

24.2 CALCULATION OF THE SEIDEL ABERRATIONS

24.2.1 Object-image relationship. From a strictly theoretical point of view, an optical system may be said to be perfect if its response is "collinear" i.e. points are imaged as points, lines are imaged as lines, and planes are imaged as planes. A further qualification is required--namely that the definition just given applies strictly and only to an optical system where the magnification is unity for all image points. While such systems do have significance, most optical systems require either minifications (telescopes, field cameras, etc.) or magnification (microscopes, etc.). We therefore qualify the concept of collinearity by adding that magnification or minification may exist, but should be constant for all points in the image. The above definition, even with its qualifications, applies more to photographic than to visual optical systems because of the reference to a flat focal surface. While curved focal surface systems have been used in photography, they are rare because of the practical problems involved in film handling. Almost all photographic systems require a flat focal surface, i.e. a focal plane. For visual optics we may relax this requirement somewhat. Indeed the ideal system is one whose curvature of field matches that of the eye.

24.2.2 The importance of Seidel Aberrations. It has been found possible by Seidel [(1)] to express the deviation of an actual image produced by a system, from the theoretically perfect system by a series expansion. This series expansion was given previously in Section 8. The monochromatic deviations from the ideal flat focal surface collinearity are called aberrations and include spherical aberration, coma, astigmatism, curvature of field and distortion. To the extent, then, that this series expansion accurately depicts what happens to an image point, the calculation of these Seidel aberrations constitute a powerful first approximation in the design of an optical system. It is equally clear that the calculation of these aberrations may be considered as a theoretical test of such a system. The method of calculating these aberrations, and the detailed significance of each has been previously treated. The subject is raised here again to point out the use of these aberrations in the theoretical tests which may be applied to an optical system. The reader should refer to Sections 8-10 for more details. It should also be pointed out that these aberrations are strictly geometrical and that

(1) Seidel: Astronomische Nachrichten, 43, 289-332 (1856).

two different systems may have the same aberrations and yet show quite different images due to the fact that the wave nature of light is completely ignored (except for the variation of index with wavelength).

24.2.3 Seidel Tolerances. The criticism sometimes levied is that it is pointless to design a system on the basis of purely geometrical optics because of the neglect of interference etc. To our knowledge no optical system has been designed, at least in recent years, without reference to the wave nature of light. Frequently this is done by explicitly placing tolerances on the aberrations by reference to the Rayleigh [2] stipulation that the maximum path deviation from a given object point to a given image point be not more than $\lambda/4$. Discussions of this may be found in Conrady [3] and Martin [4]. These optical tolerances are:

For primary marginal spherical,

$$\text{permissible primary } LA' = 4\lambda/N' \sin^2 U'_m \qquad (1)$$

For primary zonal spherical, (assuming LA' = 0)

$$\text{permissible } LZA' = 6\lambda/N' \sin^2 U'_m \qquad (2)$$

For primary Coma ($Coma_s$)

$$\text{permissible } Coma_s = \pm \lambda/2N' \sin U'_m \qquad (3)$$

For focal range,

$$\text{Focal range} = \lambda/N' \sin U'_m \qquad (4)$$

For astigmatism, Ast's

$$\text{permissible Ast's} = \lambda/4N' \sin^2 U'_m \qquad (5)$$

For curvature of field,

$$\text{permissible } X' = \text{focal range} = \lambda/N' \sin^2 U_m \qquad (6)$$

Note: U'_m is the angle between the ray and the axis, N' is the index of refraction in image space; and λ is the wavelength of the radiation.

24.2.4 Use of the Seidel Tolerances. One should use these tolerances with exceeding care particularly with high speed systems. This occurs because the focal range allowed by the $\lambda/4$ path difference criterion is assumed small compared with the actual focal length. Secondly the field angle is assumed sufficiently small so that $\sin^2\left(\frac{U'_m}{2}\right) = 1/4 \sin^2 U'_m$. One should further regard these tests as representing a theoretical arbitrary standard which may be too tight or too loose in special circumstances. For fast systems (microwave antennas are a good example outside of the field of visual optics), the tolerance on spherical aberration as computed from (1) is too loose--usually by a factor of 4 or more. The tolerance on coma is too loose for many visual systems where the coma may be the most serious aberration and every attempt should be made to reduce it sensibly to zero. The astigmatic tolerance is usually too tight, and a lens may be expected to produce good results even if the astigmatic tolerance is exceeded by a factor of 2.

24.2.5 Conclusions. The subject of Seidel aberrations from purely geometrical optics is considered here in conjunction with tolerances imposed by physical optics because they have been the prime standards against which lenses were compared until the relatively recent present. Most lenses still are designed on this basis today although there are some who think that sine-wave response calculations may replace them in future years. In conclusion we may say that the reduction of aberrations to within, or at least close to, the stipulated tolerances is a necessary but not sufficient condition that to assure a lens so constructed will perform well. Actually the reduction of the aberrations to the specified limits results in a wavefront that is sensibly spherical in image space. The true image, however, involves amplitude as well as phase, and the Seidel aberrations give no explicit information regarding amplitude.

24.3 THE SPOT DIAGRAM

(2) Lord Rayleigh, Collected Papers, vol. 1, pp. 415-459.
(3) Conrady, Applied Optics and Optical Design, pp. 136, 395, 434 et seq., Dover, (1957).
(4) Martin, Technical Optics, vol. 1, p. 139, Pitman, (1948).
also Jacobs, Fundamentals of Optical Engineering, 443, McGraw Hill, (1943).

24.3.1 Introduction. In the past, the labor involved in doing any but the simplest of ray tracing was such that relatively few rays were traced in the actual lens design process. With the advent of electric desk calculators, it became possible to trace more rays in the same time. As a result tracing rays out of the meridional or tangential fan became more common. It was not until the relatively recent present that the designer was freed of this time limitation by the development of the high-speed, electronic-computing machinery. It is now possible to trace hundreds of rays in the same time it took to trace just a few some years ago. This has resulted in lenses being designed much more carefully than ever before. The aberrations determined by tracing rays as just discussed are definitely an approximation that is very good under some circumstances, but the usual Seidel third-order aberrations are frequently misleading: higher order aberrations sometimes being dominant.

24.3.2 Aspherics. Another factor brought into being recently is the use of aspheric surfaces. Desk calculators or no, tracing through aspheric surfaces can be a monumental task when done by hand. There is ample evidence, however, that freed from the restriction of purely spherical surfaces, the designer can almost always do a far better job with aspherics than he can with spherical surfaces.

24.3.3 Development and limitations. One of the first testing techniques that took full advantage of the power of the large computers was that evolved by Herzberger (5) and later by Hopkins (6) and was called the "spot diagram." In essence the entrance pupil is divided into equal areas, and a ray is traced through the center of each area--the assumption being that the energy represented by each ray is the same. The intersection of these rays with an assumed focal plane was a spot, hence the term "spot diagram." The more compact this spot, the more nearly perfect was the lens judged to be by the standards of geometrical optics. This is discussed in Section 8. We should thus clearly realize that this technique is restricted to non-diffraction limited systems. In this connection we should also realize that while most optical systems today are not diffraction-limited, there is a growing class of high precision systems widely emphasizing aspherics where the only aberration left is color, and where the performance is almost an order of magnitude better than it was ten years ago. For such systems, the spot diagram can serve only as a rough first approximation. The vast majority of visual and photographic optical systems are aberration-limited rather than diffraction-limited so the spot diagram is still a powerful tool.

24.3.4 Techniques. There are basically two techniques for getting a spot diagram. In one the required number of rays is actually traced, and the intersection points with the assumed focal surface are plotted. In the other a relatively small number of rays is plotted, and the intersection coordinates of the others are obtained by an interpolation and extrapolation process developed by Herzberger. It should be noted here that the interpolation process does more than just give the intersection points. Via the series expansion required for the interpolation it also gives a set of terms not unlike those of Seidel. The difference is major, however, in that the Seidel aberrations work particularly well near the axis while the "Herzberger aberrations" fit well over the entire aperture. Space does not permit us to go more deeply into this use of spot diagrams, but the reader is encouraged to refer to Herzberger's articles on this subject (5), (7), (8).

24.3.5 Examples. Those interested in this subject are also urged to obtain National Bureau of Standards Report No. 5640 entitled "Numerical Analysis of a 6" f/3.5 Aerial Camera Lens (006BC035 - 15)". This report by Stavroudis and Sutton shows clearly the extent to which the spot diagram testing is currently employed. Not only are the spot diagram shown for various assumed focal plane positions and angles of obliquity, but also the values of vignetting, distortion, chromatic aberration, energy distribution, and resolving power are derived for this lens directly from the spot diagrams. It is interesting to note the excellent correction that seems to have been achieved in this lens. For full aperture the diameter of the Airy disk is 4.0 microns. If we inspect the following table, Table 24.1, taken from Stavoroudis report, we see that 80% of the total points fell within a circle on axis whose diameter was 3.93 microns. For an aberrationless system theory indicates there will be 83% of the total energy within the Airy disk. The close agreement between theory and spot diagram prediction indicates the excellence of the design, at least for on axis work. In another series of experiments Stavroudis and his colleagues at the National Bureau of Standards calculated the spot diagram of a completed lens. The comparison of the spot diagrams and corresponding actual photographs for two given positions is shown in Table 24.1.

24.4 PHASE FRONT CALCULATIONS

24.4.1 The spherical wavefront. It has been pointed out that the Seidel Aberrations, when they are fully corrected, result in a spherical wavefront converging on the image point. Modern computing machinery has enabled the designer to calculate directly the wavefront and thus determine not only the phase errors over the aperture but where the focal point should be placed.

(5) Herzberger, J. Opt. Sec. Am 37, 485 (1947).
(6) Hopkins, J. Opt. Sec. Am 44, No. 9, 692-698 (1954).
(7) Strong, Concepts of Classical Optics, Appendix L by Herzberger, p. 537, Freeman (1958).
(8) Herzberger, Optical Image Evaluation, National Bureau of Standards Circular No. 526, U. S. Gov't. Printing Office (1954).

% Total points	0^o μ	7^o μ	11^o μ	14^o μ
10	0.674	3.66	4.88	4.02
20	1.22	6.54	12.2	13.2
30	1.69	14.0	25.6	27.2
40	1.97	24.7	43.7	45.7
50	2.43	37.8	66.2	67.6
60	3.05	53.3	89.3	92.2
70	3.71	71.7	118.	119.
80	3.93	97.8	149.	148.
90	6.08	132.	187.	189.
100	12.1	247.	266.	311.

Focal length = 5.972460

Plane of best focus at -0.042 mm

Table 24.1- Energy Distribution 006 BC01515.

The table gives the diameters of the smallest circles containing specified percentages of the total number of points in each of the four spot diagrams at the plane of best focus. The common center of the circles for a given spot diagram was taken where the density of the points appeared greatest.

The diameters are listed in microns to three significant figures. Note that the diameter of the Airy disk for a perfect lens as a full aperture of f/3.5 is 4.0μ. Dr. R. N. Wolfe of Eastman Kodak Co. Research Laboratories made a similar series of experiments in 1947 in conjunction with some of Herzberger's early work in this field (9). The subject has been extensively investigated as regards automatic data reduction by Goetz and Woodland (10) at IBM. Miyamote (11), Keim and Kapany (12) as well as many others have studied this very interesting optical test.

24.4.2 Technique. There are many ray tracing programs that will give this information. The one developed by Feder(13) is offered here. Again the techniques of using this method of testing are varied but the following one is typical. See Figure 24.2. Three or more rays are traced from plane PP through the entrance pupil, the optical system into image space. The entrance pupil is EE. Frequently among the rays of interest are the upper rim ray (U), principal ray (Pr), and lower rim ray (L). A point B' on the principal ray in image space is picked arbitrarily and, from the ray tracing data, the optical path length BB' is determined. From the ray tracing data for rays U and L as well as those originating at other points (frequently zonal) such as D and F, optical path lengths equal to BB' are laid off along the rays. The termination points C', D', F' and K' are then marked and the curve passing through them constitutes the equiphase front in the plane of the paper. The deviations from a perfect circle (or sphere in three dimensions) are clear and corrections may be made as necessary.

24.4.3 Applications and limitations. This phase front technique has long been used in the design of microwave antennas because of the optical simplicity (generally speaking) of such systems. It is particularly useful in optical design as the phase front may be determined experimentally by long established techniques. This gives the designer an immediate check on how well the optician has fulfilled the prescription given to him. It should be pointed out that the diffraction pattern may now be determined, providing the amplitude distribution over the front is known. In some cases it is simpler to use basically the same technique but actually determine the phase variation over the exit pupil. The amplitude distribution over the exit pupil is determined and the diffraction pattern calculated as before. The possibility of varying the amplitude over the aper-

(9) Herzberger, J. Opt. Sec. of Am. 37, 485 (1947).
(10) Goetz and Woodland, J. Opt. Soc. of Am. 48, 965 (1958).
(11) Miyamoto, J. Opt. Soc. of Am. 48, 57, (1958); 48, 567 (1958), and 49, 35 (1959).
(12) Keim and Kapany, J. Opt. Soc. of Am. 48, 351 (1958).
(13) Feder, J. Opt. Soc. of Am. 41, 630 (1951).

ture by control of aperture shape, variation of transmission, or illumination with radius has been known for some years. A few of the efforts in this direction are the work of Conder and Jacquinot [14] in spectroscopy, the work of Osterberg and Wilkins [15] with microscope objectives, and the work of Silver [16] on tapered illumination of microwave antennas.

20° Off-axis at Gaussian Focus

10° Off-axis, 0.3mm in from Gaussian focus.

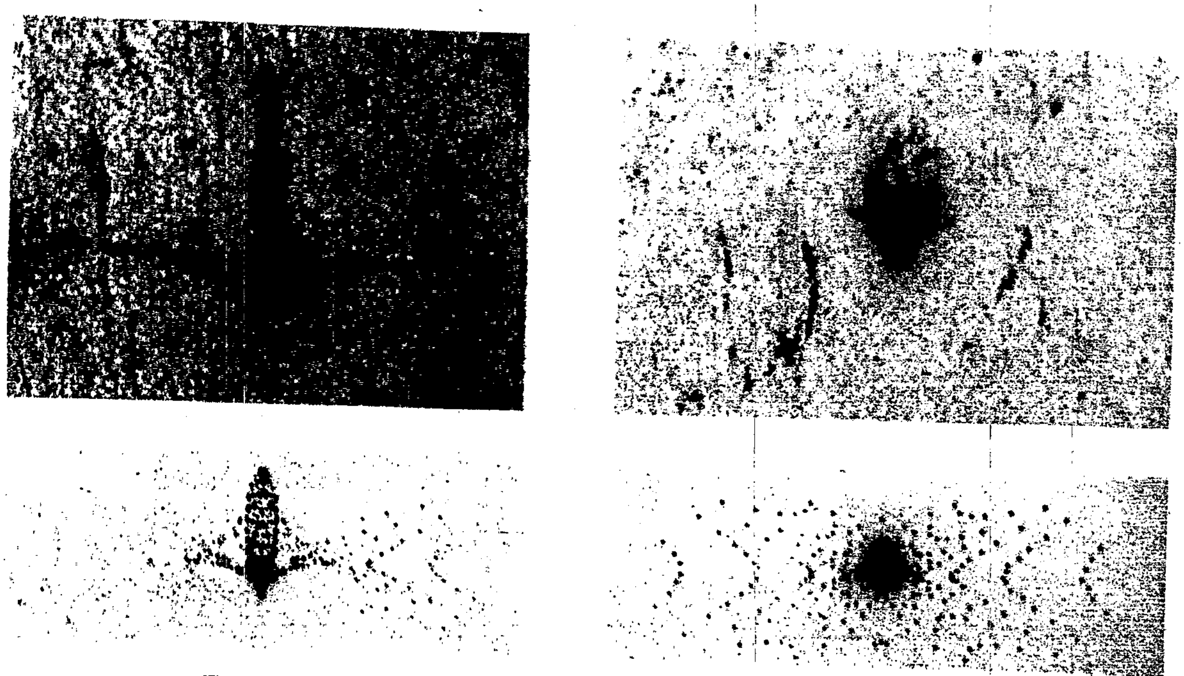

Figure 24.1- Comparison of spot diagram and actual photograph.

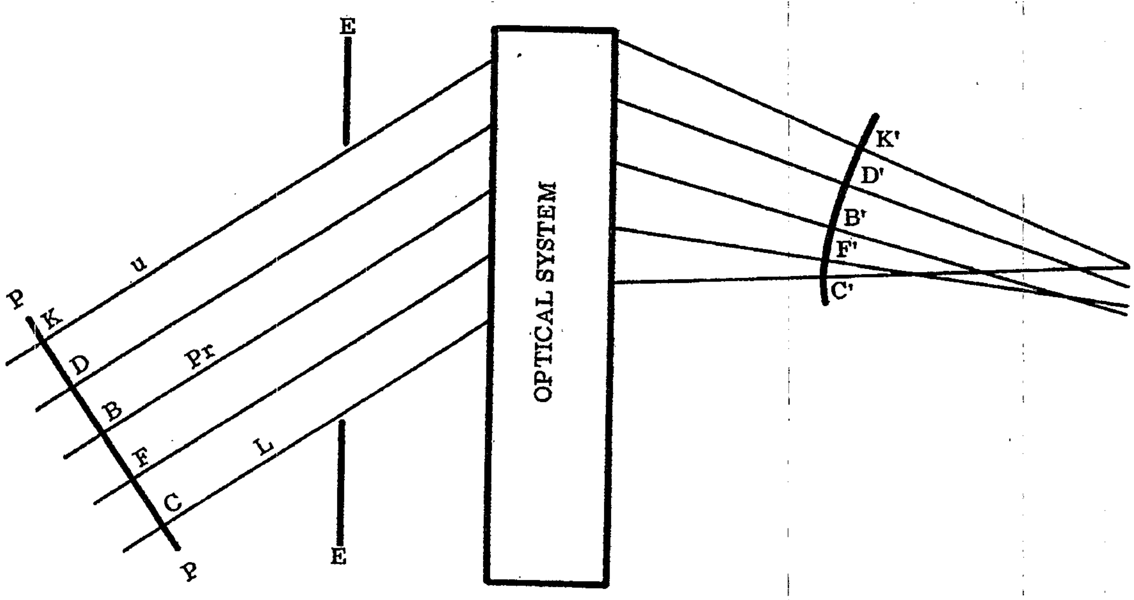

Figure 24.2- Determination of constant phase front from ray tracing data.

(14) Conder and Jacquinot, "Méthode pour l'observation des radiations de faible intensite au voisinage d'une raie brillante" Compte Rendus de l'Académie des Sciences (Paris), 208, 1639, (1939).

(15) Osterberg and Wilkins, "The Resolving Power of a Coated Objective," J. Opt. Soc. of Am. 39, 553 (1949).

(16) Silver, "Microwave Antenna Theory and Design" 187, McGraw Hill (1949).

25 PRODUCTION PHASE OPTICAL TESTS

25.1 INTRODUCTION

25.1.1 General. Intrinsic in the design of most optical systems is the calculation of the Seidel aberrations. In this section we will outline procedures for measuring these aberrations experimentally during either the production or the evaluation phase. In this connection it should be noted that over the years different laboratories have developed their own techniques for making these measurements. Frequently the difference between techniques is not so much a matter of difference in basic principle, as it is in the equipment that a particular laboratory happens to have on hand. While there are, then, many, many different ways to make each measurement, we will limit ourselves to one example of each. The interested reader may consult the references for additional information.

25.1.2 Theory vs practice. Before leaving this introduction to the measurement of Seidel aberrations, a few words of caution are in order. Aberrations may be completely isolated only in theory. The actual image embodies, simultaneously, all aberrations pertaining to it. This, of necessity, complicates the measurement, and particularly complicates the detailed checking of the theoretical predictions as to the values of the individual aberrations. It should be pointed out also that the accuracy with which the aberrations need to be measured is a function of the importance of the particular aberration to the job at hand. The experiments to be described generally assume a white light source. Chromatic effects are determined by use of the appropriate filters.

25.2 FOCAL LENGTH

25.2.1 Importance of focal length. Certainly one of the fundamental constants of any optical system that is of prime importance in the evaluation of the significance of all Seidel aberrations is focal length. Not only is the value of the focal length of importance, but also a precise statement of the point from which the focal length is to be measured is mandatory. Some years ago an aerial camera lens was designed and simultaneously the camera body was fabricated, presumably for the same focal length systems. When the lens was installed in the body, a photographic check showed hardly any semblance of an image. To say that it was "out of focus" was charitable. The error was tracked down ultimately to the fact that focal length meant measurement from the secondary principal point to the lens designer and meant from the rear surface to the machinist. Through human error, both lens and body were allowed to be fabricated on this erroneous basis. Since the secondary principal point lay several inches inside the lens, the horribly blurred image was not surprising. Recently a similar situation developed in a missile-tracking system where the optical designer measured the focal point with respect to the front surface and the machinists assumed that it was measured from the rear surface (the optics involved a thick mirror). Since the system was quite fast with short focal length, the one inch central thickness of the thick mirror played havoc with the performance of the system when finally assembled.

25.2.2 Measurement of focal length. While there are many methods for measuring the focal length of an optical system (1) (2) (3) (4), one of the most accurate for lenses of medium focal length employs the nodal slide. A photograph of one in use at the National Bureau of Standards is shown in Figure 25.1. The essential part of the nodal slide is the provision for moving the lens system longitudinally with respect to a vertical axis of rotation. This vertical axis is mounted so that it may be positioned longitudinally with respect to a collimator of appropriate size. Usually the object for the collimator is a very small point source set at the focal point of the collimator.

25.2.3 Test setup. The equipment is set up as shown schematically in Figure 25.2. In use the magnifier or microscope is set up approximately at the focal point. The lens under test is then moved backward and forward along the nodal slide until rotation of the nodal slide through a small angle, B, produces no sidewise shift in the image. The focal length is then the distance between the axis of rotation of the nodal slide and the appropriate focal point of the magnifier or microscope. There are many variations on this technique, some employing auto collimation, some focusing the image on a card, etc. Negative optics may also be tested in this manner by the addition of a positive lens of known characteristics. Knowing the position of the secondary nodal point (coincides with the principal point if the index of refraction of image space is air), the focal length may be specified with respect to the vertex of the rear surface (this distance is known as the "back focal length") or to any other convenient part of the lens.

(1) Cheshire, Trans. Optical for (London) 22, 29 (1920-1921).
(2) Kurtz, Jour. Opt. Sci. of Am. and Rev. of Sci. Instr. 7,103 (1923).
(3) Searle, Experimental Optics, Exp. 37, 185 Cambridge Univ. Press (1925).
(4) Wagner, Experimental Optics, Exp. 67, 136, Wiley (1929).

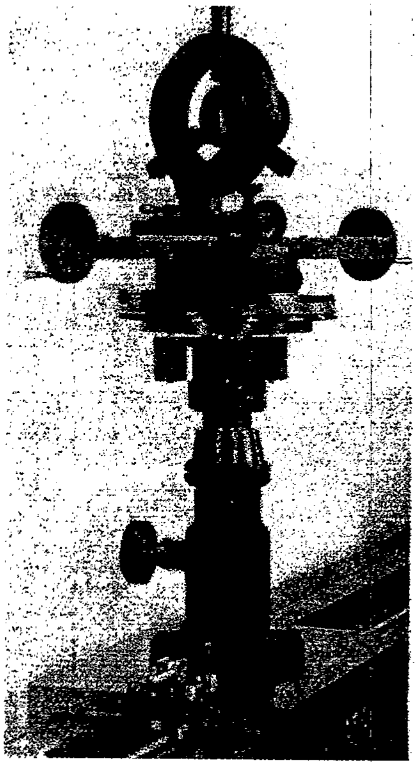

Figure 25. 1- Nodal slide developed at the U. S. National Bureau of Standards.

L_c = collimating system
L_x = system under test

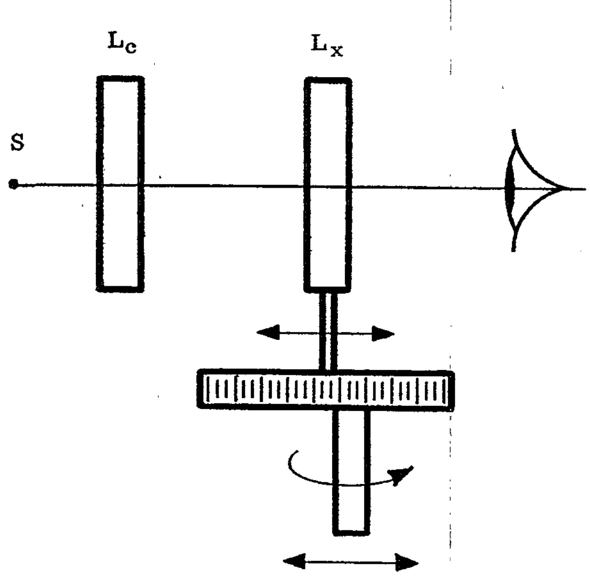

Figure 25. 2- Measurement of focal length by use of visual nodal slide.

25.3 LONGITUDINAL SPHERICAL ABERRATION

25.3.1 On-axis performance. Of considerable importance in almost all optical systems is the on-axis performance. Since the principal use of many visual optical systems is tracking in one form or another, systems are ultimately pointed directly at the target. The nature of the image on-axis is thus important. A factor also of much significance is the degree to which the system may be "opened up" and still maintain a good image. This latter requirement involves spherical aberration.

25.3.2 Hartmann test. While there are many techniques for doing this (5) (6), the simplest is perhaps the Hartmann test (7) (8) (9). It may be done either photographically or visually and can be made reasonably sensitive. It is probably not as accurate as a newer method developed by Washer, but is chosen here for its directness and simplicity.

25.3.3 Test procedure. Blocking off all but holes 1 and 8 in the Hartman Disk shown in Figure 25.3 will give the marginal focus. Holes 2 and 7 should be located at the zonal positions, and their intersection will give the zonal focus. The paraxial focus may be determined with holes 4 and 5, or by direct inspection of the lens stopped down to a very small circular aperture. From the data just obtained the longitudinal spherical aberration may be determined. Filters may be used to get the aberration for different colors if so desired.

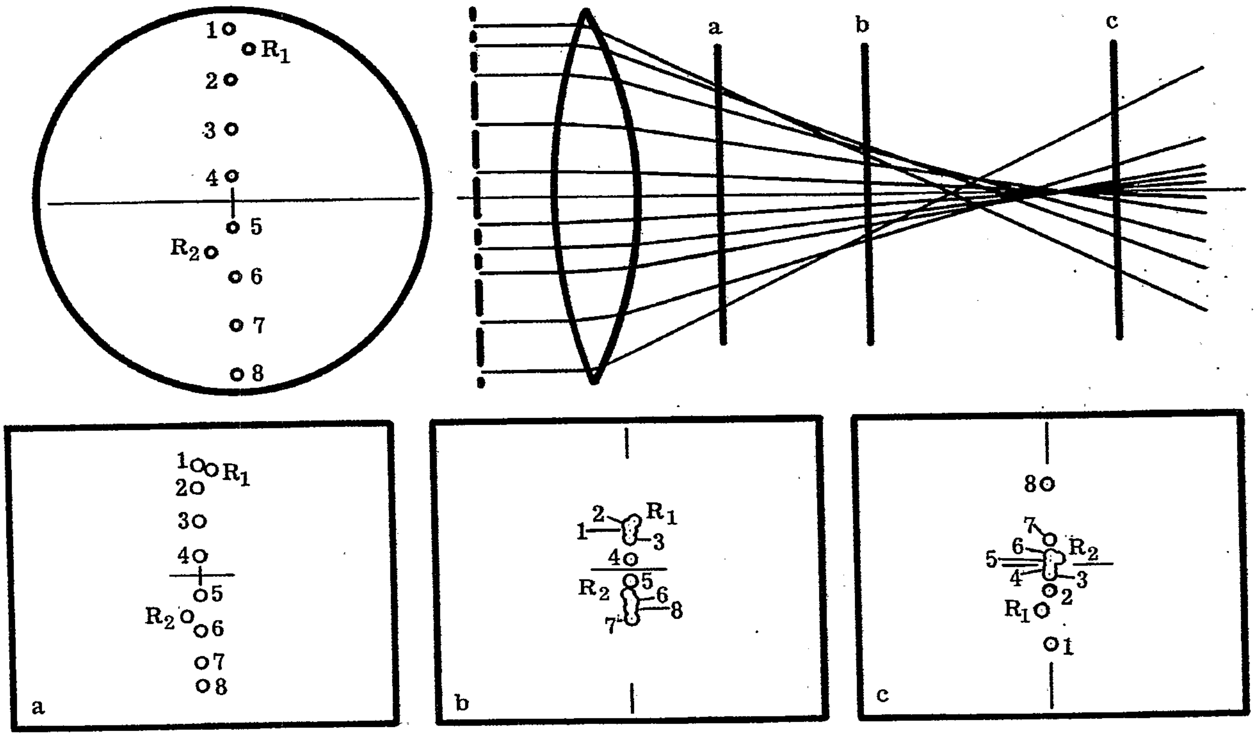

Figure 25.3-Measurement of spherical aberration by the Hartman Test.

(After Strong's, Concepts of Classical Optics, W.H. Freeman and Co. 1958)

(5) Washer, Jour. of Res. of Nat'l Bureau of St'nds 61, No. 1, 31, (July 1958).
(6) Monk, Light-Principles and Experiments 349, McGraw-Hill (1937).
(7) Strong, Concepts of Classical Optics, 354 Freeman (1958).
(8) Hartmann, Zeit. f. Inst. XX IV, 1 (1904); and subsequent papers in 1904.
(9) Bureau of Standards Scientific Papers No. 311 and 494.

25.4 COMA

25.4.1 Asymmetrical flare. Asymmetrical flare produced by coma is one of the most important aberrations to eliminate. The reason for this is that most of the other aberrations produce an image degradation that is more or less symmetrical with respect to the principal ray. For example this means that even though astigmatism may be present, the system may be pointed with a high degree of accuracy by centering the point of greatest density of the image on the cross hairs, etc. When the image is degraded asymmetrically, this same procedure can produce a pointing, or boresight, error.

25.4.2 Collimator check for coma. Coma, being an off-axis aberration, is somewhat difficult to separate from astigmatism. Usually in testing optical systems the optician will simply use a collimator to illuminate his lens at successive angles off axis. The focal plane image is then studied, and, if the flare is more than that allowed in the specifications, the system is reworked.

25.4.3 Hartmann disk. Coma may be demonstrated to a fairly successful degree by use of the Hartmann disk placed before the lens with the lens illuminated by off-axis parallel light and image space then studied, as indicated in the measurement of spherical aberration. Another simple method for measurement of coma using the Hartmann method is described in Hardy and Perrin (10), and refers to a method described previously in the National Bureau of Standards Scientific Papers No's. 311 and 494.

25.5 ASTIGMATISM AND CURVATURE OF FIELD

25.5.1 Measurement of astigmatism. Astigmatism may be measured accurately by a series of Foucault Tests with the knife edges at right angles in the basic manner described in the section devoted to the Foucault test. It may also be measured quite simply by the arrangement illustrated in Figure 25.4. In practice, the lens under test, L_x, is rotated and the traveling microscope, M, is adjusted until the image of the reticle, R, is found. The microscope is then adjusted; first until the vertical lines are in best focus; then until the horizontal lines are in best focus. L_x is then rotated to successive angles up to the maximum field angle, and the positions of best focus as just described measured at each angle. A plot of the positions of best focus for the vertical lines will give the sagittal (secondary) focal surface, and the corresponding plot of the positions of best focus for the horizontal lines will give the tangential (meridional or primary) focal surface. The reason why the tangential plane images the horizontal lines best is shown clearly in Jenkins and White (11). The microscope must of course be movable laterally as well as longitudinally to examine the astigmatism at various points on the focal plane. If in addition to making determinations of the position of best focus of the horizontal and vertical lines, one also notes the position of best overall focus of the central point in the grid system, the curvature of field may be determined.

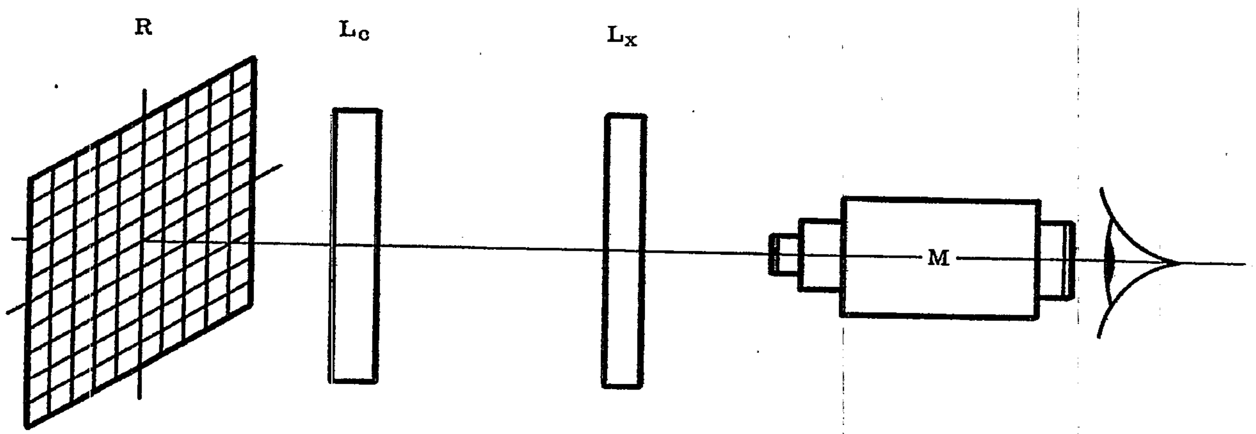

Figure 25.4- Measurement of astigmatism with a grid reticle.

(10) Hardy and Perrin, The Principles of Optics, 382, McGraw-Hill, (1932).

(11) Jenkins and White, Fundamentals of Optics, (2nd edition), 139, McGraw-Hill, (1950).

25.5.2 Determination of curvature of field. Generally, curvature of field may be determined with respect to the flat focal plane of a camera by placing a flat glass plate with a grease pencil mark across a diameter in the position occupied by the film. The grease pencil mark is towards the camera lens. One then notes the position of the traveling microscope when focused on the grease pencil mark. The camera being set up similar to that in Figure 25.4, the microscope is then focused on a star image (or central point of the reticle). The difference between the two readings is a measure of the curvature of field. Curvature of field measurements are very important in visual systems as the curvature of field of the object must match that of the eyepiece or else considerable image degradation ensue.

25.5.3 Consistency of test procedure. One should note clearly in all of these testing methods that if a system is to be used visually, then ideally it should be tested visually. Photographic testing does have its advantages, however, as it furnishes a record.

25.6 DISTORTION

25.6.1 Importance of distortion study. In optical systems designed essentially for visual observation and study of objects on-axis, the aberration known as distortion is really not too important. There are many systems, however, where, while the target may be centered in the eyepiece, measurements must be made over the entire field of view. An example of such a system is a rangefinder.

25.6.2 A rapid check for distortion: Distortion may be measured photographically very simply by replacing the microscope in Figure 25.4 by a good quality camera, known to be well corrected over the field of the optical system under test. The grid reticle is then photographed and the distortion, whether pin cushion, barrel, or irregular, is immediately obvious when D is set = 0.

25.6.3 An accurate distortion measurement for small optical systems. An excellent method of making this measurement for small optical systems with the basic nodal slide has been outlined by Washer, Tayman, and Darling (12). The procedure is as follows:

(a) The optical system under test is placed on the nodal slide shown in Figure 25.2.

(b) A measuring microscope is adjusted with respect to the lens until a focus is found.

(c) The lens system is then moved in the usual way along the nodal slide until small rotations (the microscope having been kept in focus by longitudinal movement) show no lateral movement of the image.

(d) Assuming that the focal length, f, is now measured or known, it is clear that if the microscope were moved off-axis yet remaining in this focal plane that the distance to the lens would now be f sec β.

(e) If now, instead of moving the microscope, the lens is rotated in the nodal slide by an angle β and moved longitudinally a distance (f sec β - f) or f (sec β - 1) toward the collimator, the microscope should again see the image clearly. Actually the image will probably not be on-axis and the microscope will have to be moved laterally a small distance to pick it up again.

(f) The reading of the micrometer measuring this lateral shift is noted as R.

(g) The lens is now rotated through an angle $-\beta$ and the microscope, when repositioned, gives a reading L.

(h) The distortion, D, at the angle β, is then given by the simple expression,

$$D_\beta = \frac{(R-L)}{2} \sec\beta \qquad (1)$$

25.7 AUXILIARY OPTICAL MEASUREMENTS

25.7.1 Introduction. In the fabrication and testing of optical instruments, it is frequently necessary to make measurements that are made considerably less frequently in regular machine shops. One of these measurements is the radius of curvature of spherical and aspherical surfaces: another is the measurement of the index refraction.

25.7.2 Radii of curvature.

25.7.2.1 The radius of curvature of an optical surface whose diameter is on the order of 1 - 3" may be done very conveniently with a spherometer (13). This device takes many forms--one of which is shown in Figure 11.9.

(12) Washer, Tayman, and Darling, Journal of Res. of N.B.S., 61, No. 6, 509 (1958).
(13) op. cit., (10), pg. 366.

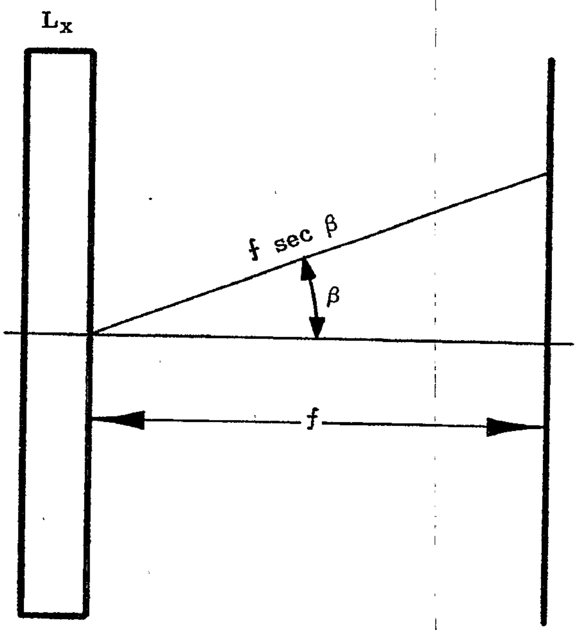

Figure 25.5- Basic diagram for measurement of distortion by nodal slide.

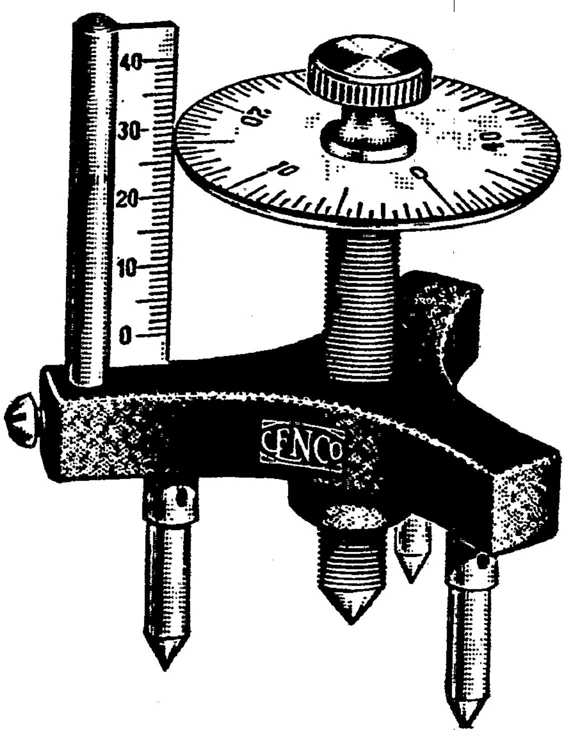

Figure 25.6- Elementary spherometer.

25.7.2.2 In use, the central spindle is screwed up and the three legs placed on the surface in question. The spindle is screwed down until it just touches the surface. The spherometer is then placed on a flat surface and the distance, S, the spindle must be advanced to meet the flat is noted. The procedure is reversed for a concave surface. The radius of curvature of the surface is then obtained from the following equation,

$$r = \frac{d^2}{6s} + \frac{s}{2} \qquad (2)$$

where d = the average distance between the legs.

25.7.2.3 For large surfaces the Foucault method described in paragraph 25.8.2 is used. For very small surfaces, less than about an inch across, a different method is employed. A provision is made for illuminating from the side, the cross hairs or reticle of a Gauss eyepiece, or equivalent, in a microscope or short focal length telescope (the choice depending upon the curvature of the sample to be tested). The microscope is focussed first on the surface of the sample, and the longitudinal position of the microscope recorded. The microscope is then racked back until there is no parallax between the illuminated cross hairs and the image from the surface. The cross hairs are then at the center of curvature. This position of the microscope is also recorded. The difference between the two positions is the radius of curvature. A telescope would be used in exactly the same way for greater radii of curvature. A similar technique can be used for positive surfaces.

25.7.3 Index of refraction.

25.7.3.1 Where it is possible to grind and polish a small sample of the material, the spectrometer furnishes a very fundamental method for measuring the index of refraction. The theory and method are outlined in Hardy and Perrin (14) and Sawyer (15). With a good spectrometer the values of the index so determined are good to ± .00003. A high precision spectrometer is shown in Figure 25.7.

25.7.3.2 For many samples it is not possible to get the sample in the form required for the spectrometer and for these the refractometer is frequently well suited. One of the many refractometers is the Pulfrich (16). This method, based on refraction at the critical angle, will give values correct to ± 2 parts in the fifth decimal place, and is shown schematically in Figure 25.8.

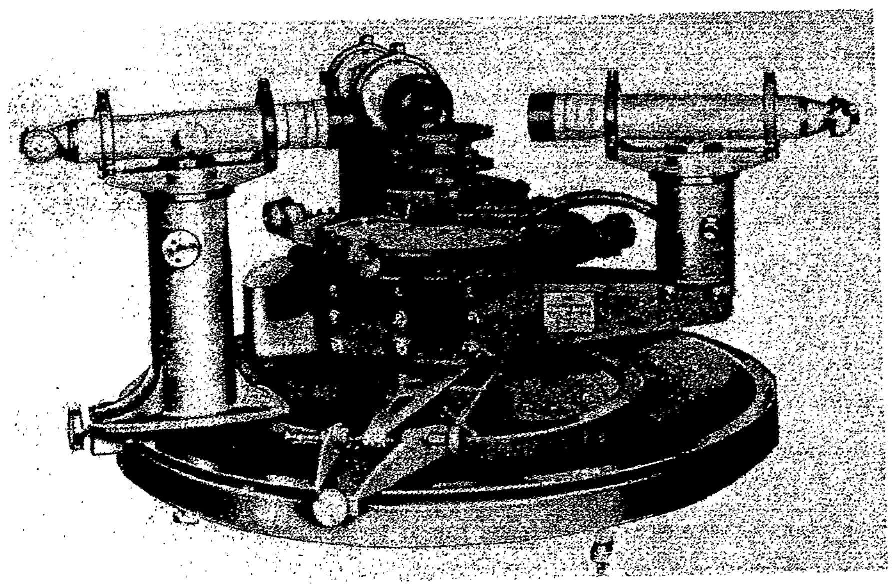

Figure 25.7 - The Guild-Watts precision spectrometer.

(14) op. cit., (10), 549
(15) Sawyer, Experimental Spectroscope, 55, Prentice Hall, (1944).
(16) op. cit., (10), 350.

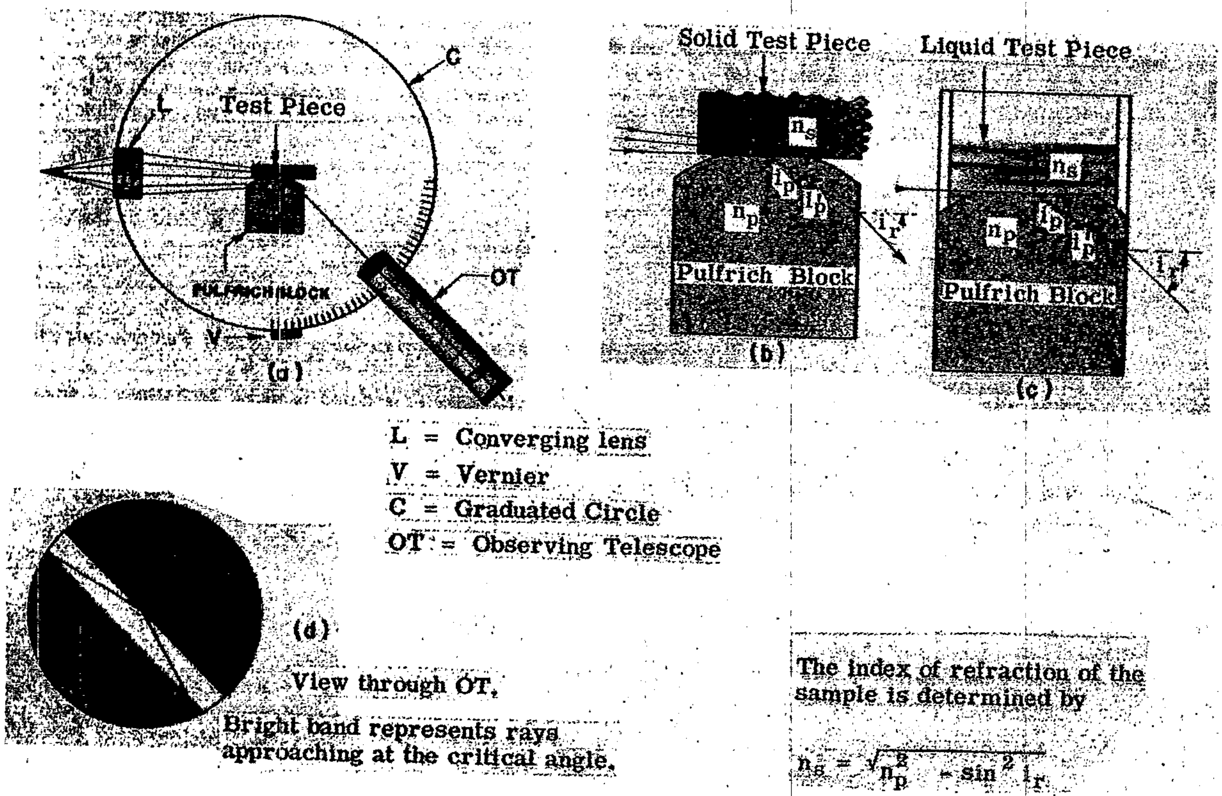

Figure 25.8 - Schematic of the Pulfrich refractometer.

25.8 OPTICAL DEVICES, TESTING SYSTEMS AND PROCEDURES

25.8.1 Interferometry principles.

25.8.1.1 The most common and simplest method for testing flatness of polished surfaces of glass or other transparent material utilizes interference fringes that are formed between the tested surface S_1 and an optically flat surface S_2 as illustrated in Figures 25.9 and 25.10. The preferred source of light is an unfiltered, tubular, Cooper-Hewitt lamp, L, which is provided with a diffusing reflector, R, and a diffusing glass plate, G. The advantage of the arrangement of Figure 25.9 is that it permits the interference fringes to be viewed at normal incidence. The positions of the light source and the eye may be interchanged. Figure 25.10 illustrates the most common arrangement where viewing at normal incidence is sacrificed to gain greater freedom as regards working space. The light emitted by the Cooper-Hewitt mercury lamp is preponderantly green. It can be rendered quite monochromatic at 5461 A, whenever desired, by means of readily available optical filters that can be held near the eye. The interference fringes are usually viewed in unfiltered light. Contrast in the fringes is improved by placing black felt or paper beneath the optical flat in the manner indicated.

25.8.1.2 It should be noted that the interferometer surfaces S_1 and S_2, Figures 25.9 and 25.10, are in close contact. Excess dust and other dirt must be removed in order to reduce the thickness d of the air-film between surfaces S_1 and S_2. Because the separation d of the surfaces S_1 and S_2 is small, the resulting interference fringes belong to a select class of fringes known as Fizeau or as Newton's fringes. The principles underlying these fringes have been discussed in paragraphs 16.12.1.2 and 16.13.1.5. These fringes are characterized by the following important properties and propositions.

(a) The interference fringes appear in good contrast when one focuses upon the air-film between the interferometer surfaces, S_1 and S_2, provided that the reflectances of these surfaces are approximately alike. It is often said that the fringes appear to be localized in the film.

(b) Because the separation, d, of the interferometer surfaces is small, the location laterally of the fringes between the surfaces does not depend markedly upon the angle of incidence, provided that one views the fringes approximately along the normal to the surfaces S_1 and S_2.

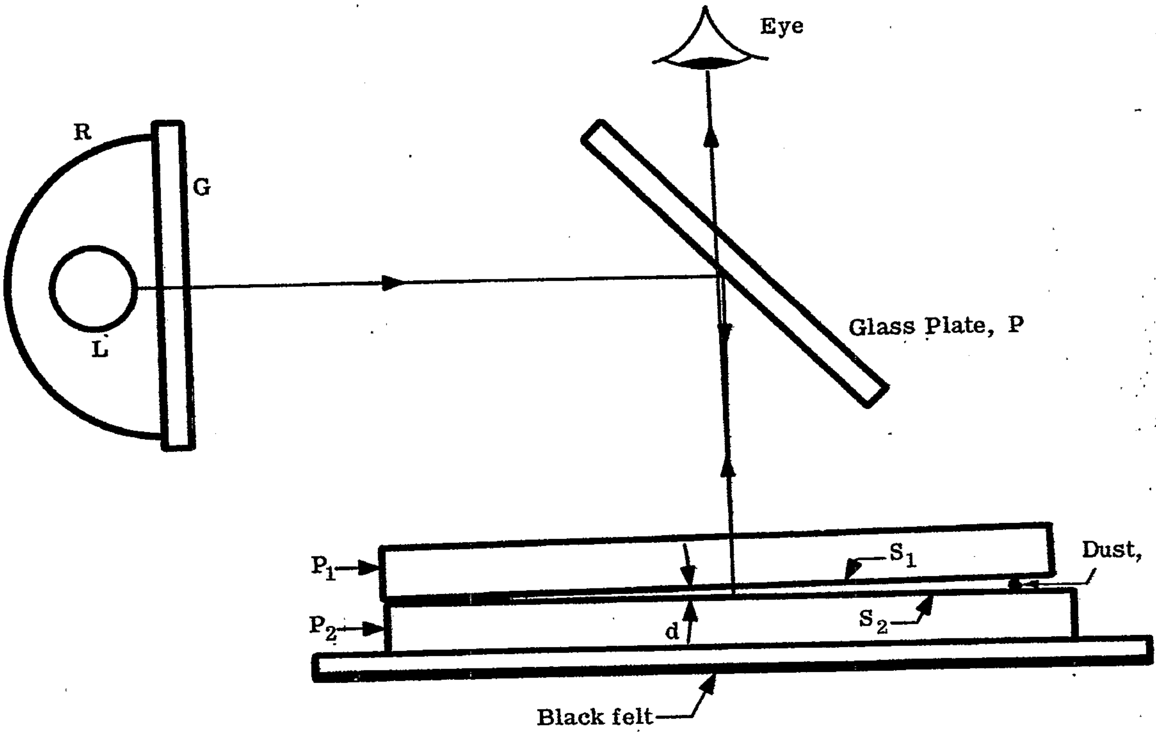

Figure 25.9 - Simple interferometer for viewing Fizeau fringes or Newton's fringes at normal incidence.

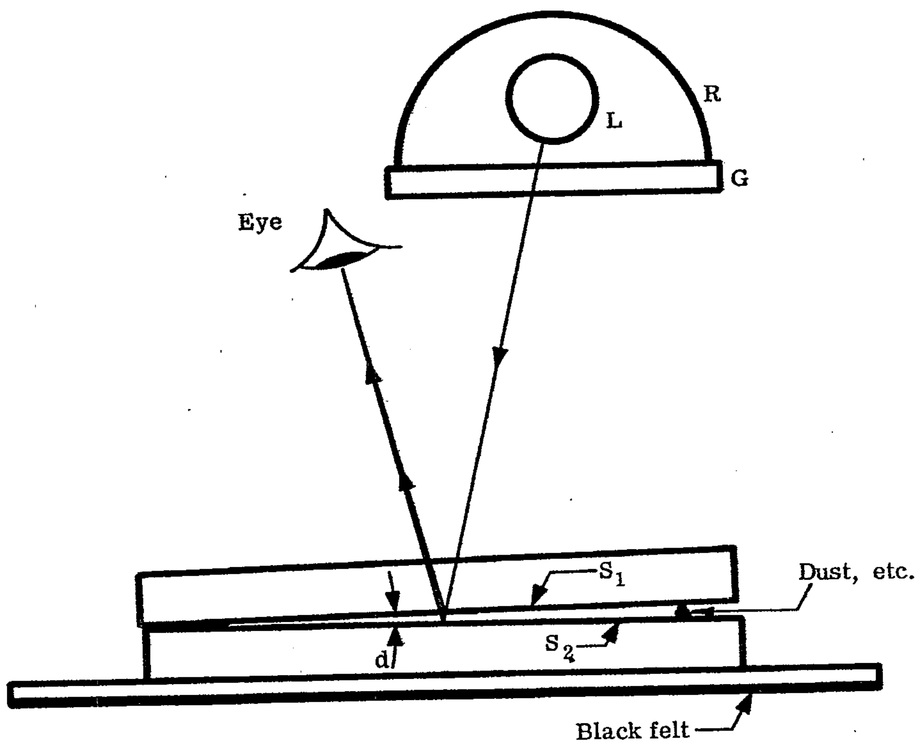

Figure 25.10- Most commonly used method for illuminating the interferometer. The fringes formed between surfaces S_1 and S_2 are observed at near - normal incidence.

(c) Each fringe marks the locus (lateral) of points for which the separation, d, is a particular constant. This constant is different for each fringe.

(d) When either surface is moved or distorted by the application of force or heat, each fringe moves in such a direction as to maintain the constant separation, d, associated with that fringe.

(e) Upon passing from one fringe to the next fringe of equal brightness or darkness, the separation, d, changes by one half wavelength.

(f) Upon passing from a bright fringe to the next dark fringe, the separation, d, changes by one fourth wavelength. It is assumed tacitly in (e) and (f) that the surfaces do not possess discontinuous jumps.

(g) When surfaces S_1 and S_2 are of nonabsorbing materials such as glass, dark fringes occur at separations, d, for which

$$d = \nu \frac{\lambda}{2} \; ; \; \nu = 0, 1, 2, 3, 4, \text{ etc.} \tag{3}$$

and bright fringes occur at separations, d, for which

$$d = \mu \frac{\lambda}{4} \; ; \; \mu = 1, 3, 5, 7, \text{ etc.} \tag{4}$$

wherein λ denotes wavelength.

Of these propositions and properties, (c) and (d) are of the greatest importance to the maker of optical flats. These two propositions or rules enable him to interpret the fringes for high and low areas on the surface under test. The optical worker recognizes fringes as contour lines on a contour map of his surface. Movement of the fringes upon application of pressure serves to distinguish the up-hill direction. Propositions (e) through (g) reveal the heights between contour lines. It is emphasized that propositions (e) and (f) are more general (and hence more often correct) than (g).

25.8.1.3 As one tests for flatness of a surface, the fringes become straighter as the surface becomes flatter. The effect of reducing the angle of the air-wedge between surfaces S_1 and S_2 by the removal or crushing of dust particles, is to widen the fringes and to increase their curvature except when S_1 is optically flat. Let, h denote the fringe width, i.e. the distance from one bright fringe to the next. For optical flats of high quality, the degree of flatness can be specified by requiring that any fringe shift from straightness shall not exceed a stated fraction of the fringe width, h, over a stated diameter or other dimension of the tested surface. As an example of the sensitivity of the method, a fringe shift h/5 corresponds to a change of separation, d, by the amount $\lambda/10$. Fringe shifts smaller than h/10 become difficult to detect and to measure in this type of interferometer.

25.8.1.4 In a second, and often preferred test for optical flats of high quality, the surfaces S_1 and S_2 are placed so closely in contact or are rendered so nearly parallel that a single fringe spreads over surface S_1. This broad fringe is examined for uniformity of color with an unfiltered source of light. It is customary to specify without further qualification that the surface shall be "polished to a uniform color".

25.8.1.5 The following procedure applies to that great class of test cases in which the departure of more than one fringe from flatness is tolerated. If the test surface is convex, only one area will contact the reference flat and this area will be surrounded by a number of alternately dark and bright Newton's fringes. The specification of flatness may be stated as the number of allowable Newton's fringes per inch, or other unit. If the test surface is concave, a ring-shaped area will contact the reference flat. The number of concentric fringes within this area can be counted and compared with the maximum tolerable number of Newton's fringes per inch or other unit. In practice, the surface S_1 is likely to display one or more convex or concave areas. Close examination of the fringes will distinguish between these convex and concave areas. If pressure is applied to a convex area in such a manner as to reduce the separation, d, between surfaces a given fringe about the area of closest contact must move outward from its center in order to maintain the locus of points for which d is a given constant.

25.8.1.6 No essential modification of the method of Figures 25.9 or 25.10 is needed for testing spherical surfaces. The reference flat, S_2, is replaced by a concave or convex reference surface whose radius is equal to the desired radius of the completed test surface. Suppose that surface S_1 has a smaller radius than surface S_2 as illustrated in Figure 25.11. Concentric Newton's fringes will appear around point O. The maximum allowed number of Newton's fringes per inch along the radial direction from O may be stated as the permissible departure of surfaces S_1 from the "test glass" having the surface of reference S_2. For surfaces, S_1, of high optical quality, the radius of surface S_1 will be made to match that of S_2. At the match point, it will

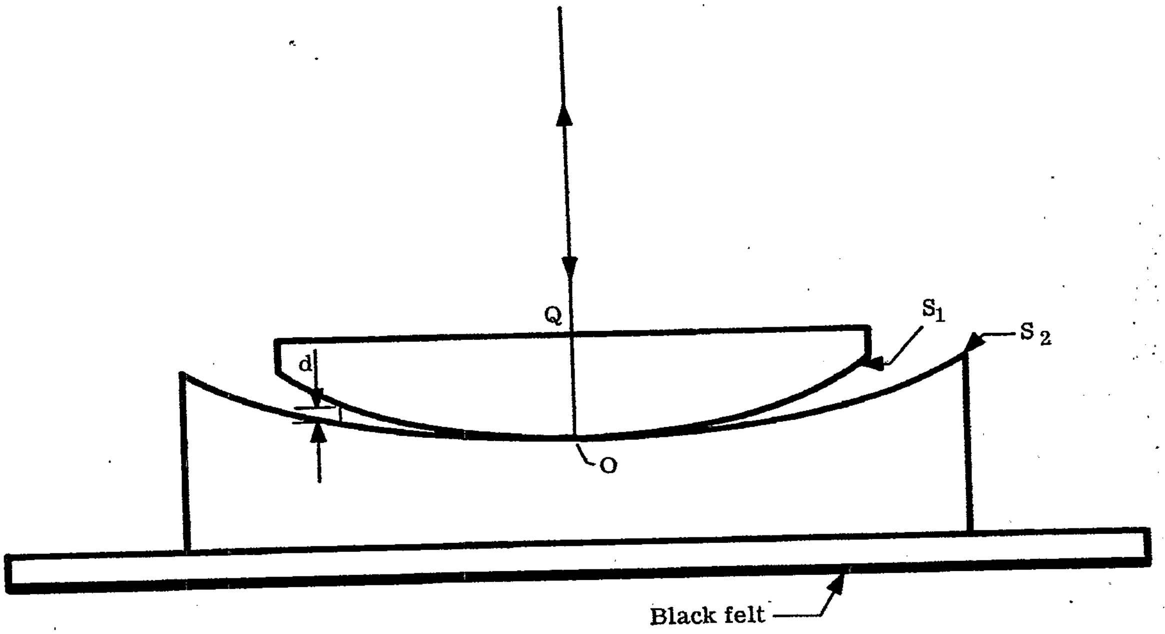

Figure 25.11- Arrangement of the interferometer surfaces S_1 and S_2 for obtaining Newton's fringes.

be possible, as in paragraph 25.8.1.4, to place surfaces S_1 and S_2 into sufficiently close contact so that a single fringe spreads over surface S_1. For work of highest quality, it is customary to specify that this single fringe shall be made uniform in color.

25.8.1.7 The method of the sagitta (see paragraphs 16.13.1.1 and 16.13.1.6) enables one to make a good estimate of the radius of surface S_1 when this radius departs only slightly from that of the test glass. Consequently, it is not always necessary to provide a test glass whose radius is equal to that of the completed surface S_1.

25.8.1.8 When elliptical fringes appear around point O, Figure 25.11, surface S_1 is not spherical. The minor and major axes of the elliptical fringes may be measured, and the ratio of the minor axis to the major axis computed. This ratio is a measure of the ellipticity of surface S_1 and is often utilized as a specification of the maximum tolerable ellipticity. When departures of many fringes from the test glass can be tolerated, another measure of ellipticity is to count the number of fringes along some convenient length in the direction of the major and minor axes of the elliptical fringes and to utilize the ratio of these fringe counts in specifying the tolerable ellipticity.

25.8.1.9 An extreme amount of irregularity in the shape of the fringes is an indication that the tested surface has been improperly polished or molded. "Orange peel" and other defects of polished surface produce irregularities in the observed pattern of fringes.

25.8.1.10 Contrast in the fringes deteriorates as the reflectances a_1 and a_2 of surfaces S_1 and S_2 become more unlike. The light beams reflected from these two surfaces can interfere to produce systems of fringes having zero intensity in the dark fringes (and hence displaying maximum contrast) only when the amplitudes, a_1 and a_2, of the two, coherent, interfering beams are alike. The distribution of intensity in the fringe system when a_1 and a_2 are unlike can be ascertained from paragraphs 16.1.1.3, 16.1.1.5, 16.8.1.1, 16.8.1.2, and 16.9.1.4. In spite of reduced contrast in the fringes, the interferometers of Figures 25.9 and 25.10 are often applied to testing polished surfaces of metals. With metals and other opaque substances, surface S_2 of Figures 25.9 and 25.10 must be that of the opaque material.

25.8.1.11 The reflectance of the "test glass" can be increased by the deposition of a high reflecting coating or by increasing the refractive index of the test glass. In this way, contrast in the fringe system will be improved in testing high reflecting surfaces. Metallic surfaces and coatings produce phase changes on reflection that differ from zero (as in the reflection from a glass-to-air interface) or that differ from $\lambda/2$ (as in the reflection from an air-to-glass interface). Consequently, Equations (3) and (4) require modification. However, the effect of the modified phase changes on reflection is only to shift the location of the fringes. As a result, the interpretation of sections 25.8.1.3 to 25.8.1.9 remains unchanged when applied to coated or metallic surfaces. For testing surfaces of high quality, any coating applied to the test glass must be extremely uniform in thickness and composition because phase changes on reflection can vary appreciably with thickness and composition of the coating.

25.8.1.12 As the reflectance of surfaces S_1 and S_2 is increased from that of polished glass, the nature of the interference fringes formed by the interferometers of Figures 25.9 and 25.10 alters gradually until, finally, these fringes are classified as multiple beam interference fringes. Inter-reflections between surfaces S_1 and S_2 serve to sharpen the fringes formed by the reflected or the transmitted light beams in the manner discussed in paragraph 16.17. With suitable changes in the technique of observation, these sharp (narrow) fringes can be used to detect and measure surface irregularities as small as 10 Angstroms in height. Polished surfaces are found to be rough terrains whose hills and valleys vary in height and depth from 10 to 120 Angstroms. These small irregularities are not visible in the "double beam" interferometer of Figure 25.10 when surfaces S_1 and S_2 are of polished glass.

25.8.1.13 The interferometer method of Figures 25.9 – 25.11 is essentially a "contact" method. Experience and care are required in order to avoid undue scratching of one surface by the other. Life of the test glass is shortened by wear and scratching. A number of convenient interferometer techniques can be applied to testing flat surfaces without placing two surfaces in contact. However, existing interferometer methods for avoiding contact between two spherical surfaces are either so inconvenient to manipulate or so difficult to interpret that the contact method remains the standard method of the optical shop.

25.8.2 <u>The Fizeau Interferoscope.</u>

25.8.2.1 The Fizeau interferoscope, Figure 25.12, is a double beam interferometer that permits one relatively flat surface, S_1, to be tested against another flat surface, S_2, without placing these two surfaces in contact. The increased "working distance", d, is made possible without undue loss of contrast* in the fringes by restricting the effective size of the light source to a pinhole, H, and by illuminating the pinhole with monochromatic light. Since improved monochromaticity and smaller pinholes entail loss of light, the ultimate working distance, d, is restricted by the required level of illumination. Distances of d greater than 2cm must be considered "large" and should be avoided in designing and planning the interferoscope. Fizeau interferoscopes have been varied in design to meet the needs of various users. The use of beamsplitters as illustrated in Figure 16.2 is to be avoided in order to conserve light. The instrument illustrated in Figure 25.12 is an example of one of the more flexible types of interferoscopes. When this instrument is to be used for testing surface S_1 against surface S_2, the two sets of leveling screws, L_1 and L_2, are adjusted in the order mentioned so that the light beams reflected from S_1 and S_2 are refocused by the collimator as images of the pinhole, H, at the aperture, A. When the pinhole images formed at A are brought almost into unison by further relative adjustments on screws L_1 and L_2, straight fringes will appear on the observer's retina as he looks through the aperture, A, provided that the test surface, S_1, is optically flat. Interpretation of the interference fringes remains the same as with the simpler interferometers of Figures 25.9 and 25.10. Except for the more convenient and elegant manner in which the relative inclinations of surfaces S_1 and S_2 can be adjusted with the aid of the leveling screws, the procedures and methods of sections 25.8.1.3 - 25.8.1.5 apply again.

25.8.2.2 Many optical workers use the Fizeau interferoscope exclusively for ascertaining the degree of parallelism of the surfaces of a plane parallel plate. One surface, S_1, of plate, P_1, is first made optically flat. With interferoscopes of the type illustrated in Figure 25.12, test plate, P_2, is removed from table, T_2. The leveling screws L_1 are adjusted so that the two beams reflected from surfaces S_1 and S_{11} are focused within aperture A as images of pinhole, H. If both surfaces of plate P_1 are optically flat but are not quite parallel, the fringes are parallel to the line of intersection of surfaces S_1 and S_{11}. The fringes curve as surface S_{11} departs from flatness. As S_{11} is made optically flat and brought into parallelism with S_1, a single fringe of uniform intensity spreads over the field of view determined by the area of plate P_1. Equations (3) and (4) must be modified to include the refractive index n of plate P_1. Thus dark fringes occur when

$$nd = \nu \frac{\lambda}{2} \ ; \ \nu = 0, 1, 2, 3, 4, \text{etc.} \ ; \qquad (5)$$

and bright fringes occur when

$$nd = \mu \frac{\lambda}{4} \ ; \ \mu = 1, 3, 5, 7, \text{etc.} \qquad (6)$$

* See paragraphs 16.4 and 16.5 for the effect of monochromaticity, pinhole size and separation, d, on fringe contrast. Other principles underlying the use and interpretation of the Fizeau interferoscope are discussed in 16.2 and 16.2.2.

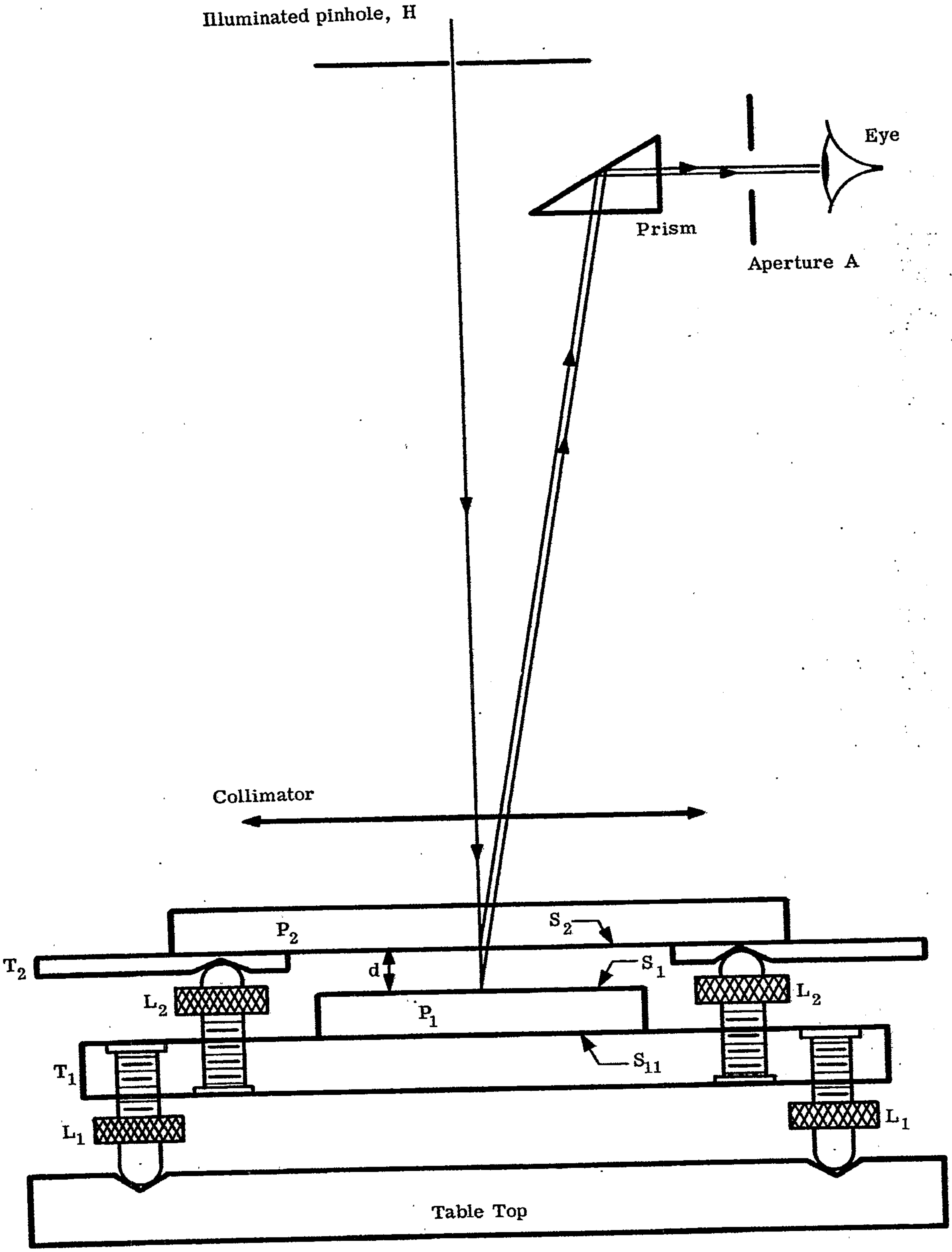

Figure 25.12 - A Fizeau interferoscope.

In other words, dark fringes occur when the optical path nd of the plate is equal to any integral number of half wavelengths, and bright fringes occur when the optical path is an odd number of quarter wavelengths. These conclusions can be expected intuitively when one considers that the phase change on reflection will be $\lambda/2$ at surface S_1, and 0 at surface S_{11}, so that the difference in the phase changes on reflection is $\lambda/2$. The beam reflected from S_{11} passes through plate P_1 twice, and thus is increased in phase by twice the optical path or 2(nd). Because the phase change on reflection is $\lambda/2$ at the air-to-glass interface, S_1, the two interfering beams proceed toward the observer with a phase difference, Δ, given by

$$\Delta = 2nd - \lambda/2. \qquad (7)$$

If now, nd is given by Equation (5), $\Delta = (\nu - 1/2)\lambda$ so that destructive interference takes place. But if nd is given by Equation (6), $\Delta = (\mu - 1)\lambda/2$. Since $\mu - 1$ must be an even number, $(\mu - 1)/2$ is an integer and Δ is an integral number of wavelengths. Hence we verify that constructive interference takes place when the optical path obeys Equation (6).

25.8.2.3 As an example of the sensitivity of the Fizeau interferoscope in testing for parallelism of the two surfaces of a plate, let us suppose that the diameter of the plate is 5cm, that its refractive index is 1.5, that the wavelength λ is 0.5461×10^{-3} mm and that the optically flat surfaces define a wedge whose optical path differs by $\lambda/2$ at the extreme ends of the wedge. Suppose that a bright fringe appears at the thin edge of the wedge. A bright fringe must appear at the thick end of the wedge since the optical path is greater by $\lambda/2$ at the thicker end of the wedge. This conclusion follows at once from Equation (6); for if nd is increased by $\lambda/2$, μ is increased to the next odd number, $\mu + 2$, the spectral order number of the next bright fringe, Equation (5) will be satisfied at the center of the plate so that a dark fringe occurs here. The field of the plate will appear very nonuniform. It presents one dark and two bright fringes. Despite this nonuniformity, the angle, α, between the surfaces of the plate is less than one second of arc. Since nd changes by $\lambda/2$ across the plate, the thickness of the plate changes by $\lambda/2n$. Therefore

$$\alpha = \frac{\lambda/2n}{\text{diameter}} = \frac{0.5461 \times 10^{-3}}{3 \times 50} = 3.64 \times 10^{-6} \text{ radians or } 0.75 \text{ seconds of arc.}$$

If the variation of intensity across the plate is reduced to 0.1 fringe, α will be reduced to 0.075 seconds.

25.8.3 A Modified Michelson Interferometer.

25.8.3.1 A flexible instrument, with the aid of which any surface (whether glass or metallic) can be tested for flatness against an optical flat without contact, is illustrated in Figure 25.13 as a specialized form of Michelson's interferometer. If S_1 is a surface of polished glass, surface S_2 is chosen as polished glass. If surface S_1 is metallic or high reflecting, an optical flat P_2 having surface reflectance approximating that of S_1 will be provided. The user can afford to supply several optical flats since these flats will not have to be replaced because of wear and scratches. The housing, H, is compact and rigid. It is designed to support the beamsplitter and the optical flat, P_2, with minimum vibration. The line OB is pointed in the vertical direction so that the test plate, P_1, is simply laid upon an auxiliary, stable support, Q. The arms OB and OA of the interferometer will be designed so that these arms are nominally of equal length and so that these arms are easily adjusted for equal lengths. Adjusting screws L can be utilized both for equalizing the lengths of the arms and for tilting surface S_2 with respect to S_1 to control the fringe width. The mechanism for tilting plate P_2 must be designed with great care because it is this mechanism that determines the operator's convenience in making quick and certain adjustments of the fringe widths as well as in checking arms OB and OA occasionally for equality by finding the "white light position". Supports Q should be ground to equal thicknesses in order to avoid hunting for the white light position each time Q is replaced by another support. An auxiliary, tiltable mirror M is provided for deflecting the light beam toward the observer.

25.8.3.2 Michelson's interferometer does not differ in principle from the interferometers of Figures 25.9 and 25.10. Consequently, the conclusions of paragraph 25.8.1.2 remain valid and the methods of paragraphs 25.8.1.3 - 25.8.1.5 apply again. Figure 25.14 illustrates why the Michelson interferometer behaves as the interferometers of Figures 25.9 or 25.10.

25.8.4 4 The Twyman-Green Interferometer.

25.8.4.1 The Twyman-Green interferometer is similar to the Fizeau interferoscope as regards basic principles* and interpretation. In both of these interferometers, the allowable optical path difference between the two interfering waves is increased by reducing the effective size of the source to that of a pinhole and by increasing the monochromaticity of the source of light. If, for example, mercury arcs are utilized, they should be operated at reduced pressure and followed by a high quality filter for 5461 Angstroms. The Twyman-Green interferometer has many points of mechanical similarity with Michelson's interferometer. However, Michelson's interferometer is invariably intended for use with broad sources of light.

* The principles underlying the Twyman-Green interferometer are discussed in paragraph 16.3.

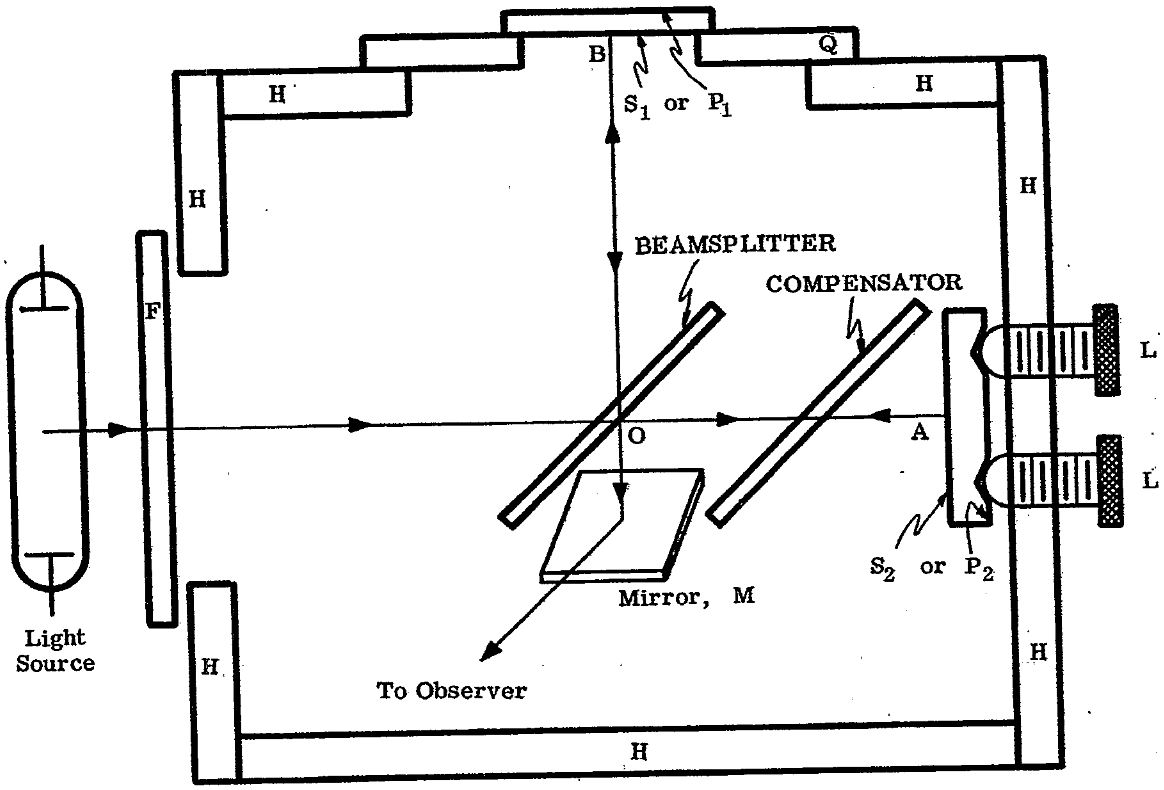

Figure 25.13- A modified Michelson interferometer.

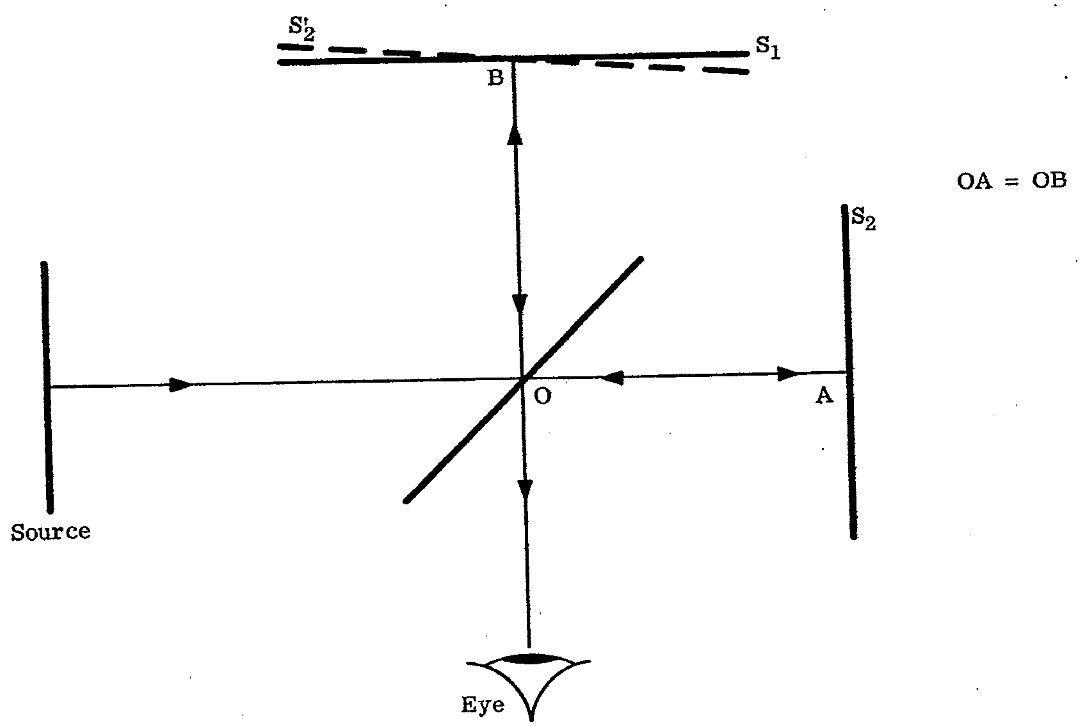

Figure 25.14- Michelson's interferometer as a method of Fizeau fringes. The observer sees surface S_2 as though it were located at S_2', consequently, the fringes are formed as by reflection from two surfaces, S_1 and S_2', that are in close contact.

25.8.4.2 Emphasis in the design of the Twyman-Green interferometer is placed upon taking advantage of the permissibly large optical path difference, d, between the two arms of the interferometer in measuring the variations of optical paths through plates or prisms. The instrument is not intended for regular use in checking flatness of surfaces. For maintaining best contrast in the fringes, the optical paths OA and OB, Figure 25.15, should be kept approximately equal. Accordingly, end mirror, M_2, is mounted on a slide that permits M_2 to be moved without appreciable wabble along the line AO. An iris diaphragm whose opening can be reduced to 0.75 mm, or less, in diameter is ordinarily used as pinhole, H. By means of this adjustable iris, the observer can choose his own compromise between brightness and contrast of the fringes. End mirrors, M_1 and M_2, are adjusted by means of suitable mechanisms (not shown) involving screws, L_1 and L_2, until pinhole images of H, formed after reflection at the end-mirrors, appear within aperture, A, at the rear focal plane of the telescope. If these pinhole images are not too far apart within A, fringes will be seen when the eye is placed behind A. One obtains the desired fringe width by further adjustments of L_1 and L_2. Failure to obtain good fringes as the pair of pinhole images is brought into unison indicates that the optical path difference between arms OA and OB is too great.

25.8.4.3 Figure 25.15 illustrates the arrangement for testing plates, P. Suppose that one knows that the surfaces of the plate are optically flat and that he wishes to check the uniformity of the optical paths through the plate. These optical paths can differ due to nonparallelism of the surfaces or due to nonuniformity in the refractive index, n. In one procedure the end mirrors, M_1 and M_2, are adjusted so that one fringe spreads over the field of view before plate, P, is inserted. The effects of introducing plate, P, are then observed. If the broad fringe is left practically undisturbed, the optical paths through the plate are sensibly uniform. The appearance of straight fringes indicates that the surfaces of the plate are not parallel. Irregularities in the fringes indicate that the refractive index is not constant. Let Δt and Δn denote variations in the thickness, t, and refractive index, n, of the plate, respectively, and let Δd denote the corresponding variation in the optical path difference, d, between the two arms of the interferometer. If Δn is negligible,

$$\Delta d = 2(n - 1)\frac{\Delta t}{\lambda} \text{ wavelength numbers.} \qquad (8)$$

If Δt is negligible,

$$\Delta d = 2\,\Delta n\,\frac{t}{\lambda} \text{ wavelength numbers.} \qquad (8a)$$

The factor, 2, enters because light waves traverse the plate twice. The following principles should be kept in mind.

(a) Each fringe is associated with a particular value of Δd.

(b) When one of the arms of the interferometer is altered in length by pressing upon the plate that supports the elements of the interferometer, each fringe moves such that Δd remains constant. With respect to the problem of interpreting the fringe system for the direction of the wedge that produces the straight fringes, one has only to shorten or to lengthen one arm of the interferometer and to note the corresponding movement of the fringes.

(c) In passing from one fringe to the next fringe of equal darkness or brightness, Δd changes by unity.

(d) In passing from a bright fringe to the next dark fringe, Δd changes by 1/2.

25.8.4.4 The base plate of the Twyman-Green interferometer is grooved or otherwise constructed so as to permit the end mirror, M_1, to be swung into orientations for testing prisms, etc. The configuration for testing right angled prisms is illustrated in Figure 25.16. Mirror, M_1, is adjusted for the desired fringe width. If all surfaces of the prism are known to be optically flat, the observed fringes reveal the degree of uniformity of the refractive index of the prism. More frequently, one will not have explored independently the degree of flatness of the surfaces of the prism. In such cases the observed fringes reveal the combined effects due to departures from surface flatness and due to inhomogeneities in refractive index. This method does not appear to have been modified to yield information about the angles of the prism or about deviation by the prism.

25.8.4.5 The following expedient is used, as the occasion demands, for distinguishing between effects due to inhomogeneity of refractive index and due to inadequate flatness of surface. The method is particularly effective in testing plates. As illustrated in Figure 25.17, plate, P, of Figure 25.15 is "immersed" between two optically homogeneous plates, E and F, that have outer surfaces of high degree of flatness. These plates are preferably, but not necessarily, plane parallel plates. For best results, the refractive indices of the immersion oil and of plates E and F should match the refractive index of the test plate, P. It can be useful to

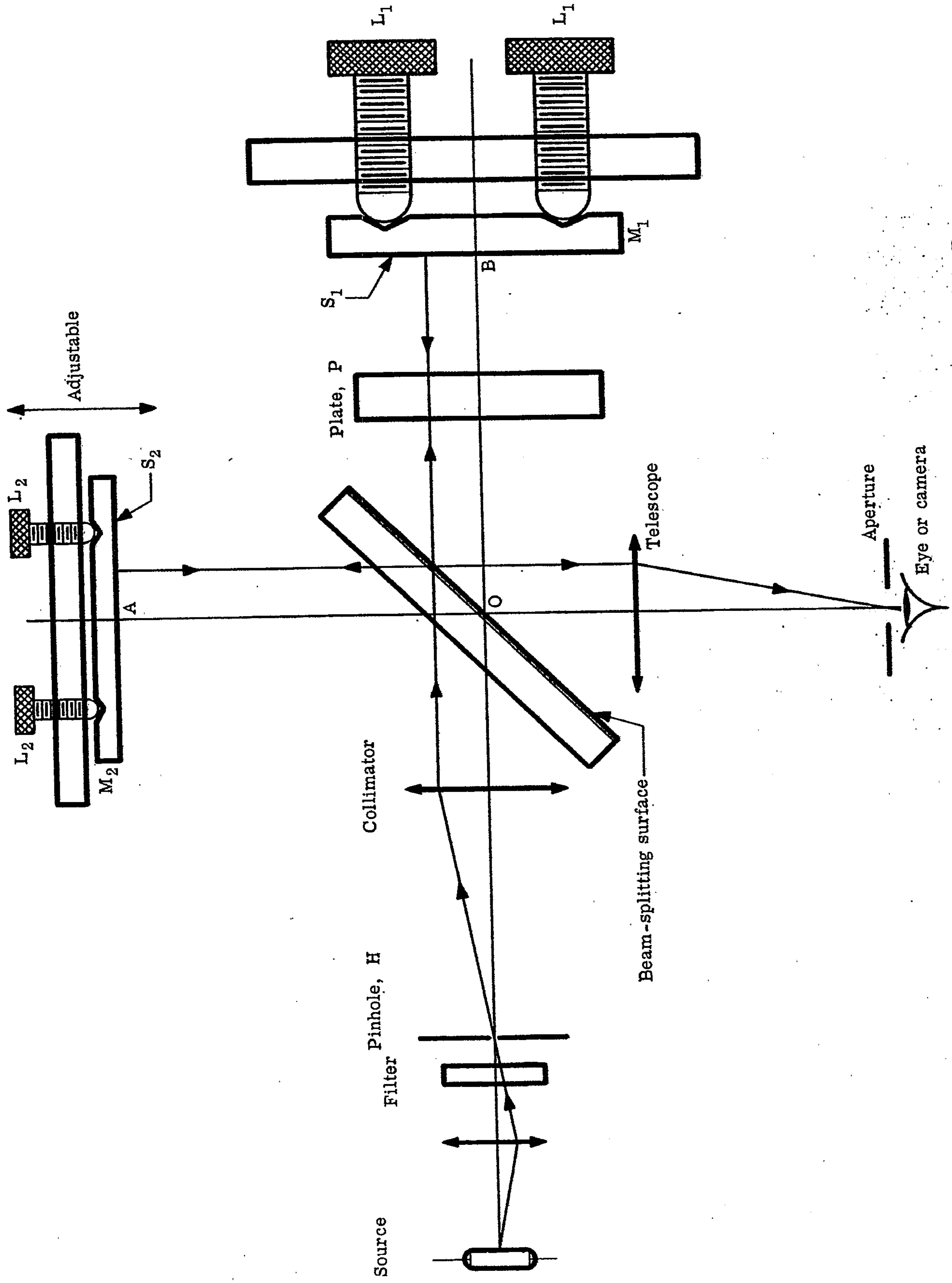

Figure 25.15- Twyman-Green interferometer as used for inspecting a glass plate P.

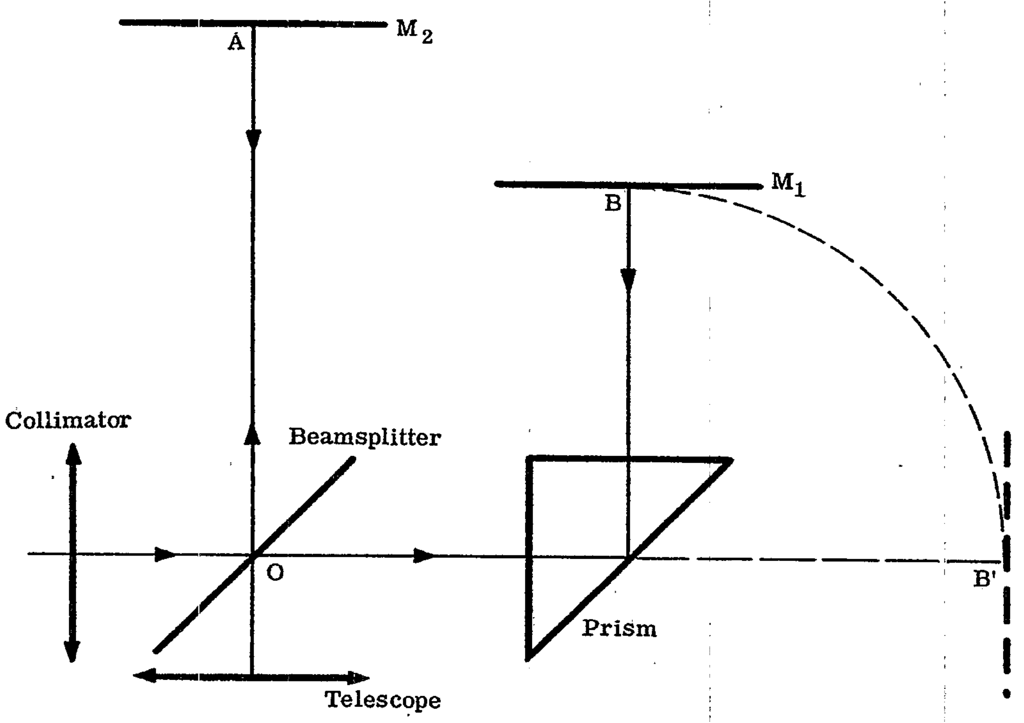

Figure 25.16- Modification of the location of end mirror M_1 for testing prisms in the Twyman-Green interferometer.

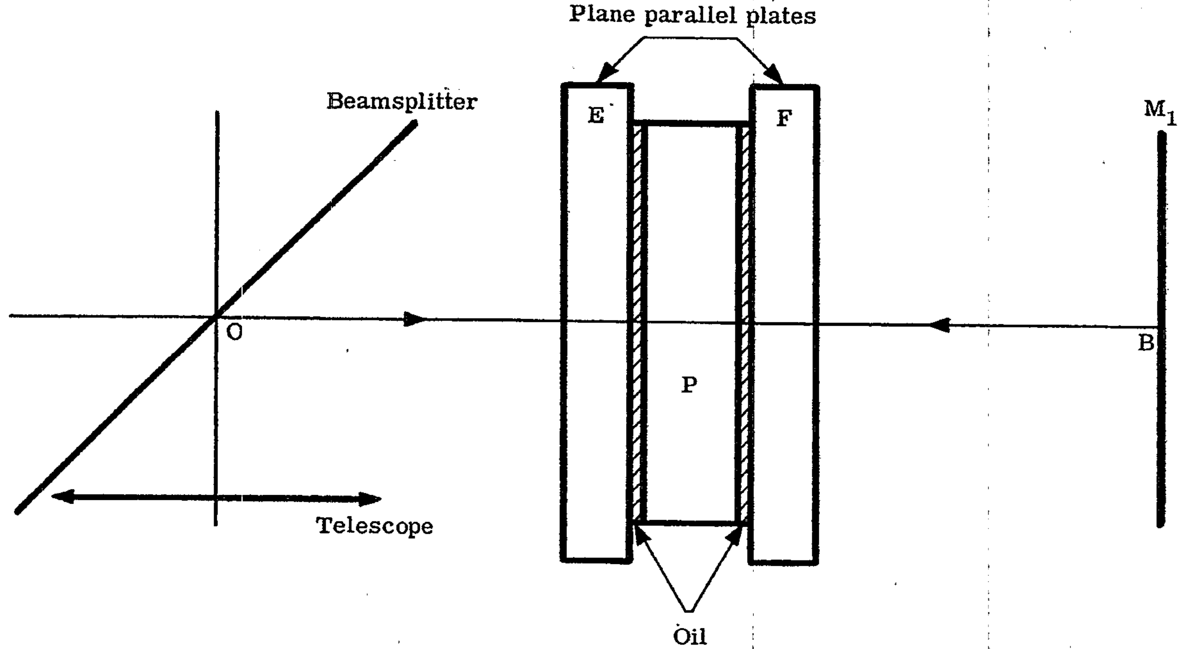

Figure 25.17- Method for obviating surface flatness of the test plate P.

"immerse" the prism of Figure 25.16 between two plane parallel optical flats. However, it is not possible to avoid lack of flatness at the reflecting surface of the prism.

25.8.4.6 Twyman-Green interferometers are provided, as illustrated in Figure 25.18, with an accessory fixture for observing spherical aberration of objectives throughout a wide range in focal lengths. Suppose that neither the collimator nor the test objective L possesses spherical aberration. Then rays from the axial point within pinhole, H, will be converged upon the axial point, C, at the rear focal plane of lens, L. If a spherical, convex mirror, M_1, is placed as indicated with its center of curvature at point C, all rays, ef, will be reflected back upon themselves and will emerge from lens, L, as normals to a plane wave that is propagated toward the beamsplitter. This plane wave interferes with the plane wave reflected from M_2 in the other arm of the interferometer to produce upon the observer's retina a family of straight fringes whose fringe width depends upon the angular adjustment of the end-mirror, M_2. In particular, a single fringe can be spread over the field of view. If the test objective has spherical aberration, all rays, ef, cannot be reflected back upon themselves. Consequently, the wave emerging from objective, L, will not be plane and will interfere with the plane wave from the other arm of the interferometer to produce interference fringes that display axial symmetry provided that the elements of objective, L, have axial symmetry and are well centered.

25.8.4.7 With objectives having long focal lengths, it is preferable to locate the convex mirror M_1 near the objective. This means that spherical reflectors having a series of radii should be provided. With objectives having short focal lengths, such as microscope objectives, the available working distance will not permit a convex reflector, M_1, but rather a concave reflector, M_1', centered about point C must now be used.

25.8.4.8 In actual practice, the exact location of the center of reflector, M_1, with respect to the axial point near the rear focal plane of lens, L, is problematical and becomes often a matter of choice. The spherical aberration can be less with respect to a focal plane that falls on one side or the other of the paraxial focal plane. Secondly, some consideration will show that the observed spherical aberration is not necessarily that of the objective alone. When the test objective has spherical aberration, the observed aberration is, in fact, the aberration of the combination consisting of the test objective, L, and the spherical mirror, M_1. Interpretation of the fringe displacements for the spherical aberration of the objective alone is not without objections of fundamental nature. But inspite of this difficulty, the Twyman-Green interferometer method is one of the better methods for indicating actual or relative amounts of spherical aberration in objectives of high optical quality.

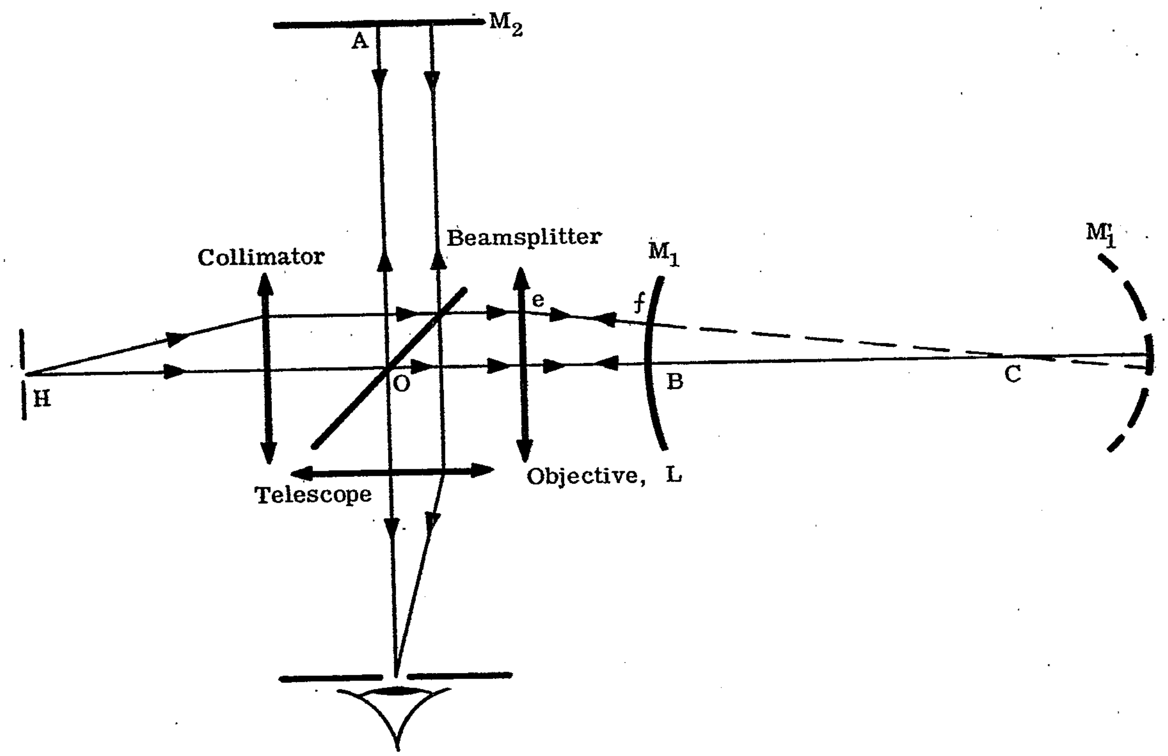

Figure 25.18- Adaptation of the Twyman-Green interferometer to the observation of spherical aberration of lenses, L.

25.9 THE RONCHI TEST

25.9.1 Introduction. One of the fairly common tests used currently by optical workers is the Ronchi Test[17]. This technique actually falls into a class known as the "shadow-fringe method". The geometrical aspects of the technique are outlined in Figure 25.19.

25.9.2 Theory.

25.9.2.1 The essence of the theory is as follows. Let us suppose as a start that a lens, L, produces a perfect star image at the paraxial focus, O, Figure 25.19. (The edge ray shown will not pass through B but through O.) Now if a plane grating of 4-8 lines/mm (Jentsch method 18 and 19) or 10-20 lines/mm (Ronchi method) is positioned at an arbitrary distance, g, from the focal point, O, as indicated in Figure 25.19, a shadow of it would be formed on a screen placed in a plane of projection arbitrarily distant p from O. Since we are, for the present, considering a perfect lens, rays from all parts of the lens aperture pass through O and this point is the single center of projection of the grating onto the plane of projection. Hence the shadow image of the grating has exactly the proportions, over all its area, of the grating itself, i.e. without distortion and with a constant magnification over its area of

$$\frac{\sqrt{\eta + \xi}}{\sqrt{y + x}} = \frac{p}{g} \qquad (9)$$

This ideal aberrationless case is usually not found and there is some spherical aberration, S, (shown for the edge ray in the figure) with the intersection points of other rays filling the space between O and B (simple undercorrection). Thus there is no longer a single point which can be considered as the center of projection for the entire grating. In this case the shadow image of the grating cast on the plane of projection will have a varying size scale over its area because centers of projection for points on the entire area of the grating lie between B and O. The magnification for any point on the grating becomes a function of the spherical aberration, S, of the ray passing through that point in accordance with the expression

$$\frac{\sqrt{\eta + \xi}}{\sqrt{y + x}} = \frac{p - S}{g - S} \qquad (10)$$

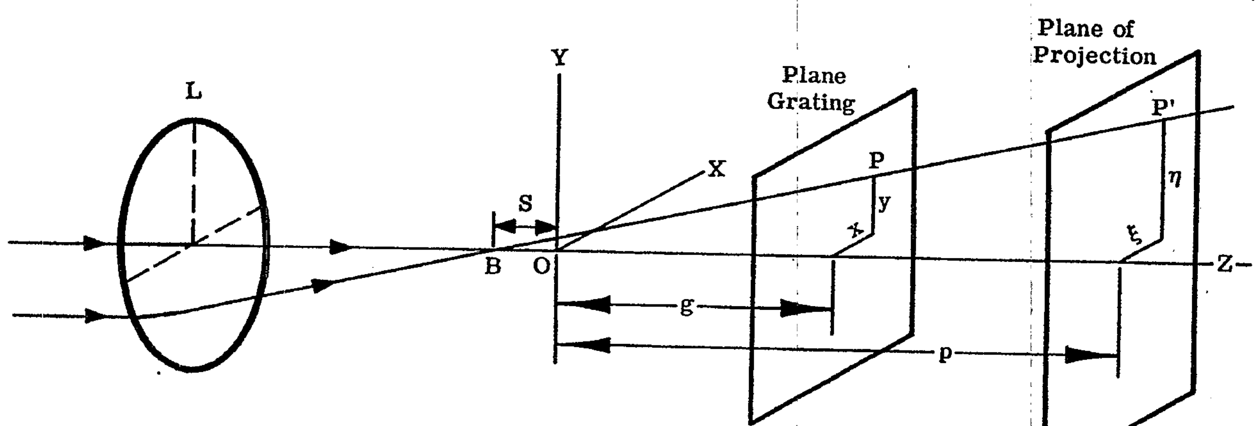

Figure 25.19-Geometrical theory of the Ronchi Test.
(After Martin's, Technical Optics, Vol. II, Pitman Pub. Co. 1950)

(17) Ronchi, Ann. d. R. Scula Normale Supriore di Pisa, Vol. XV (1923)
(18) Jentsch, Physikal Zeitschr, XXIX, 66, (1928)
(19) Martin, Technical Optics, Vol. II, 289, Pitman, 1950

If the grating is composed of straight lines its shadow image will show the lines as curved, and from the geometry of the figure, it can be shown that the curvature indicates the amount of spherical aberration present.

25.9.2.2 The complete theory must take into account not only the geometrical aspects outlined briefly here, but also the fact that interference may well be significant if the grating is as fine as those used by Ronchi or if more definitive interpretations are required. F. Toraldo Di Francia (20) has treated this subject in quite some detail, and the interested reader is urged to consult his paper.

25.9.3 Ann Arbor Tester.

25.9.3.1 There has appeared a commercial unit known as the Ann Arbor Tester based on this principal and manufactured by the Ann Arbor Optical Co. The tester is the device on the right of Figure 25.20.

25.9.3.2 The following Figures 25.21 and 25.22 are taken from the instruction booklet furnished with the instrument. Figure 25.21 [4(a)-(g)] shows the testing of an eight-inch focal length spherical mirror as a 175 line/inch grating is moved through focus on axis. Figure 25.21 [(5(a)-(d)] shows the patterns obtained with the Optical Tester and a thirty-inch focal length paraboloid cut 7° off axis. The pattern in [5(a)] shows the tester on the optical axis while [5(b)] shows the tester off axis; [5(c)] and [5(d)] were taken in the same positions but the parabolic mirror was rotated. The experimental arrangement is shown in Figure 25.22.

25.9.4 Jentsch's grid method. A similar testing technique using the coarser gratings of Jentsch is shown in Figure 25.23 taken from Martin (21) and showing the presence of spherical aberration. One optical shop checks all its work with this technique finding it a very sensitive and simple method for examing mirrors and lenses. The shadow - fringe method has much in its favor as an experienced worker gains a feeling quickly as to the nature of the defects of the system under test.

25.9.5 Summary. In the last analysis, however, all optical tests depend upon evaluation, and the experience of the optical worker himself is a vital factor. It is largely a matter of what the workers in a particular laboratory have previously used. One of the largest laboratories in the United States does practically no Ronchi-type testing as they have accumulated other equipment and know-how over the years that gives them the information they need.

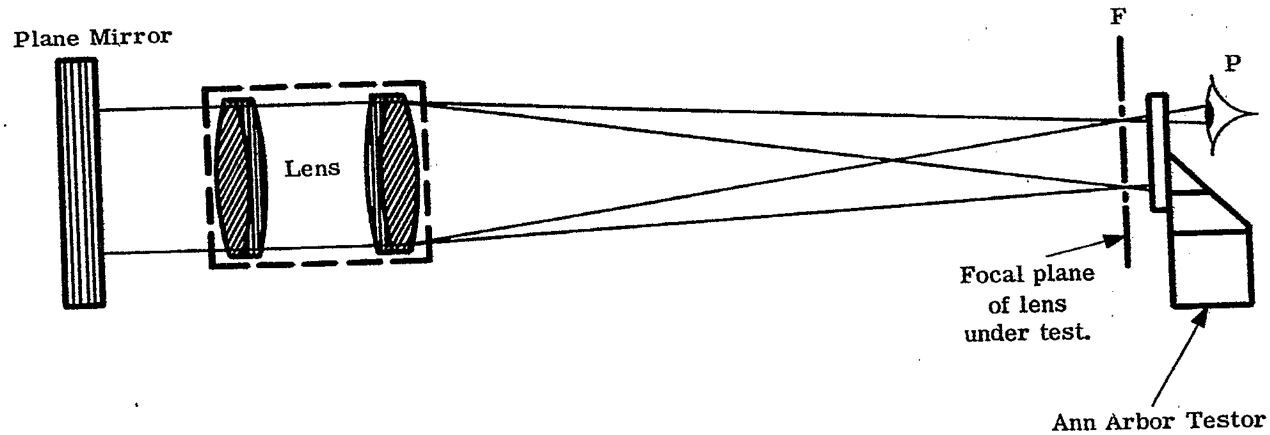

Figure 25.20- The Ann Arbor Tester.

(20) di Francia, Optical Image Evaluation, (NBS Circular 526), 161, U. S. Gov't. Printing Office, (1954).
(21) Martin, Technical Optics, vol. 1, p289, Pitman, (1948). also Jacobs, Fundamentals of Optical Engineering, McGraw Hill, (1943).

(a) -0.063" (b) -0.031" (c) -0.006"

(d) 0.000" (e) 0.008" (f) 0.025" (g) 0.051"

Figure 4

(a) (b) (c) (d)

Figure 5

Figure 25.21- Patterns seen with the Ann Arbor tester for various optical systems.

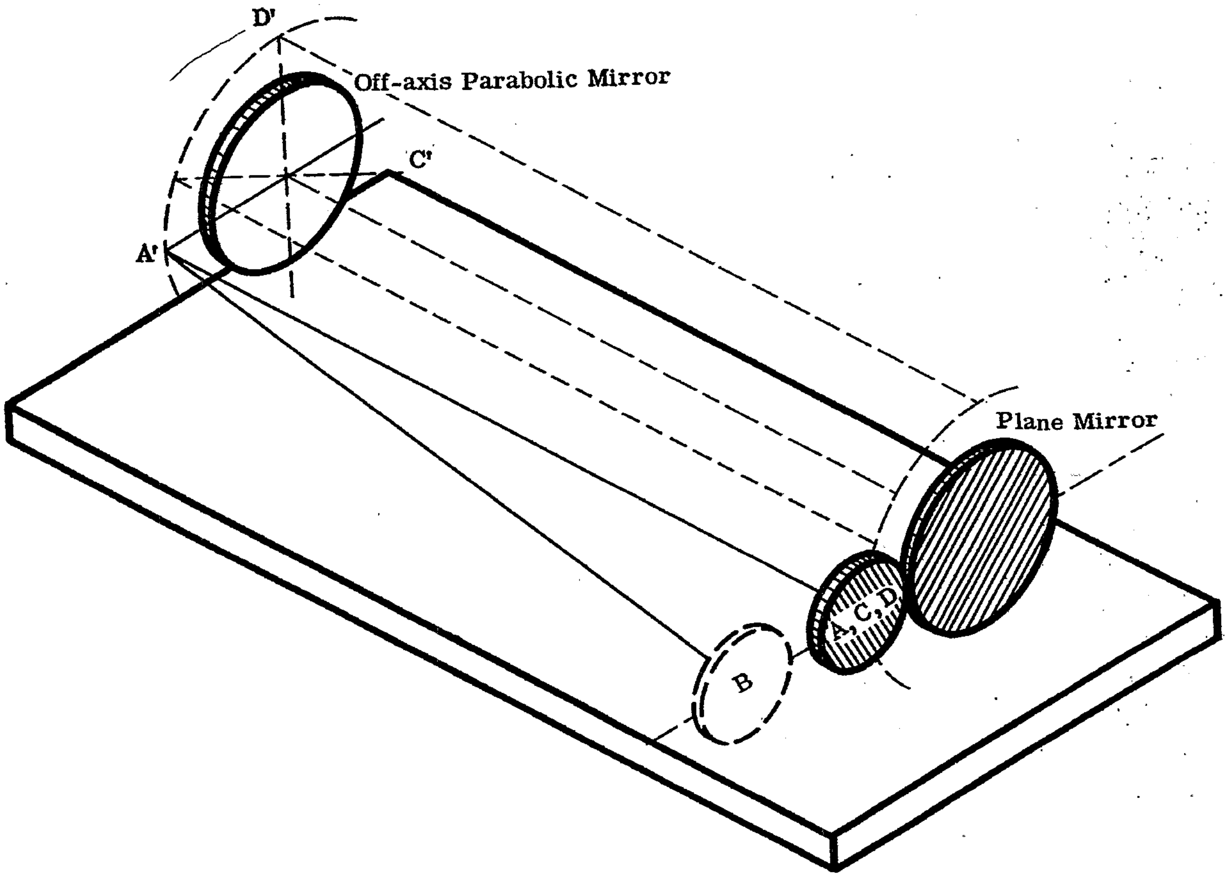

DETERMINING THE OPTICAL AXIS OF OFF-AXIS PARABOLIC MIRRORS

Often off-axis parabolic mirrors are received from the fabricator without markings indicating the side of the mirror which is toward the optical axis. Also, even with such markings, only the plane containing the axis is defined, and it is still necessary to locate the axis.

The position of the optical axis is easily determined by observing the pattern obtained with the Optical Tester. Only when the Tester is on the optical axis will the fringes be equally spaced and parallel to each other and to the lines in the grating when using an arrangement as shown in Figure 25.20.

The resulting patterns for the Tester in the correct and other positions with respect to the axis can be seen from the patterns pictured in Figure 25.21. Figure 5(a) in 25.21 shows the pattern obtained with the Tester on the optical axis of a 30" focal length parabolic mirror cut 7° off-axis. This position is illustrated above, with the Tester at A and the edge of the parabolic mirror closest to the optical axis at A'. Figure 5(b) in 25.21 shows the pattern when the Tester, parabolic mirror, and plane mirror are still in the correct plane, but the grating is located outside the optical axis (B in the Figure above).

Figure 25.22- Determining the optical axis of off-axis parabolic mirrors with the Ann Arbor Tester.

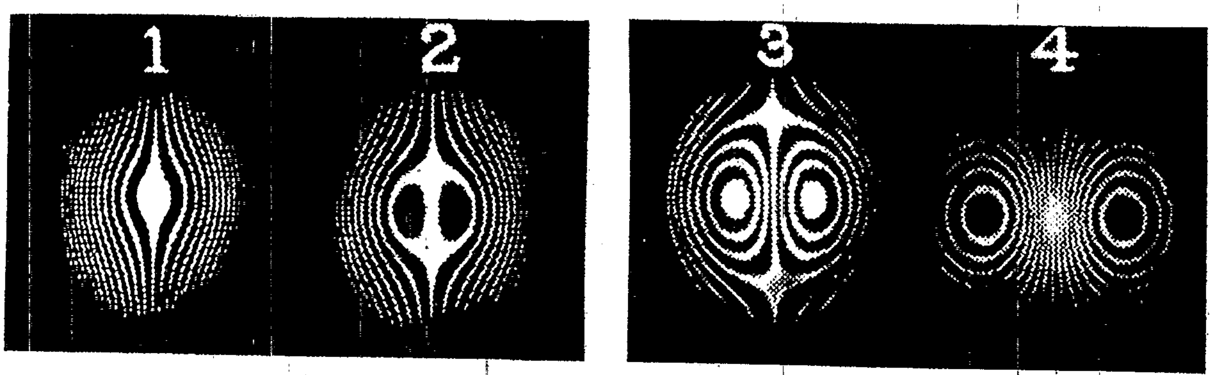

1 and 2 are shadow fringes outside the caustic. 3 and 4 are shadow fringes inside the caustic.

The appearances follow in the progression 1, 2, 3, 4.

Figure 25.23-Jentsch's grid method.
(From Martin's, Tech. Optics, Vol. II, Pitman Pub. Co. 1950)

25.10 FOUCAULT TEST

25.10.1 Introduction.

25.10.1.1 Having been given a lens or mirror surface prescription and having ground and polished the surfaces by hand or machine methods, the question arises as to what areas need to be "figured", i.e. be repolished to achieve perfectly the prescription. While helpful, the viewing of the image in toto is of less value than might be supposed, in that it represents the summation of the contributions from all parts of the surface. A technique which allows for inspection of the surfaces themselves is obviously required. One of the simplest and yet most delicate of all such techniques of surface testing was developed by Foucault (22) in 1859. The method requires, in its simplest form, merely a pinhole, a knife edge, the lens or mirror, and the eye of the observer. The system is shown diagrammatically in Figure 25.24 for a mirror.

25.10.1.2 In essence, the pinhole provides a small source of light which illuminates the surface of the mirror but which is so shielded that it sends no light directly into the eye. If we assume that the spherical surface is perfect and that the longitudinal aberration is negligible, then all rays striking the mirror will be focussed at some point, F. If the pinhole is located at the center of the curvature of the system, then F also will be at the center of curvature.

25.10.1.3 Assuming that the eye is placed close enough to the image so as to view the mirror in the Maxwellian sense (i.e. the eye receives all the rays coming to the focus), then the mirror surface will be evenly illuminated. (Actually even a perfect surface will show some deviations which will be discussed later.) If now a knife edge K is advanced in the direction indicated, the mirror surface will appear to go from completely bright to completely dark as the knife passes through F. Again for reasons to be discussed later this does not quite happen. If the knife edge is displaced toward the mirror from F then as it cuts into the beam the lower side of the mirror is darkened gradually and not until the beam is completely occulted will the eye see no light. If the knife edge is displaced from F away from the mirror, the reverse occurs. Clearly then the point where the intensity varies most rapidly with knife edge movement from bright to dark is the focus. If the knife edge always remains in the plane of the pinhole, then there will be only one place where the mirror darkens uniformly and rapidly with lateral displacement of the knife edge. This point is of course the center of curvature.

25.10.1.4 The extreme delicacy of this measurement will become more obvious if we study Figure 11.28 where a highly exaggerated error is present. Suppose there is an error of slope, angle, θ. The rays hitting

(22) Foucault, Ann de L'Obs. de Paris, V, 197 (1859).

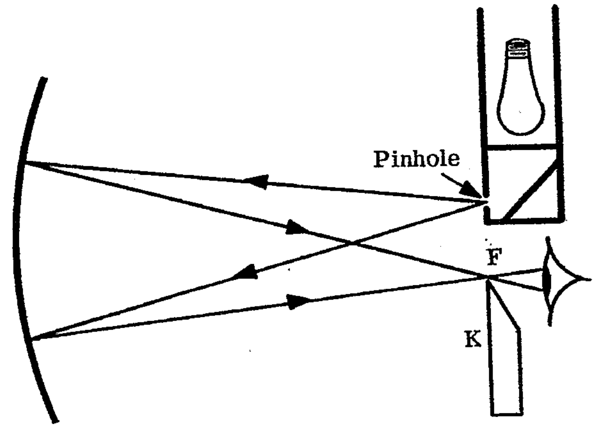

Figure 25.24- Experimental arrangement for a Foucault Test of a mirror.

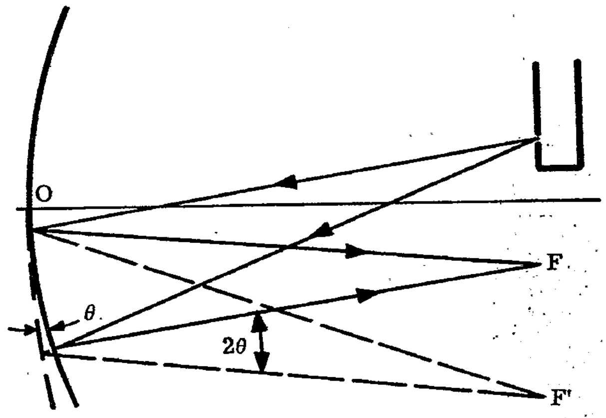

Figure 25.25- Schematic demonstration of sensitivity of Foucault testing.

this area will then be deflected from the correct focus by an angle of 2θ and the focal point for this area will be moved laterally a distance approximately equal to FO x 2θ. If the surface has a radius of curvature of ten and a slope angle error of 10^{-5} radian, then the deflection is 10^{-4} inches or .025 mm. An error this size on a lens of such small curvature would be barely detectable but on a larger focal length system it would be clearly visible. The test is actually so sensitive that slope angle errors of 10^{-6} radians are easily seen on the long focal length mirrors used in some telescopes.

25.10.1.5 Errors of this type usually appear as zones on the surface rather than isolated areas. Unfortunately while Foucault tests are very common, they are almost always done visually and few photographs are taken. The photographs of some drawings from Strong (23) are shown in Figure 25.26. The artistry of Roger Hayward, illustrator for Strong, clearly shows the variations in mirror illumination produced under the Foucault Test.

25.10.2 Detailed discussion of Foucault Test for spherical surfaces.

25.10.2.1 The preceding discussion has been highly qualitative and obviously over-simplified in some respects. To begin with the focus is never a pure geometrical point as we have demonstrated earlier. Secondly, the surface of even a "perfect" mirror does not appear all bright or all dark. It has been known for a long time that at the edge of a circular mirror there appears a very bright ring even when the knife edge has apparently cut through all of the rays. Banerji (24) has also observed that the surface for a real system with finite focal area does not grow continuously darker as the knife edge advances but rather the entire surface presents large variations in illumination. The peak illuminations get smaller and smaller until finally the whole surface is dark. Lord Rayleigh (25) attempted to explain the first of these two effects and was relatively successful. It remained for Zernike (26), Gascoigue (27), and recently Linfoot, in his articles and more recently in his book (28), to carry the interpretation of the Foucault patterns into the realm of the quantitative. Linfoot shows that the patterns may be determined analytically for an aberration-free system by assuming that electromagnetic waves originate at the surface being tested and combine according to the usual interference principles. In the event that the system is not aberration free, one must assume that the electromagnetic waves start at the pinhole and are reflected from the surface in the usual way.

(23) loc. cit., (7), 296,297
(24) Banerji, Astrophysical Journal 48, 50, (1918)
(25) Rayleigh, Phil. Mag. 33, 161, (1917)
(26) Zernike, Physica 1, 689 (1934)
(27) Gascoigue, M. N. 104, 326, (1945)
(28) Linfoot, Recent Advances in Optics, 128 at req. (1955) Oxford

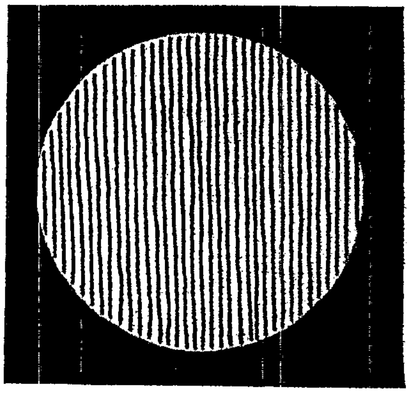

(a) Spherical mirror tested at the center of curvature.

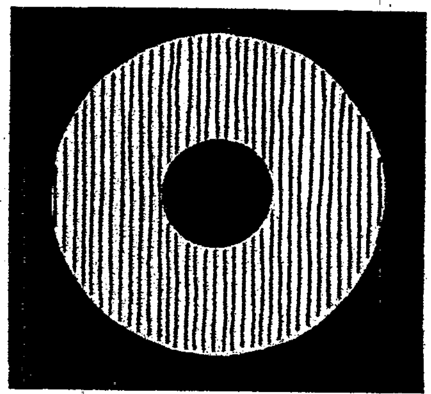

(b) Parabolic mirror tested with a flat testing mirror.

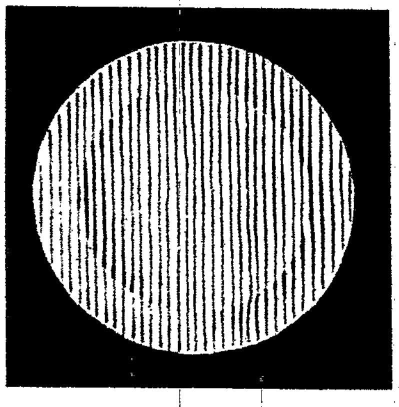

(c) Spherical mirror with a raised annular ridge as tested at the center of curvature.

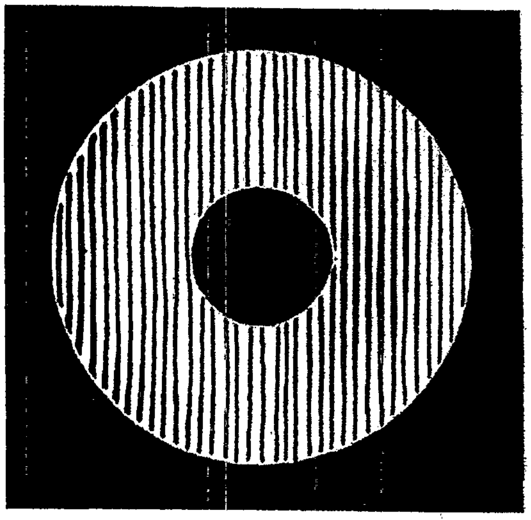

(d) Spherical mirror tested with a flat testing mirror.

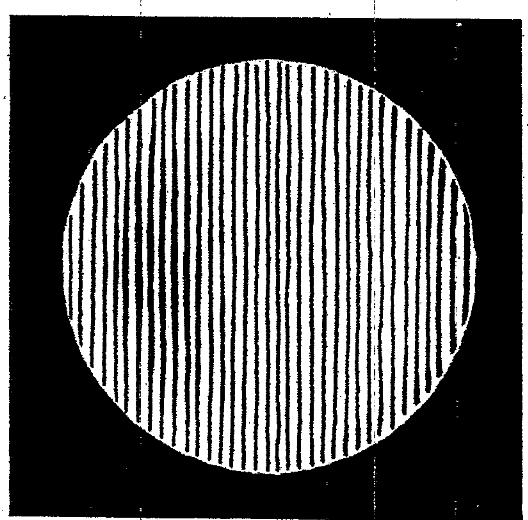

(e) Parabolic mirror tested at the mean center of curvature.

Figure 25.26-Foucault test appearances.
(From Strong's, Procedures in Experimental Physics, Prentice-Hall Inc., 1938)

25.10.2.2 Linfoot concludes that the <u>variation of illumination,</u> D(x', y'), of the knife edge is given, to a good approximation, by the equation

$$D(x', y') = \frac{1}{2\pi} \int_0^{\infty} du \int_{-\infty}^{+\infty} e^{(-iux' - ivy')} W(u, v)\, dv \qquad (11)$$

Where

$$u = \frac{2\pi x_1}{\lambda s}$$

$$v = \frac{2\pi y_1}{\lambda s}$$

$$i = \sqrt{-1}$$

s = distance from the vertex of the surface to the knife edge.

$$W(u, v) = \frac{1}{2\pi} \int \int E(x, y)\, e^{(iux + ivy)}\, dx\, dy$$

E(x, y) = illumination over the surface

Note carefully that (x, y) represent coordinates of a point on the surface under test; (x_1, y_1) represent the corresponding coordinates in the plane of the knife edge; and (x', y') represent the corresponding coordinates in the image of the x_1, y_1 plane.

25.10.2.3 An application of this equation to a true mirror with knife edge central gives Figure 25.27 (from Linfoot). Here the brilliant zone around the edge of the mirror is clearly predicted.

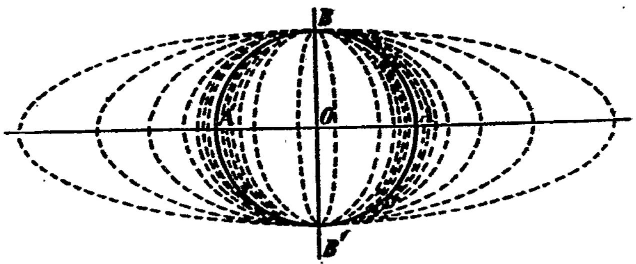

Isophotal lines for a true mirror under the Foucault test, with the knife edge central.

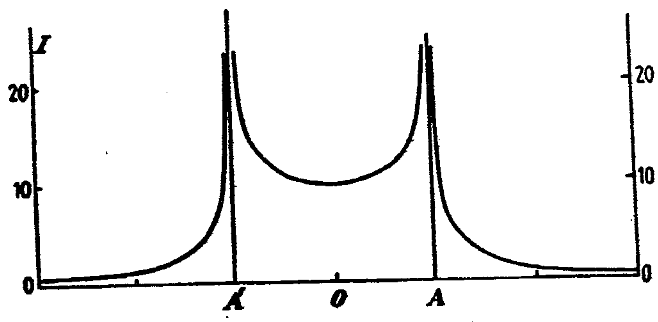

Intensity distribution along the horizontal diameter (after Linfoot).

Figure 25.27 - Isophotal lines and intensity distribution for a mirror under the Foucault test
(From Linfoot's, Recent Advances in Optics, Oxford Univ. Press, 1955)

25.10.2.4 If the knife edge is kept in the central plane but moved a distance, C, laterally we see the oscillations of Benerji (29). In this diagram $C' = \frac{2\pi C}{\lambda S}$, where C' is the distance moved in the plane of the image of the knife edge.

25.10.2.5 A practical problem frequently occurs in using the Foucault Test for surfaces of low reflection. The small pinhole that must be used results in very low light intensities, and the low light intensities make detection of the Foucault shadows difficult. To improve the situation a slit may be used. The slit must not only be narrow, but also of a length such that the aberrations of the system under study are effectively constant over this length. The details for interpreting the pattern resulting from this type of source are given in Linfoot (30).

25.10.3 The Foucault Test applied to non-spherical mirrors.

25.10.3.1 The Foucault Test can be used for paraboloidal as well as spherical mirrors. To simplify the interpretation, an additional flat is required as shown in Figure 25.28. For paraboloidal mirrors one may use several modifications of the basic Foucault test. One employs a flat mirror with a hole in the center. The arrangement is equivalent to that shown, but the observer looks along the axis of the surface being tested.

25.10.3.2 Another modification is the technique developed by Gaviola (31). This method is more sensitive than the basic test and is particularly useful as a guide in very close control of zonal errors. The experimental arrangement is shown in Figure 25.29. The Gaviola technique depends on the fact that for off-axis areas of a paraboloid the positions of best focus do not lie on the center line of the paraboloid but rather lie on a caustic which originates at the center of curvature. The method is essentially as follows. First the paraxial focal point is determined by the regular knife edge method. From this datum the equation of the caustic for the non-aberrated paraboloid is calculated. Next one calculates where the center of curvature (ξ_i, n_i) should be for a given facet or area. A knife edge is then used to determine where the center of curvature actually is - all of the paraboloid except the facet in question being covered up. The deviations $\Delta\xi$, Δn_i of the actual center of curvature from the ideal center of curvature for various facets are used to map the true surface of the mirror. Symmetry about the center line is assumed.

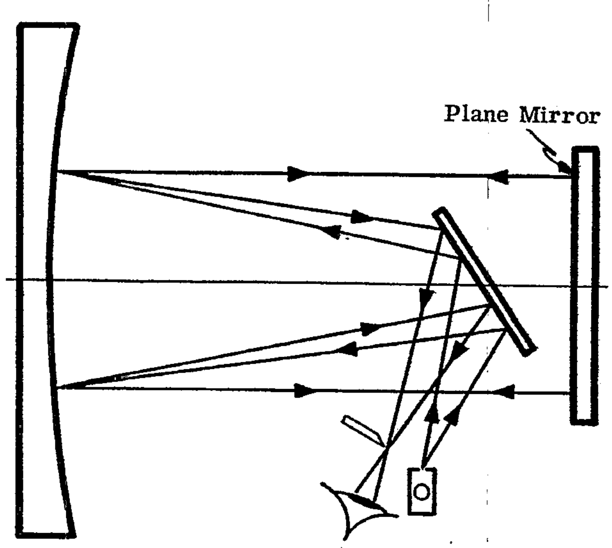

Figure 25.28- Foucault Test set-up for paraboloidal mirrors.

(29) loc. cit., (24)
(30) loc. cit., (28), 146
(31) Gaviola, JOSA 26, 163 (1936); also Strong, loc. cit., 23, p. 298

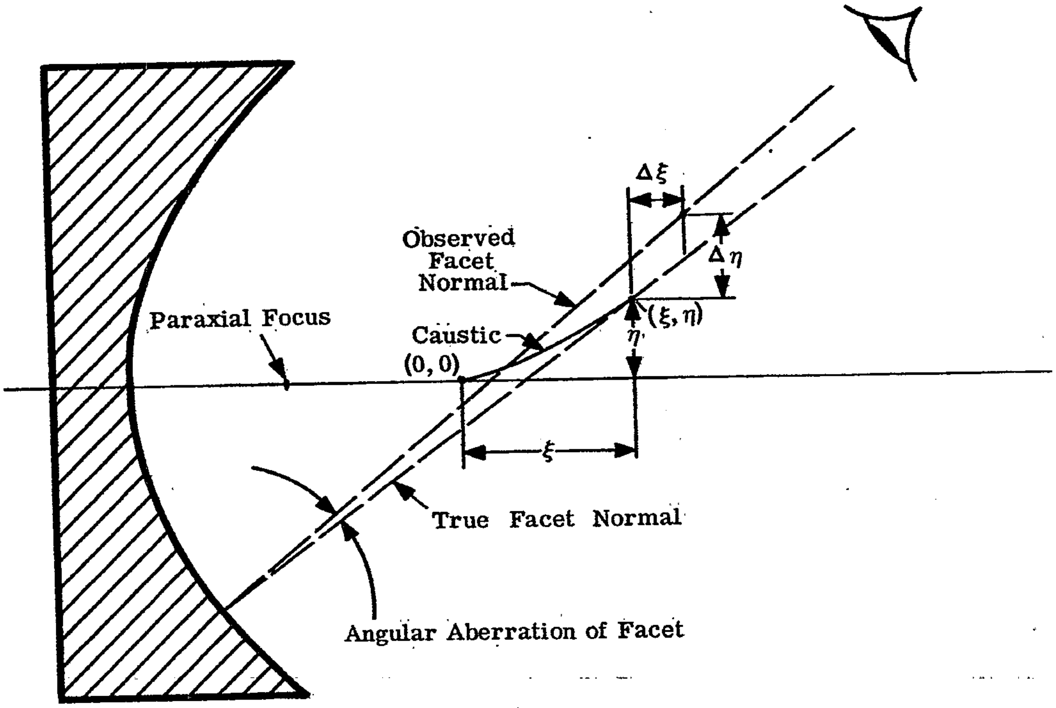

Figure 25.29-The Gaviola technique of Foucault Testing.

(After Strong's, Concepts of Classical Optics, W. H. Freeman and Co. 1958)

25.10.4 The Foucault Test applied to lenses. The previous discussion may have left the impression that the Foucault test is really applicable only to mirrors. This is not so. Basically any type of system may be tested with the same advantages accruing. Several examples are given in Strong (32). The essential technique is the same in each instance with modifications made as dictated by the system under test. In each case, it is the possibility of inspecting the zonal contributions more or less individually rather than seeing them in their integrated form which makes this test so important. Recently one of the leading precision optical makers commented that due to the increasing use of aspheric surfaces, virtually all of his lenses and mirrors were tested by this method.

25.11 THE STAR TEST

25.11.1 Introduction. It has been pointed out before that the choice of optical testing technique is frequently strongly related to the individual and his particular experience. It is generally acknowledged that H. Dennis Taylor carried the star test to its present heights and his disparaging comments on the knife-edge, or Foucault, test are interesting to read (33).

25.11.2 Technique.

25.11.2.1 The star test, as practiced by Taylor actually used a star as source of parallel light. The most frequently used star was Polaris although for checking achromatism, he also used the bluish star, Vega, and the reddish star Orionis. Today with the press of work, etc., it is seldom practical to depend on the visibility of the night sky, and artificial stars are used. One of the best "stars" is made by piercing a needle point, well honed, to varying degrees into layers of very thin tinfoil backed up by something like a very hard plastic or ebonite. Several trials should result in a very small perfectly round hole. The resulting aperture is then illuminated by a Pointolite lamp or equivalent and placed at the focus of a well corrected collimator as shown in Figure 25.30. Without much doubt, one of the best collections of star test photographs appears in Taylor's book and repeated also in Twyman's (34). It is reproduced in Figure 25.31. For convenience reference will be made using the figure numbers that appear in the photograph from Taylor, following in parentheses our figure number e.g. Figure 25.31(10a) is Taylor's Figure 10a, etc.

(32) Strong, Procedures in Experimental Physics 70-72 Prentice Hall (1953)
(33) Taylor, The Adjustment and Testing of Telescope Objectives, 50, Grubb, Parsons and Co. (1946)
(34) Twyman, Prism and Lens Making, 369, Hilger (1957)

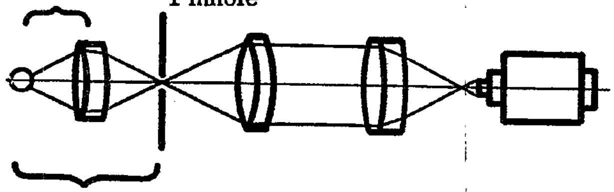

Figure 25.30- The experimental arrangement for a star test.

25.11.2.2 The star test technique consists of examining the image of the star with a fairly high power magnifier or telescope. It is pointed out clearly by Taylor that a careful examination of the observer's own eye is mandatory if a correct analysis of the system under test is to be obtained. The tests such as rotating the objective are simple to make. If the astigmatism rotates with it, the fault is with the objective, if not, the fault is with the eye.

25.11.2.3 In most instances more information is to be gained by examining the image out of focus and watching what happens as it goes through focus than trying to evaluate the system by an examination of only the in-focus image. The perfect figure will expand concentrically in an even fashion as the image passes through focus, with the intensity varying regularly in the ring structure. A perfect lens is shown in Figure 25.31 (17) while Figure 25.31 (18) shows the variation as a well-corrected lens passes through focus. It will be instructive to consider the principal star tests in the manner of Taylor, and this will now be done with frequent reference to Figure 25.31.

25.11.3 Squaring-on.

25.11.3.1 A telescope objective is considered "square-on" when the optical axis of the objective passes directly through the center of the axis or stated another way -- when the optical axis of the objective and the eyepiece coincide. Should the objective be cocked with respect to the eyepiece, the appearance of the image will depend upon the residual aberrations in the objective (assuming the eyepiece is effectively perfect). Usually the aberrations at focus that distort the image will be coma and astigmatism. Such a system is shown in Figure 25.31 (10a).

25.11.3.2 Reference should be made to Taylor for the actual process of squaring-on the objective, but the principle is clear from the photographs, viz. that the incorrectly adjusted objective will result in even the best focus being non-symmetric. Further, as the eyepiece is racked through focus, the image does not expand concentrically about the best focus image, but does so about a point to one side of the best focus image.

25.11.4 Achromatism.

25.11.4.1 It is a fundamental principle of instrumentation that we are interested in the performance of the whole instrumentation system and not just a part of it. Thus with visual optics and the known defects of the eye, we must design systems that take these defects into consideration. Occasionally we can put the defects to good use, but at all times we must be conscious of their effect upon the rest of the system. Even a perfect reflector will show a colored star test visually because of the achromatism of the eye. This may be checked easily and due account taken of it in judging systems whether they be reflective, refractive, or a combination thereof.

25.11.4.2 The defects of the eye are of course involved in the choice of eyepiece with which to judge the objective. Usually a fairly high power objective with a magnifying power of 50 - 100 times is suitable for use with a well-corrected eyepiece. Lower power objectives involve more of the eye aperture and consequently are affected more by the achromatism of the eye.

25.11.5 Astigmatism.

25.11.5.1 The nature of astigmatism has been discussed elsewhere in this manual so its details will not be reworked. It suffices one to say that the aberration known as astigmatism results in a star being focussed into two "lines" that are at right angles to each other, and displaced by an amount that depends upon the angle of view. This aberration is very easily detected with the star test. As the eyepiece is racked through focus one might see the image vary as in Figure 25.31 (12 d, d", d'). For corresponding positions inside and outside of focus one might see images as in Figures 25.31 (13) and (14).

25.11.5.2 A study of the photographs in Figure 25.31 and of the aberrational theory indicates that the star test is indeed a marvelously simple, and yet accurate, method for testing for astigmatism. It must be understood that seldom will a system have just one aberration and that particularly as one goes off axis, it becomes increasingly difficult to stipulate exactly the cause of the image degradation. It is here that experience plays such a vital role.

25.11.5.3 Assuming in the present case that only astigmatism is involved, one will usually find that the position of best focus will show a roughly circular image - the disk of least confusion - half way between the two astigmatic focal lines and of a diameter approximately equal to one-half the length of either focal line. While astigmatism is not as bad an aberration as some, if one is interested in "pointing" because of its symmetry, it may increase the spot diameter several hundred percent. This clearly decreases the resolution possible with the system. Once again we call the attention of the reader to the fact that the requirements of a good pointing system are not as stringent as those for a system of high resolution. This fact is too often overlooked.

25.11.5.4 As previously indicated, the defects of the eye must be taken into account and a truly stigmatic system may appear to the eye to be astigmatic. It is not only possible to separate the astigmatism of objective, eyepiece, and eye, but careful design can result in a system that shows no astigmatism to the eye, yet each component of the system, objective, eyepiece, and eye, each have demonstrable amounts of this aberration. Again the tests of the eye should be made initially with a low power eyepiece. More detailed drawings of star effects showing astigmatism, after Zernike and Nienhuis (35) are shown in Figure 25.32.

25.11.6 Zonal and marginal spherical aberration.

25.11.6.1 Perhaps the best way to get a feel for how the star test demonstrates zonal and marginal spherical aberration is to refer to Figure 25.33 where three possible extremes are depicted: (a) no spherical (b) marginal spherical and (c) zonal spherical. In each instance the lens under test (the element could of course be a mirror, etc.) is directed toward a distant star or equivalent as previously explained. In case (a) there is no spherical aberration at all and geometrically all rays come to point focus. Actually of course interference spreads the point into the familiar interference pattern and such a lens would show a perfect figure such as Figure 25.31 (17) at focus. Either side of, but not far from focus, such a lens might produce images such as Figure 25.31 (22) and (23). A glance at Figure 25.33 (a) demonstrates why this is so.

25.11.6.2 If the lens has marginal spherical aberration but little or no zonal, then we might see within focus an image similar to that in Figure 25.31 (15). Note carefully that there is no very bright center as contrasted with Figure 25.31 (22). Note also the way the intensity of the rings varies with transverse distance. Figure 25.31 (15) shows positive marginal spherical, i.e. the edge rays come to focus between the paraxial focus and the lens. Figure 25.31 (15a) shows negative marginal spherical aberration. The reason for Figure 25.31 (15) is again clear by reference to Figure 25.33 (b). Within focus there is a greater concentration of light for the marginal than for the central rays.

25.11.6.3 Where the marginal spherical aberration has been corrected, there may be residual zonal. This manifests itself, as might be expected, by an image of the form of that shown in Figure 25.31 (20) (inside focus) and 25.31 (20a) (outside focus). That there should be this high concentration in the third and fourth rings inside focus and in the 2 and 3 and 5th rings is reasonable providing the zonal error is as shown in Figure 25.33 (3c).

25.11.6.4 When checking for zonal or marginal spherical, the best technique is to check through focus and not just at focus. Further, the inspection should be made far enough from focus so that several rings appear as this is a more sensitive test. Generally speaking, the rules for interpreting zonal spherical aberration are

(35) loc. cit., (26), 96, Plate V

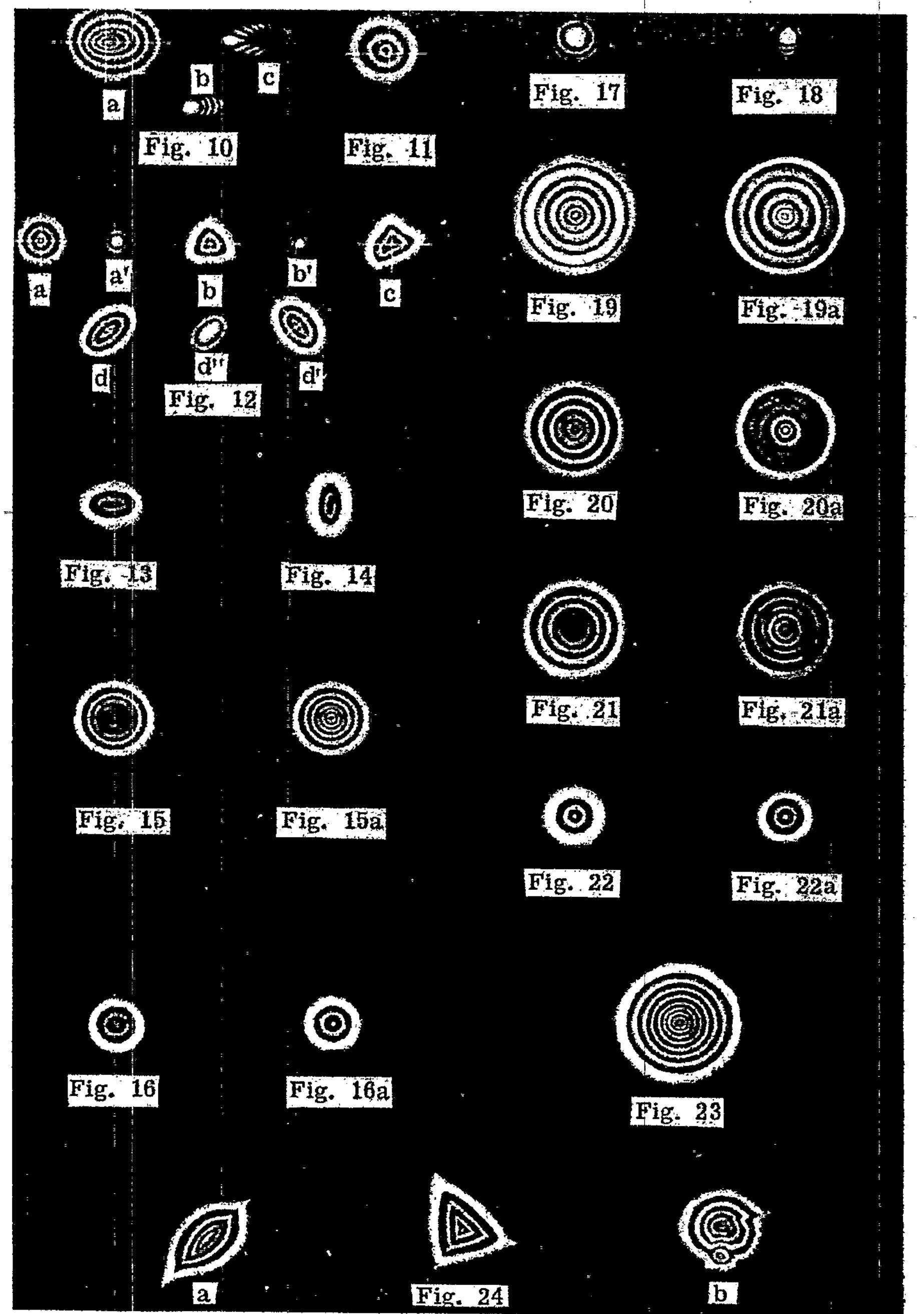

Figure 25.31-Star testing. (From Taylor's, The Adjustment and Testing of Telescopes Objectives, Grubb, Parsons and Co. 1946)

Fig. 10a.- Eccentric appearance of interference rings, due to the objective being out of adjustment.
c.- The focussed image of a star, when the maladjustment is about as much as in the last case.
b.- The focussed image, as visible when the objective is moderately out of square.

Fig. 11. - A section of the cone of rays taken closer to the focus, exhibiting a more moderate degree of maladjustment.

Fig. 12. - a, b, c, d, and d' are out-of-focus sections, as will be seen when the objective is correctly "squared on," and quite irrespective of other faults.
a', b' and d" are appearances of the focussed image corresponding respectively to a, b and d.
d, d and d" are also examples of astigmatism.

Fig. 13. - A section taken a very little way within focus, under a high power, exhibiting the fault of astigmatism.

Fig. 14. - The corresponding appearance to Fig. 13, as shown by a section taken at the same distance beyond focus.

Fig. 15. - Section within focus, showing result of positive spherical aberration.

Fig. 15a.- The corresponding section, taken at the same distance beyond focus.

Fig. 16. - A section taken closer to focus under a high power, exhibiting a slight residual spherical aberration; the central rings rather weak.

Fig. 16a.- The corresponding appearance at the same distance beyond focus; the central rings relatively strong.

Fig. 17. - The spurious disc or image of a star yielded by a perfect objective, and viewed under a very high magnifying power.

Fig. 18. - The spurious disc sometimes yielded by a large objective when resting upon three points, without intermediate supports being supplied to counteract the flexure due to the weight of the lenses.

Figs. 19 and 19a.- An example of marked zonal aberration, being sections of the cone of rays taken inside and outside of focus respectively.

Figs. 20 and 20a.- Another example of zonal aberration.

Figs. 21 and 21a.- Example of the general figure of an objective being tolerably good, but there is a region in the centre having a focus somewhat beyond the main focus.

Figs. 22 and 22a.- Two sections of the cone of rays yielded by a perfect objective, taken very near to and on opposite sides of focus, and viewed under a high power.

Fig. 23. - A section of the cone of rays yielded by a perfect objective, taken at about 1/4-inch on either side of focus, and viewed under a moderately high magnifying power.

Figs. 24 and 24a.- Examples of violent mechanical strain, due to imperfect mounting or bad annealing.

Fig. 24b.- Example of the effects due to the presence of veins in the material of the objective.

Index to Figure 25.31
(From Taylor's, The Adjustment and Testing of Teles. Objectives, Grubb, Parsons and Co., 1946)

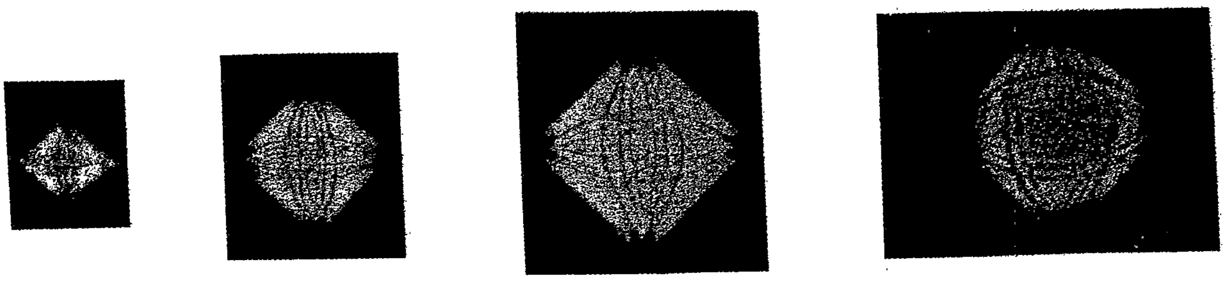

± 1.4λ ± 2.7λ ± 3.5λ ± 6.5λ

Figure 25.32-Star tests showing astigmatism of varying degrees.
(From Linfoot's, Recent Advances in Optics, Oxford Univ. Press, 1955)

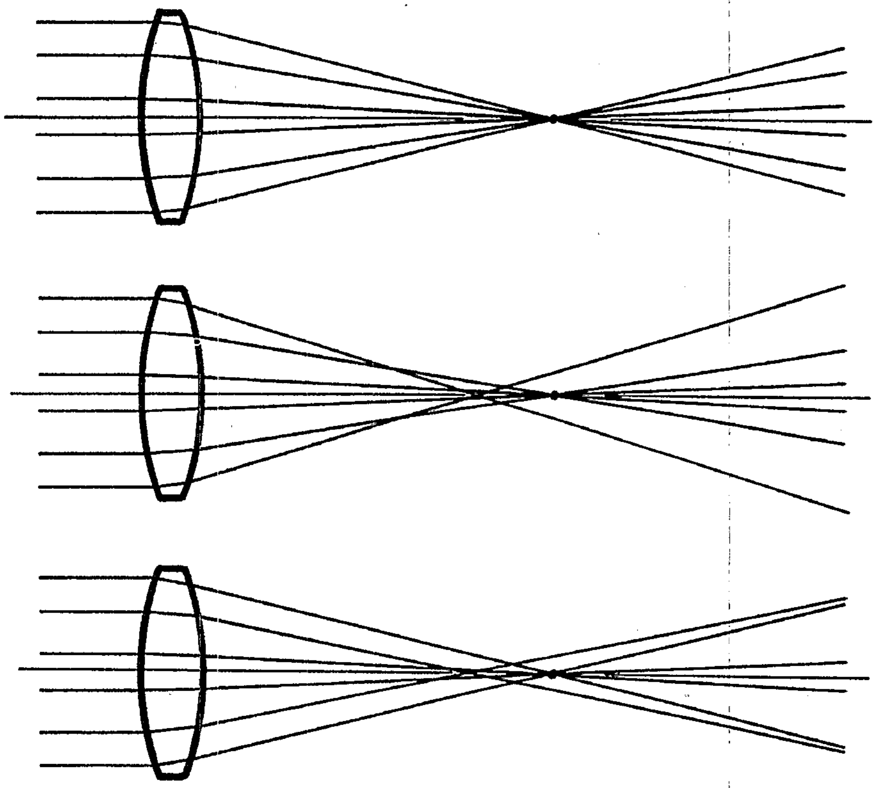

Figure 25.33- Various types of spherical aberration.

fairly straightforward with a bright zone or ring inside focus corresponding to a zone that focusses short. A bright zone or ring outside focus corresponds to a zone that focusses long. This corresponds of course to positive and negative zonal aberration. Again, Nienhuis (36) gives somewhat more detailed data, but not quite as much general information as Taylor. Figure 25.34 shows star images with varying degrees of primary spherical aberration at various focal positions.

25.11.6.5 It is clear that the star test furnishes a sensitive measure of the integrated effect of the whole lens. There is some question as to whether it gives as much information about a specific part of the lens or mirror as might a Foucault Test.

25.11.7 Coma. A good photograph of the effect of coma appears in Kingslake (37) and is reproduced in Figure 25.35.

(36) loc. cit., (26) 48, Plate II; also, Thesis, Groningen (1948)
(37) loc. cit., (28) 84, Plate IV

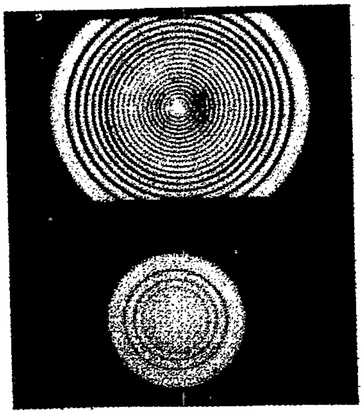

(a) Images in presence of primary spherical aberration of amount 16λ, at marginal focus and at circle of least confusion.

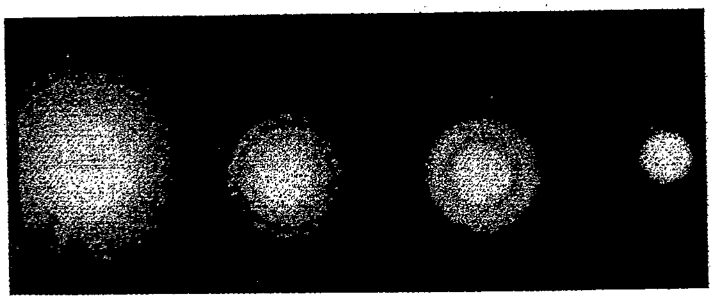

17.5λ 8.4λ 3.72λ 1.4λ

(b) Images in plane of paraxial focus, in presence of primary spherical aberration.

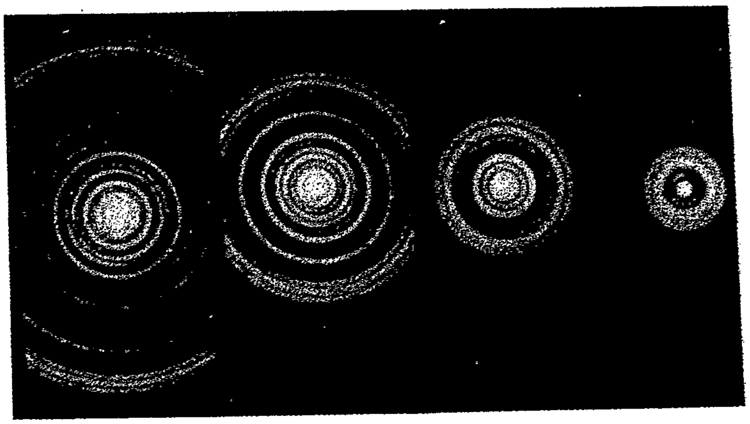

17.5λ 8.4λ 3.72λ 1.4λ

(c) Images in plane of least confusion, in presence of primary spherical aberration
scale three times that of (b).

Figure 25.34-Star images showing various amounts of primary spherical aberration.
(From Linfoot's, Recent Advances in Optics, Oxford Univ. Press, 1955)

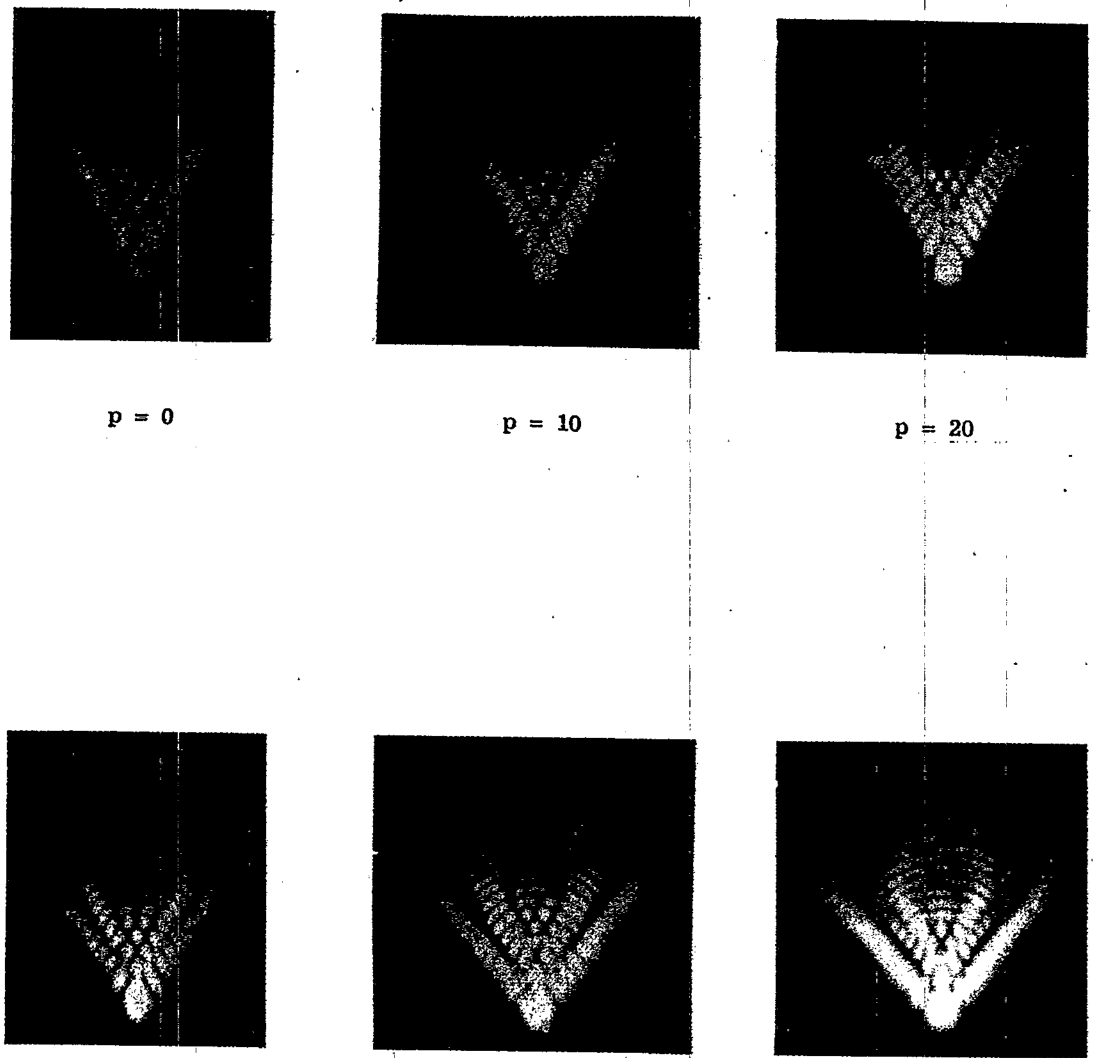

Primary coma - ϕ is $2\lambda\,(r^3 - 2/3\,r)\cos x$ at focal settings corresponding approximately to the given values of p.

Figure 25.35-Star images exhibiting coma.
(From Linfoot's, Recent Advances in Optics, Oxford Univ. Press, 1955)

26 EVALUATION PHASE OPTICAL TESTS

26.1 RESOLVING POWER TESTS

26.1.1 Introduction.

26.1.1.1 The reason for the popularity of this general method stems from the feeling that, artistic considerations aside, the function of an optical system is to give information as to the detail in an object which is usually quite some distance away. Short of looking at the actual detail of the type on which the instrument under test is to be used, it has seemed reasonable to use some sort of artificial but definite target. Since many targets of military significance have sharp edges, targets with sharp edges seem to make sense. The nature of optical system performance is such that the edges should occur in at least two orientations and these preferably at right angles to each other. This deceptively simple process culminates then in a statement as to how many lines per millimeter can be resolved on the film of a camera, or as seen by the eye in a visual device. Actually it makes more sense to talk about a limit of resolution in terms of lines per unit solid angle, etc.

26.1.1.2 It will pay us to look somewhat more closely as to why this apparently straightforward process is called "deceptively simple". To begin, we have the fundamental question of what kind of target are we going to choose as a representative sampling of the in-use object. The USAF has been using the target in Figure 26.1 for years, while the National Research Council of Canada (1) has been using annuluses on a dark background as shown in Figure 26.2 along with a sector target proposed by Nutling. The U. S. National Bureau of Standards until recently used a line target as shown in Figure 26.3 . This target and its applications were discussed in the reference cited. Recently NBS has adopted a new target and this is shown in Figure 26.4 .

26.1.1.3 In addition to these, other groups have chosen targets made up of letters or numbers or combinations of special symbols or objects (2) . To get informative as to the response of the optical system, at all angles, a target consisting of alternate black and white sectors has been used. (3) Apparently even the choice of the form of the target has been far from unanimous!

26.1.1.4 Let us look deeper. Even putting aside the question of form there is a considerable controversy over the contrast to be used between the dark and light portions. At least until the new NBS low contrast target came out, the British and Canadians were maintaining stoutly that the USAF high contrast targets were unrealistic as most of the objects photographed from an aircraft exhibited low contrast on the majority of days when photo-reconnaissance could be performed. We need not labor this point further except now we realize that not only the form but also the contrast is the subject of controversy.

26.1.1.5 With all this controversy the fact still stands that the system does have merit. Pestrecov (4) gave an excellent survey of the methods to date, and the serious student is referred to his work as regards relative merit of each. The particular claim for this technique is that it does give a single number that may be used to compare the performance of different lenses. The big question obviously is "granted it does give a figure by which to compare lenses but so do other techniques such as f- numbers, T- numbers, etc.", but does this really enable one to evaluate how a lens will perform in the field or does it merely tell how it would perform when photographing the very uninteresting lines and spaces on the test target? Unfortunately the answer to this question is not an unqualified "yes it does serve to state positively that this lens will be better than that in the field."

26.1.1.6 Having discussed these general ideas, let us now look at how the resolving power charts are actually used. As can be gathered from the above, different laboratories have their own techniques so we will sample three of the more common methods.

26.1.2 The NBS method.

26.1.2.1 Figure 26.4 shows the high and low contrast NBS charts. The dimensions of these patterns are given in the table below the charts. The contrast of the black on white is 1.4 while that of the black on grey is 0.20. The numbers on the chart "14, 20, 28", etc. refer to the number of lines/mm when this chart is used at a minification of 25X. The numbers refer to both the horizontal and vertical patterns whose linear extention

---

(1) Howlett, L. E., Photographic Resolving Power, Canadian Journal of Research, Vol. 24, Sec. A, No. 4, 15-40 (1946)
(2) MacDonald, NBS Circular 526, 51
(3) Jewell, A Chart Method of Testing Photographic Lenses, JOSA Vols. 2-3, Nos. 3-6, 52, (1919)
(4) Pestrecov, Photographic Resolution of Lenses, Photogrammetric Engineering, Vol. 13, (1947)

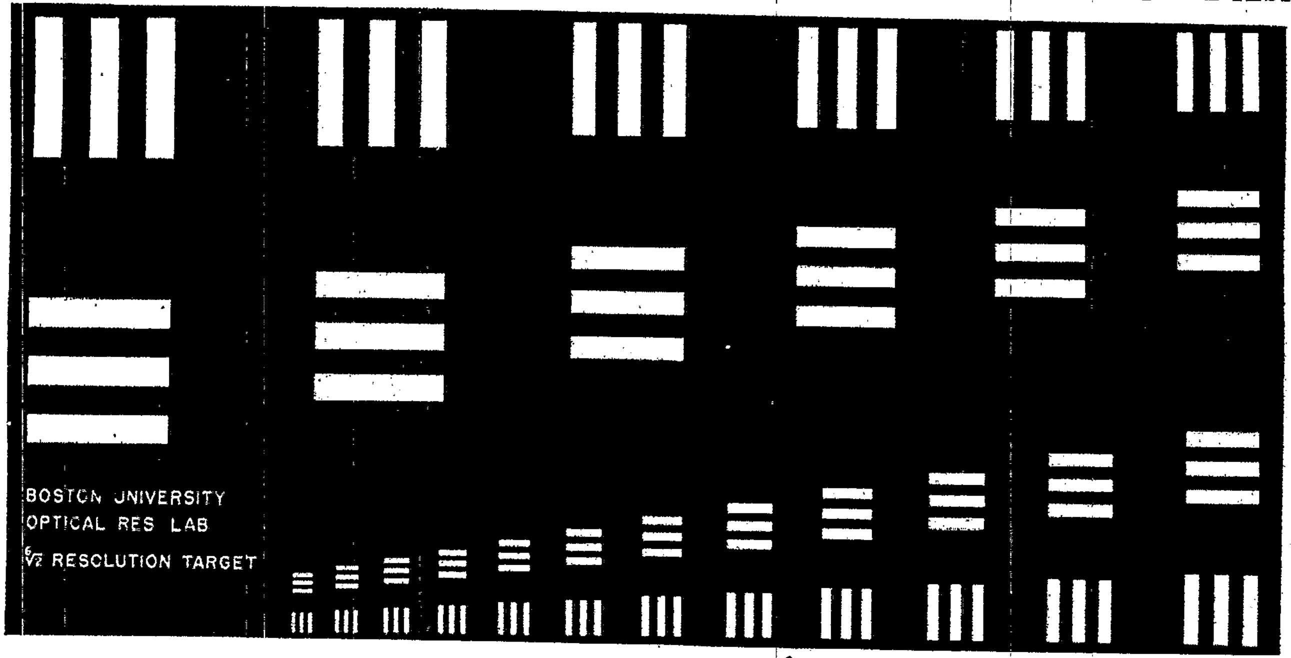

Calibration Sheet for B. U. O. R. L. $\sqrt[6]{2}$ Target

Unit	1	2	3	4	5	6	7	8	9	10	11	12	13	14	15	16	17	18
Conversion Figure	21.5	24.1	27.1	30.4	34.2	38.3	43.0	48.3	54.2	60.8	68.3	76.7	86.0	96.6	108	122	137	153

These are resolution values for a B. U. $\sqrt[6]{2}$ target of 1mm. width. To determine resolution for each unit in lines/mm for any size target, divide each figure listed above by the width of the target measured from the extreme edge of unit 1 (the largest) to the extreme edge of unit 6.

Figure 26.1 - The USAF resolving power target.

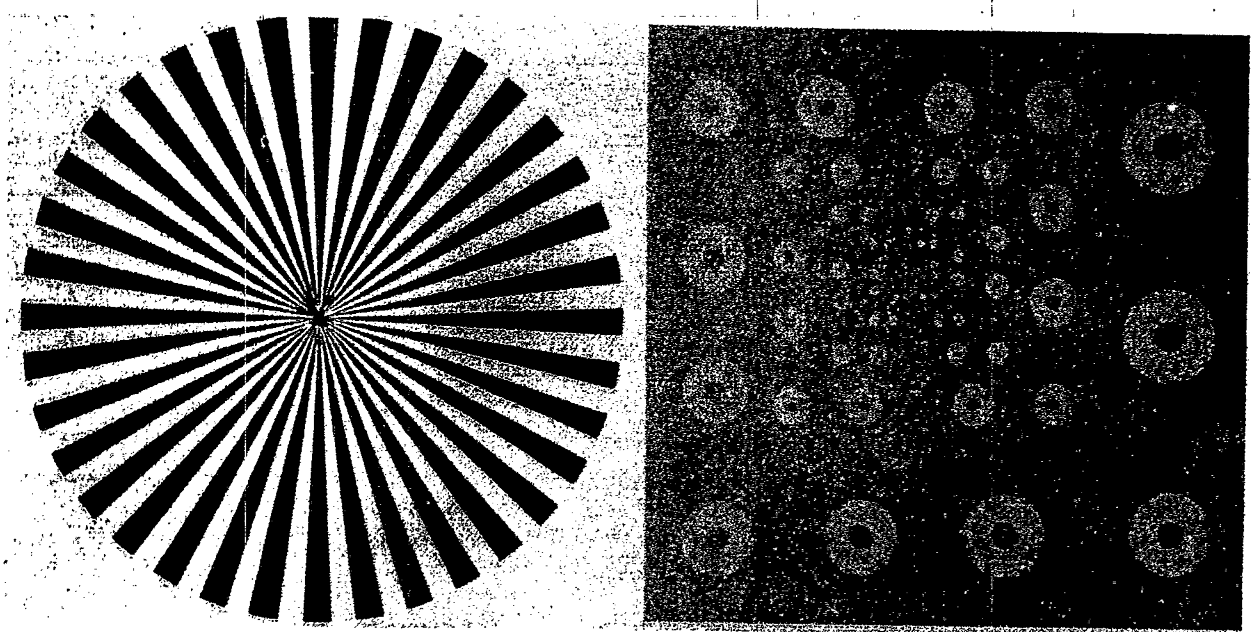

Sector target introduced by P. G. Nutting.

Canadian annulus target of 1.6:1 contrast ratio. The resolution values of the adjacent annuluses are in the $\sqrt[6]{2}$ ratio.

Figure 26.2 -The Nutting and Annuli resolving power targets.

(From Pestrecov's, Photographic Resolution of Lenses, Photogrammetric Engineering, Vol. 13, 1947)

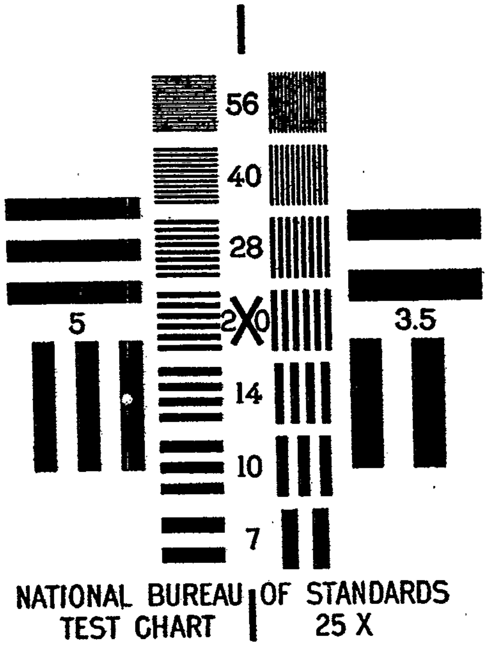

This chart formed part of NBS Circular 428. The ratio of the line spacings in successive patterns of this chart is equal to $\sqrt{2}$. When the chart is photographed at the standard distance of 26f, the values of resolving power that can be measured with this chart range from 3.5 to 56 lines/mm.

Figure 26.3 - Old NBS resolving power target.

(A Test of Lens Resolution for the Photographer, NBS Circ. 428)

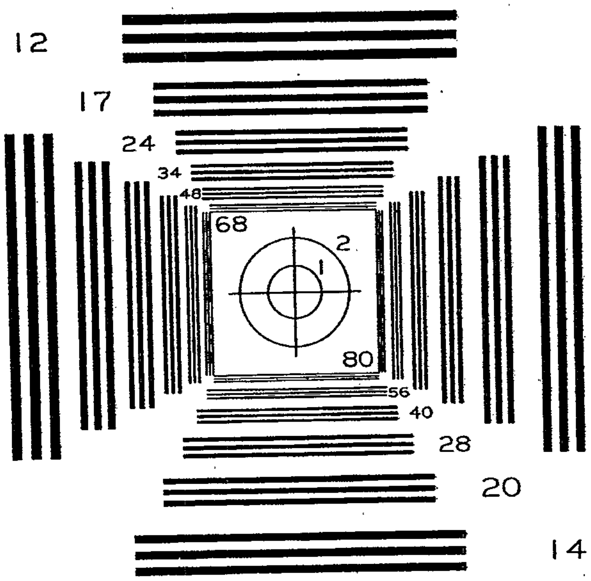

High-contrast N. B. S. resolution test chart

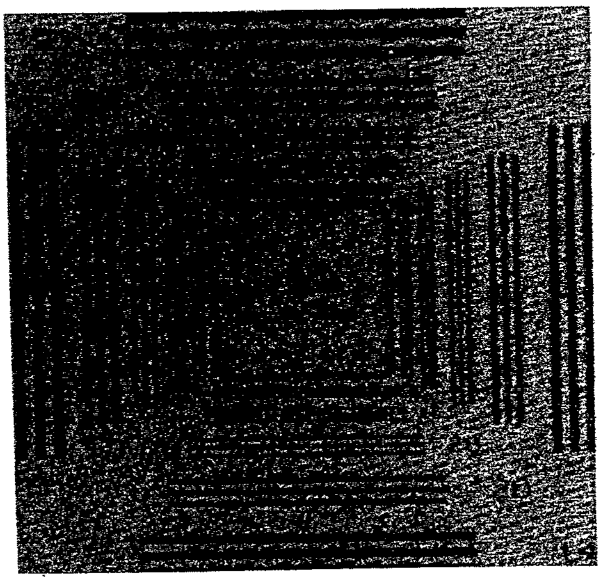

Low-contrast N. B. S. resolution test chart.

Pattern Number	80	56	40	28	20	14	68	48	34	24	17	12
Width of single black or white line	0.156	.233	.312	.446	.625	.893	0.184	.260	.368	.521	.735	1.042
Width of 3-line pattern	0.781	1.116	1.562	2.232	3.125	4.464	0.919	1.302	1.838	2.604	3.676	5.208
Width of space between patterns	0.781	1.116	1.562	2.232	3.125		0.582	.825	1.164	1.649	2.328	
Length of lines	18.0	19.6	21.9	25.1	29.6	36.1	18.0	19.6	21.9	25.1	29.6	36.0

Figure 26.4 -The new N. B. S. resolving power targets.

(Charts for Testing the Resolving Power of Photographic Lenses, F. E. Washer and I. C. Gardner, NBS Circ. 533(1953)) would run into the number. The chart used in this manner should be 26 focal lengths in front of the lens. The charts of course may be used both off as well as on axis. A common arrangement is to make a rack holding a series of the charts arranged in roughly the form of a square so that a photographic lens may be tested at all angles simultaneously. If the lens is to be tested visually, then it may be somewhat more desirable to reposition the test chart to the various angles of interest.

26.1.2.2 The observer after setting up the chart at the requisite distance determines which group is just distinguishable as three distinct lines and reports the corresponding number of lines/mm as the maximum resolving power of the lens at the given angle etc. Note that the measurement made in this way gives little or no information as to the response of the system to targets at fewer lines/mm.

26.1.2.3 Table 26.1 taken from NBS 533 shows the variation of resolving power of several hand held cameras. In this connection it is interesting to note the effect of using the high and low contrast targets. Inasmuch as we judge lines to be separated on the basis of contrast, it is important to note particularly Figure 26.5. The high contrast targets clearly may well be a more revealing as to what the actual resolution limits of the lens are. Further, the increased slope of the high contrast curve makes far more accurate measurements. Again we must warn that if the lens is to be actually used on low contrast targets, then we had better check it

Lens	EFL mm	F-number	Resolving power in lines per millimeter (angular separation from axis): Tangential					Radial				
			0°	5°	10°	15°	20°	0°	5°	10°	15°	20°
A--	50	2	68	56	56	48	28	68	56	56	48	40
		2.8	68	68	68	68	56	68	68	68	68	56
		4	80	68	56	56	56	80	68	68	68	68
		5.6	80	80	68	68	80	80	80	80	80	80
		8	80	68	68	68	68	80	68	68	68	56
		11	80	80	80	80	68	80	80	80	80	80
		16	56	56	56	56	48	56	56	48	48	48
		22	56	56	48	48	48	56	56	48	48	40
B--	50	4.5	56	34	20	14	24	56	40	40	48	48
		5.6	56	28	17	20	34	56	40	40	56	56
		8	56	28	24	34	48	56	56	48	80	80
		11	56	34	34	34	56	56	56	56	80	80
		16	56	56	56	48	48	56	56	56	68	68
C--	85	2	68	68	34	17	--	68	68	48	34	--
		5.6	68	68	48	20	--	68	68	68	56	--
		11	68	68	48	24	--	68	68	68	80	--
D--	101	4.5	34	34	28	28	28	34	34	28	20	28
		5.6	40	34	28	28	28	40	40	28	14	28
		8	40	40	40	34	34	40	48	48	24	28
		11	40	48	48	40	40	40	48	48	34	34
		16	34	48	48	40	40	34	48	48	40	40
E--	101	4.5	28	28	24	12	7	28	34	34	28	20
		5.6	28	28	20	12	7	28	28	24	28	20
		8	34	28	24	17	14	34	34	34	28	28
		11	28	28	28	20	12	28	40	40	28	28
		16	34	34	28	17	12	34	40	40	28	20
		22	34	28	28	17	5	34	40	40	34	24
		32	34	28	24	17	12	34	34	34	34	28
F--			5.6	5.6	5.6	5.6	4.8	5.6	5.6	5.6	4.8	4.8

Table 26.1 - Resolving power at various apertures of several lenses of the type used on small hand-held cameras.

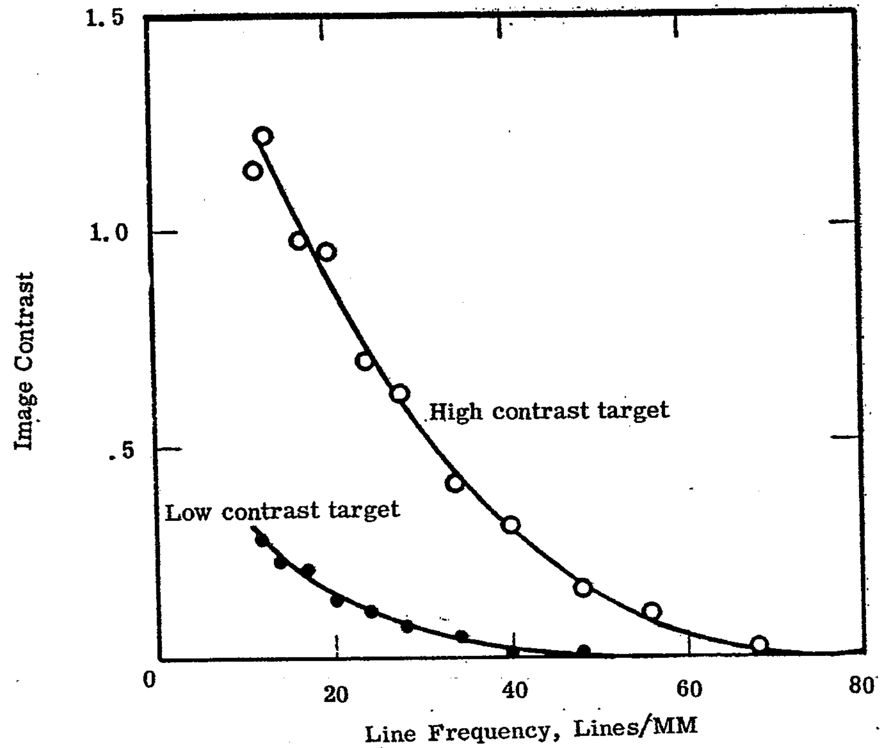

Figure 26.5-Variation of contrast in the image as a funtion of line frequency.
(Charts for Testing the Resolving Power of Photographic Lenses, F. E. Washer and I. C. Gardner, NBS Circ. 533(1953))

on low contrast targets. This also is shown clearly by Figure 26.5: if we want to resolve 50/mm at low contrast, then the lens examined is not suitable. If we want to resolve the same number of lines/mm at high contrast, then the lens might well be satisfactory. This is a crucial point in considering the usefulness of resolving power targets as evaluation tools.

26.1.2.4 Looking again at the question of visual optics such as binoculars, telescopes, periscopes, etc. we realize, as previously pointed out that here the most important characteristic is not lines/mm but rather lines/unit solid angle. We can also state this by saying that we are interested in the angular rather than the linear resolving power of the system. Tables 12 and 13 from NBS 533 enable the user to determine from the chart group just resolvable, the corresponding maximum angular resolving power for either the circles or the lines around them.

26.1.2.5 Care must be exercised in judging the resolving power of a visual system to be certain that the resolving power of the eye is taken into consideration. This means that the lines under study must all subtend an angle greater than that just resolvable by the eye--usually about 60 seconds of arc. This means then that the product of the resolving power of the target and the magnification of the system must be greater than, say 60 seconds of arc, if we are to obtain a true test of the resolving power of the system.

26.1.2.6 In this same connection, the resolving power of a sequence of optical systems is analogous to the effective bandwidth, or the effective rise time of a number of sequential amplifiers; the overall resolving power, Re, in terms of the resolving power of the individual components R_1, R_2 etc., is given approximately by

$$\frac{1}{Re} = \sqrt{\frac{1}{R_1^2} + \frac{1}{R_2^2} + \frac{1}{R_3^2} + \dots} \qquad (1)$$

26.1.2.7 The NBS chart, when used in this standard manner, will cover a range of 14 to 80 lines/mm. For systems having higher or lower resolving powers the targets may be moved closer or further away. In some instances it may be convenient, where systems capable of resolving several hundred lines/mm are repeatedly encountered, to avoid the long working distances involved in the method above and reduce the targets photographically. Should this be done, great care must be exercised to see that the resolving power of the film and copying camera are such as to not degrade the targets.

26.1.2.8 While the NBS charts were developed primarily for lens studies, they may also be used as a basis for compliance with certain government specifications, for example

Federal Specification:

GGG-G-501b	Goggles, eyecup, protective, impact-resisting (chippers', grinders' etc.).
GGG-G-511a	Goggles, eyecup, protective (welders).
GG-T-621	Transits, 1-minute; and transit tripods.

Military Specification:

MIL-O-13830 Ord	Optical components for fire control instruments; general specification governing the manufacture assembly, and inspection of.

Commercial Standard:

CS159-49	Sun glass lenses made of ground and polished plate glass thereafter thermally curved.

26.1.3 <u>The U.S.A.F. resolution target.</u>

26.1.3.1 Originally suggested at the Bureau of Standards and carried to its present status by the U.S.A.F. Photographic Laboratory at Wright-Patterson Air Base, the U.S.A.F. target was designed primarily to evaluate the performance of aerial camera lenses. While the use of this target is controversial, it is probably the most widely used of all at the moment. The following comments of A. Katz (5), then of Wright Field, are much to the point. They were made during a discussion following a paper by R. E. Hopkins.

> "In connection with the points raised by Dr. Pestrecov and in earlier papers, I notice that a number of people have been gleefully trying to kick the three-line resolution target to death. I want to point out again--and I have done this in other meetings--that it has served its purpose well. This purpose, simply stated, is to serially grade lenses in a manner that will correlate with their photograph-making rank. I have yet to be shown that our use of the three-line target in the judging of lenses to be used for aerial photography has led to any error, let alone consistent error."

> "Now we have lots of data, most of which is not neat and packaged. The exigencies arising with the working conditions in the Air Force are such as to effectively preclude the careful running of planned experiments. We substitute large numbers of airplane flights and tests, and after a number of years we come to pretty definite conclusions--by statistical osmosis, if you will. We know by now that when we get a lens that performs well in the laboratory (on the much maligned three-line high-contrast target) it will take high-quality photographs in the air on good days as well as bad days. The converse is also true. Laboratory test enable us to predict the quality of actual aerial photographs. I can't expect much more of a laboratory test. Let us not forget that it is only within the last 10 years that lens performance began to be specified in terms of resolution requirement over the field and that manufacturers began to use these tests, and it is only within the last couple of years that photointerpreters have begun to hear of lines per millimeter as a measure of performance."

26.1.3.2 The type of tests (6) to which Mr. Katz is referring are well demonstrated in a portion of a series of through-focus trials shown in Figure 26.6 on a 40-inch f/5 Baker telephoto aerial camera looking through a <u>window</u> of poor quality. The target was the standard high contrast U.S.A.F. target plus a low contrast version of same plus a two variable frequency high contrast targets first introduced by Washer and Rosberry (7). The target was distant from the camera some 35 focal lengths to minimize the effects of spherical aberration. The term "window" here refers to the glass covering the hole in the skin of the aircraft through which the <u>aerial camera sees the ground.</u> More or less comparable focal positions are shown side by side for ease of

(5) NBS Circular No. 526, 200

(6) These tests were run by Mr. William C. Britton while at the Boston University Physical Research Laboratories and under a U.S.A.F. contract. Mr. Britton is now with Itek Corp.

(7) Washer and Rosberry, JOSA vol. 41, No. 9, 597, (1951)

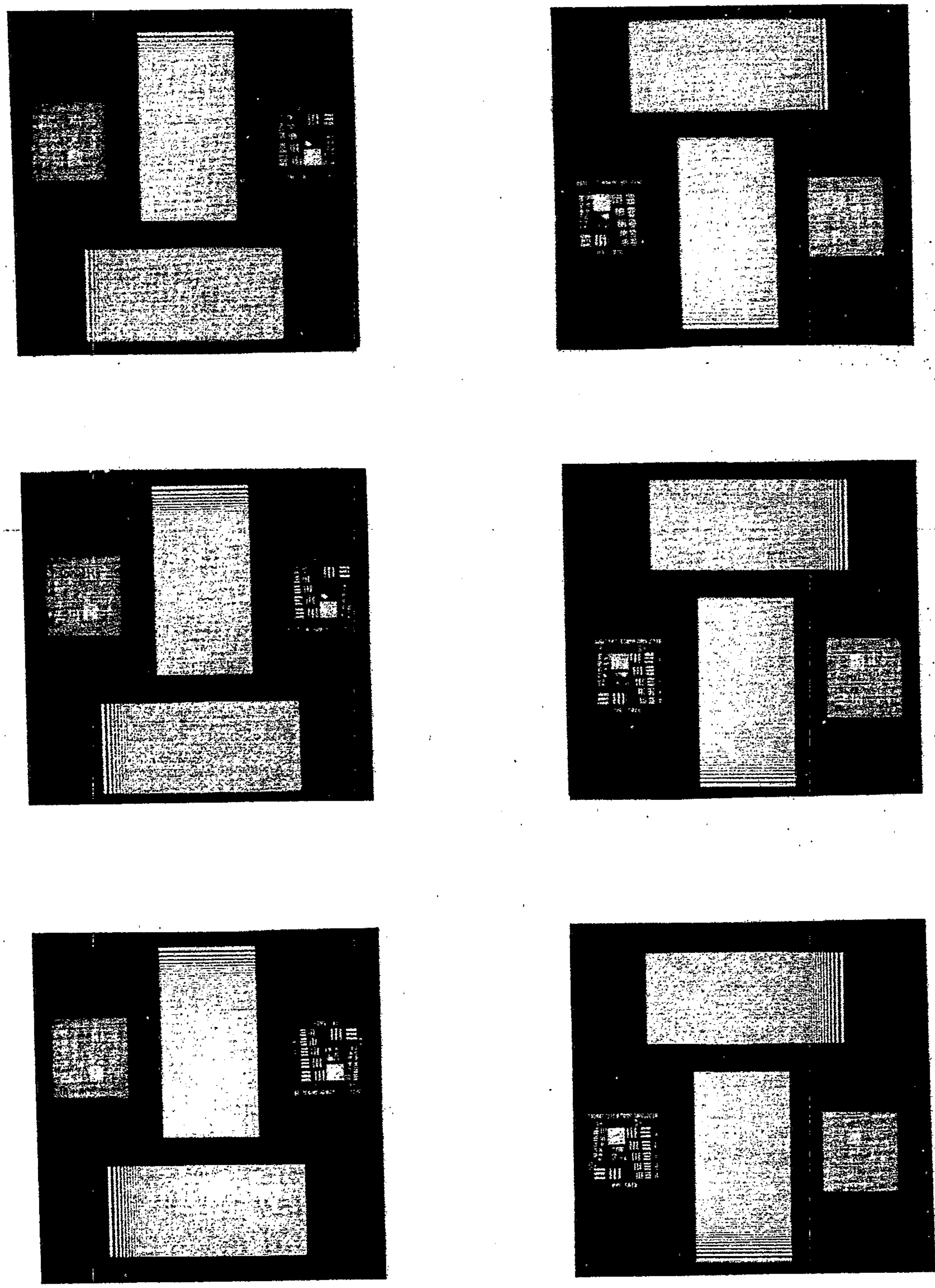

window 45° Obliquity

No Window

Figure 26.6 - Resolution target testing for Baker 40" f/5 telephoto aerial camera.

comparison. The focal settings was changed by .005" between successive exposures. The variation of the resolution limit with the high and low contrast targets is clear. The effect of off-axis aberrations is also clear.

26.1.3.3 Composite target tests such as these demonstrate the difficulty of deciding on which target, if any, to settle on to the exclusion of all others. In fact it is pretty generally the opinion of the "conservatives" that no one target gives all the information that is needed to fully evaluate a lens. Were a given optical system always to be used on exactly the same type target, that would give a one to one correlation between laboratory testing and field performance. It, thus, is the very versatility of optical systems that gives rise to our difficulty.

26.1.4 <u>The Kinetic Definition Chart.</u>

26.1.4.1 There was developed during World War II (8) and subsequently improved upon (9 and 10) a routine system for checking the resolving power of visual optical systems. The system is essentially a resolving-power target approach, but incorporates many features not formed in the spur-of-the-moment setups commonly found in laboratories. The targets employed, as well as plan and side view schematics are shown in Figure 26.7.

26.1.4.2 The apparatus derives the word "kinetic" from the motorization of some of its parts, but the term is misleading nonetheless. A glance at the charts will show that they are of constant line spacing but of various contrasts and situated in four positions. The ratio of lines/spaces is 1:1, and is essentially the chart first advanced by Foucault (11) in 1858. The variation in line spacing required to determine the resolving power of a system is effected by the optical reduction unit. This unit consists of four highly corrected microscope objectives of focal length 4, 8, 16, and 32 mm. By varying the distance from the target to the reduction unit by the adjustable space gauge shown in Figure 26.7, the lines/inch may be changed from coarse to fine.

26.1.4.3 There are several interesting aspects to the KDC Apparatus. One of these is the "artificial sky" which not only simulates (by varying its illumination) the sky against which many objects must be seen, but also the stray light found in most optical systems. This apparatus thus takes into account not only the low control of the object itself, but also the surround so important in retinal response. Incorporated into the KDC Apparatus is a standard telescope with an aperture that is variable. This very carefully constructed telescope is of superior quality and allows the observer, in effect, to set up a standard against which the test instrument is compared. Once again we see a recognition of the need for removing as far as possible the limitations of the particular observer's eye from the testing procedure. Here this is done by inclusion of an auxiliary telescope of such magnification that the limit of resolving power is determined by the instrument under test rather than the eye. The rest of the system is rather straightforward and all designed to give maximum ease of assessment to the observer.

26.1.4.4 The final report on the NBS chart or the USAF chart is the resolving power limit of the system. In this technique the final report is called the <u>K.D.C. efficiency</u> and is defined as follows:

$$\text{KDC efficiency} = \frac{\alpha_e}{\alpha_i \, Mi} \times 100 \qquad (2)$$

where

α_i = minimum angle resolvable using the instrument under test.
α_e = minimum angle resolvable with the eye alone.
Mi = magnification of the instrument under test.

Clearly then, this definition is not a statement of the resolving power of the instrument alone, but rather it is a comparison of the effective improvement the instrument affords over the eye alone.

26.1.4.5 The factors directly preportional to α_e and α_i are conveniently determined directly from the KDC apparatus as follows. With the auxiliary telescope in place (if it will be required with the instrument under test as previously explained) the observer adjusts the target-to-turret spacing until the target is just resolved and the K.D.C. scale (lower left of drawing, just above the reversing switch) is read. The pointer on this scale is coupled to the target holder. The instrument under test is then inserted in its proper place and the K.D.C. scale again read. The K.D.C. efficiency is now obtained from the equation:

(8) NDRC Report (classified)
(9) Coleman and Harding, JOSA 37, 263, (1947)
(10) NBS, 526, 95, (1954)
(11) Foucault, Ann. de L'observation de Paris, 5, 197, (1859)

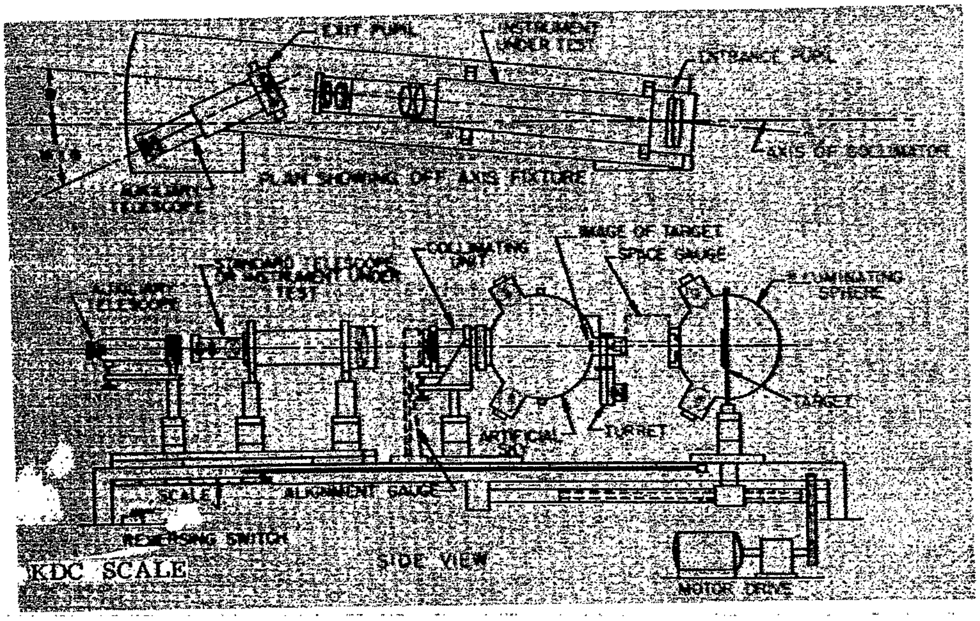

Figure 26.7 (a)- The KDC apparatus schematic.

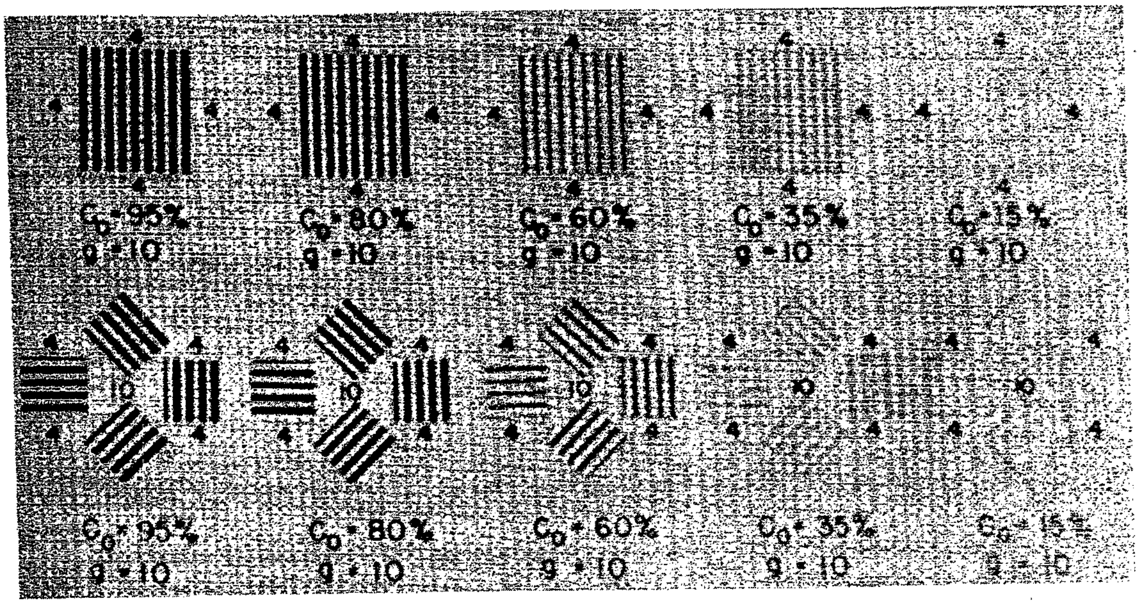

Modified Foucault resolution targets.

$$C_o = \frac{B-b}{B} = \frac{\text{Reflectivity of white band} - \text{Reflectivity of dark band}}{\text{Reflectivity of white band}}$$

C_o = inherent target contrast: g = number of white bands per inch.

Figure 26.7 (b)- The KDC apparatus targets.

Figure 26.7 - The KDC apparatus and target charts.

$$\text{K.D.C. efficiency} = \frac{Xi}{MiXe} \times 100 \qquad (3)$$

where

Xi = K. D. C. scale reading with the instrument under test (and of course the eye)
Xe = K. D. C. scale reading with the eye alone
Mi = the magnification of the instrument under test.

If it is desired to compare a production instrument with the standard telescope, the K. D. C. reading taken with the standard telescope replaces Xe in the above equation.

26.1.4.6 There are many other uses of the K. D. C. apparatus but certainly its versatility and ease of manipulation recommend it when a large amount of work of this type must be done.

26.2 GENERAL DISCUSSION OF SINE WAVE TESTING

26.2.1 Introduction.

26.2.1.1 At about the time the controversy as to just what type of resolution target should be used was reaching its zenith, a paper given by Schade (12), an electrical engineer, brought to bear on the problem of optical system evaluation, the full resources of a completely different field viz., communication theory. While others such as Selwyn (13) and Duffieux (14) had preceded Schade in their investigations into this general area, there is little doubt in most minds that Schade (15) was responsible for focusing the attention of the optical world on the optical possibilities of this method.

26.2.1.2 It will be of interest to look briefly at Schade's original problem. Schade was studying the problem of optimizing the response of a television system starting with the optical pick-up in the studio through the electronic and electromagnetic systems to the final presentation on a kinescope in the home. His background here as an electrical engineer had taught him that one may study the response of an ordinary amplifier two ways (a) by feeding a single transient pulse to the amplifier and noting its response or (b) using sine waves of different frequencies and noting the phase shift and/or amplitude change as the sine wave signal passed through the amplifier. Fourier analysis shows that all the information contained in (b) is actually implicit in (a) but the transient is harder to use experimentally.

26.2.1.3 With the knowledge that this testing technique was a proven method, Schade in effect asked "why can't I do the same sort of thing for the optical part of the system? If I can do this, then I should be able to use the theories already developed for optimizing cascaded amplifiers." The question then arose as to what there was about an optical system that corresponded to the electrical sine waves. After the idea was conceived that the variation in intensity with angle as seen by the lens did indeed constitute a frequency, albeit a "spatial Fourier frequency" and not the frequency associated with $v = f\lambda$, the way was clear. There did remain then (and still does now) much theoretical work to do but at least the direction was indicated. The problem of translating the Fourier spatial frequencies into the temporal frequencies used in electronic amplifiers was easily solved by scanning techniques already under study in the sister field of flying spot scanner television.

26.2.2 Basic theory.

26.2.2.1 Inasmuch as this manual is not intended to develop all the pertinent theory but rather to acquaint the reader with possible methods, most of the details of the mathematical treatment will be omitted. The reader, however is invited to study closely the many excellent articles in this field. Some of these are in the following

(12) Schade, A New System of Measuring and Specifying Image Definition: Symposium on Optical Image Evaluation, NBS, Oct., 1951. Proceedings published in NBS circuler 526, (1954).

(13) Selwyn, Theoretical Estimation of Combined Effects of Film and Lens on Resolution; RAE Report N. H. 698, April, (1940).

(14) Duffieux, L'intégrale de Fourier et ses Applications à L'optique, Besançon, Faculté des Sciences, (1946).

(15) Schade, Electro-Optical Characteristics of Television Systems, RCA Rev., 9:5-37, 245-286, 490-530, 653-686; (1948).

references: (16) through (23)

26.2.2.2 As indicated above and by Schade and Duffieux, an optical system may be considered as a two dimensional electrical filter. Further in electrical work we normally think in terms of amplitudes and at least in normal circuit work do indeed measure our signals by determining their amplitude. In optics, however, we cannot measure amplitude directly but instead measure intensity. A negative amplitude has no physical significance (although it can be interpreted as indicative of a 180° phase shift) for optics while it is a common and significant occurrence in electronics. As an aside we might note, however, that in the detection of electromagnetic radiation we can measure only power directly. The spatial frequencies to which we are referring are thus variations of intensity. This is an important point.

26.2.2.3 Let us assume that the coordinates in an object plane are denoted by ξ and η and in the image plane by x and y. The intensities in the object and image plane are then indicated by $O(\xi, \eta)$ and $i(x, y)$ respectively. We should note here that the terminology is not yet standardized and we are here following that of O'Neill (loc. cit. 16, p E-3). An object point $O(\xi, \eta)$ is then spread out into an image point $i(x, y)$, this "spread function" being denoted by $i(x, y)$. If we now apply this spread function to each point in the object, we can predict the appearance of the image by convolving the spread function with the object distribution according to equation (3).

$$i(x, y) = \int_{-\infty}^{+\infty}\int S(x-\xi, y-\eta)\, O(\xi, \eta)\, d\xi\, d\eta \qquad (4)$$

Assuming for the moment that this convolution is amenable to the techniques of the Fourier transform, we can do the same thing as (4) in the spatial frequency domain by utilizing equation (5).

$$i(\omega_x, \omega_y) = \tau(\omega_x, \omega_y)\, O(\omega_x, \omega_y) \qquad (5)$$

where $i(\omega_x, \omega_y)$ and $O(\omega_x, \omega_y)$ are the image and object expressed in terms of Fourier spatial frequencies and $\tau(\omega_x, \omega_y)$ is the so called "transfer function" of the system (for details see loc. cit. (16) p 232, et seq.)

26.2.2.4 Note clearly what has happened. We have replaced the convolution integral which is difficult to compute, by a product. The two equations of course say basically the same thing and their interrelationship is clearly seen by the more complete definition of the transfer function (loc. cit. (17), p26).

$$\tau(\omega_x, \omega_y) = \frac{1}{2\pi} \int_{-\infty}^{+\infty}\int S(x, y)\, e^{i(\omega_x x + \omega_y y)}\, dx\, dy \qquad (6)$$

Clearly we must be able to calculate, or otherwise determine, the spread function in (4) before the $i(\omega\ ,\ \omega\ )$ may be calculated theoretically. This is a sizeable task. It turns out, however, to be relatively simple to do it experimentally and this is effectively where the art stands at present. The technique, based on experimental determinations of $\tau(\omega_x, \omega_y)$ has lead to a new, although still controversial, method of evaluation of optical systems. Synthesis by use of this principle as a design method is still in its infancy.

26.2.2.5 Let us back off again and look at why equation (5) is so important an evaluation tool. The reason rests in part on the fact that the object and image are related in the spatial frequency domain by a multiplicative factor while in the spatial domain they are related by a complex summation. If we have two systems

(16) Proceedings of Symposium on Communication Theory and Antenna Design AFCRC - TR-57-105 (ASTIA Document No. AD117067). While this symposium was aimed primarily at antenna designers, the organization of it was such that not only is the optics covered rather well by O'Neil and Parrent but also the basic mathematics and physical requirements are outlined in detail. One should note particularly the bibliography prepared by Parrent on Page M-1.

(17) O'Neil, Selected Topics in Optics and Communication Theory Itek Corp. (1958) Note - This publication has an exceptionally complete bibliography of work in this field.

(18) O'Neil, Publications of the Theoretical Optics Section, Itek Corp. (1958)

(19) Marechal, The Contrast of Optical Images and the Influence of Optical Aberrations, NBS Circular No. 526, p9, (1954)

(20) Elias, Optics and Communications Theory, JOSA, 43, 229, (1953)

(21) Hopkins, H. H., The Frequency Response of a Defocussed Optics System, Proc. Ray Soc (London), 321A, 91, (1955)

(22) Blanc-Lapierre, Upon Some Analogues Between Optics and Information Theory, Symposium on Microwave Optics, McGill University, (1953) - Proceedings published by Antenna Section Air Force Cambridge Research Center.

(23) Parrent and Drane, The Effect of Defocussing and Third Order Spherical Aberration on the Transfer Function of a Two Dimensional Optical System, Optica Acta, 3: (1956)

one of which clearly shows a better high frequency response than the other, we can be sure that this system will have the higher resolving power. Further the process of obtaining the sine wave response, or $\tau(\omega_x, \omega_y)$, will give (or usually does) the response at all frequencies and not only at the maximum resolvable condition as with the resolution target system. It is thus, theoretically, possible having $\tau(\omega_x, \omega_y)$ to predict the image for any object by the use of equation (5).

26.2.2.6 As might be expected, nothing is ever quite this rosy. Always there is the needle in the haystack or thorn in the rose. The difficulty here lies in the fact that the transformation from equation (4) to equation (5) presupposes that the optical system is perfectly linear and invariant over the object and image fields. Unfortunately this does not hold very well in poor systems. In good systems Linfoot and Fellgelt (24) have shown, however, that over the normal working field the assumptions are reasonably valid. A rather good discussion of the restrictions involved in making the jump from (4) to (5) has been given by Zucker (25) both for the case at hand, optical systems, and also for the allied problem-antennas. Much as it would be interesting to go into here more of the basic theory, the limitations of space require that we get on to the actual experimental techniques of measuring the transfer function and its applications. The interested reader will find the references given, however, replete with pertinent information. There are several methods of determining $\tau(\omega_x, \omega_y)$ or the equivalent, of which the following are representative only.

26.3 SINE WAVE TESTING WITH SINE WAVE TARGETS

26.3.1 The Schade system.

26.3.1.1 In Schade's original presentation, he demonstrated a system that, stripped to its basic features, was essentially that shown in Figure 26.8 wherein F represents a continuous film with a series of discrete sine wave targets. Each target was made by varying the intensity of the exciter lamp in a sound track camera sinusoidally with time while the film was moving at a constant rate through the camera. Sections of the film are shown in Figure 26.9 (26). P is a projector that allows the test pattern to be seen at any effective distance from the system under test, S. The light from S is focussed (usually with the aid of an auxiliary microscope) onto a scanning aperture, A. This aperture might be of any shape but usually it is most convenient to use a circle. Behind the aperture is a photomultiplier tube, PM, which feeds into a recorder, R.

26.3.1.2 In action then, the film moves through the projector producing a spatial frequency sine wave. The fact that the film is moving means that there will be a sinusoidally varying electrical signal from the photomultiplier tube. The sine wave response is then given simply by the ratio of this ac signal at a spatial frequency, N, to that which the system would give if the frequency were extrapolated to zero. In Schade's terminology $r_{\bar{\psi}} = \bar{\psi}_n/\bar{\psi}_o$ where $r_{\bar{\psi}}$ is the sine wave response. Typical sine wave response factor curves are shown in Figure 26.10. These response curves were taken from research done in this field by Shack (27) when at the National Bureau of Standards. Figure 26.11 from the NBS Report gives the variation of $r_{\bar{\psi}}$ with focal position for a fixed spatial frequency while Figure 26.12 gives the variation of $r_{\bar{\psi}}$ with focal position for a fixed color. Figures 26.13 and 26.14 show the variation of $r_{\bar{\psi}}$ with spatial frequency for different colors. Note the negative amplitude in these figures. It is due to a 180° phase change. Schack's apparatus was much the same as Schade's but Shack used a scanning slit instead of a scanning pinhole.

26.3.2 The Lamberts system.

26.3.2.1 Lamberts (28) and Lamberts, Higgins, and Wolfe (29) have studied the sine wave response particularly in connection with their lens evaluation program at Eastman Kodak. The reader will find Lamberts' article particularly interesting as he not only discribes the basic theory very lucidly but also presents a rather novel variation on the fundamental method.

26.3.2.2 In the Schade method the scanning aperture is very small and usually circular or square. In the Lamberts system the scanning aperture is a long slit. By the use of the slit it is possible to replace a target whose intensity varies sinusoidally by a target with a variable area as shown in Figure 26.15. This type of target has also been used by Lindberg (30). The scanning slit is indicated by SS in Figure 26.16. It can be shown the light distribution in the image is given by,

$$F(x) = b_o + b_1 \, |A*| \, \cos (2\pi\gamma x - \phi) \qquad (7)$$

Where b_o and b_1 have the meaning shown in Figure 26.15, and b_1/b_o is the "normalized amplitude" as discussed in Lamberts' article. γ is of course the spatial frequency and x is the shift of any particular aspect

(24) Linfoot and Fellgelt, On the Assessment of Optical Images, Trans. Roy. Soc. (London) 247, (1955)
(25) Zucker, loc. cit. 5, p L-1
(26) Schade loc. cit. 1, p 233
(27) Shack, Investigations Into the Correlation Between Photographic and Photoelectric Image Evaluation, NBS Report No. 5483
(28) Lamberts, JOSA 48, 490 (1958)
(29) Lamberts, Higgins, and Wolfe, JOSA 48, 487 (1958)
(30) Lindberg, Optica Acta 1, 80 (1954)

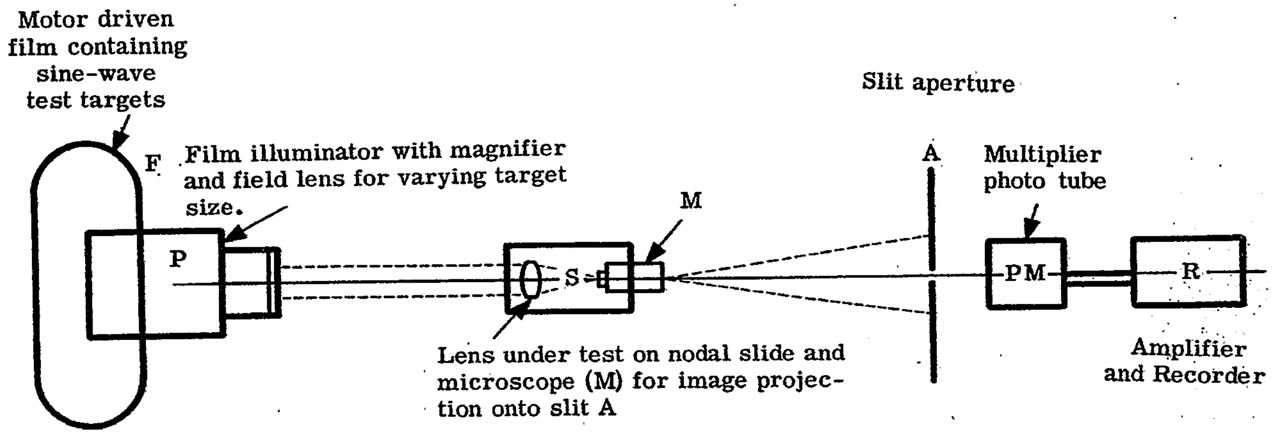

Figure 26.8 - The basic Schade system for determining the sine wave response of an optical system.
(Based on O.H. Schade's, Electro-Optical Characteristics of Television Systems, RCA Review, Vol. 9, 1948)

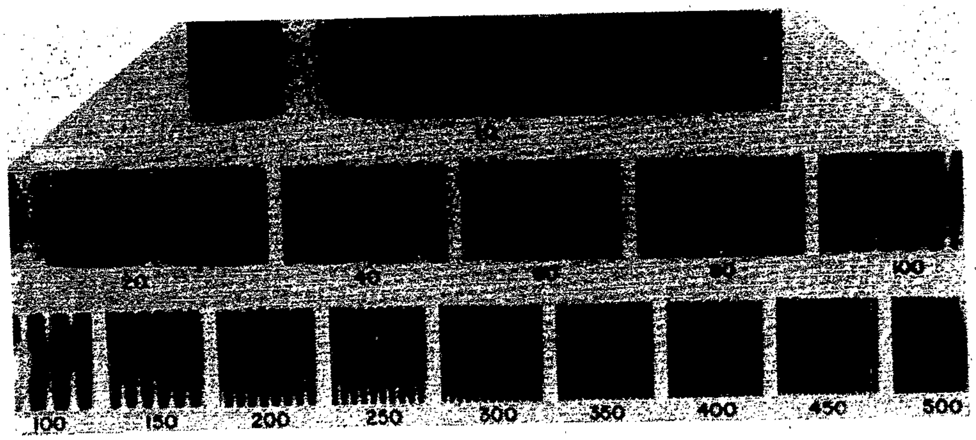

Figure 26.9 - Sine wave test targets.
(Based on O. H. Schade's, Electro-Optical Characteristics of Television Systems, RCA Review, Vol. 9, 1948)

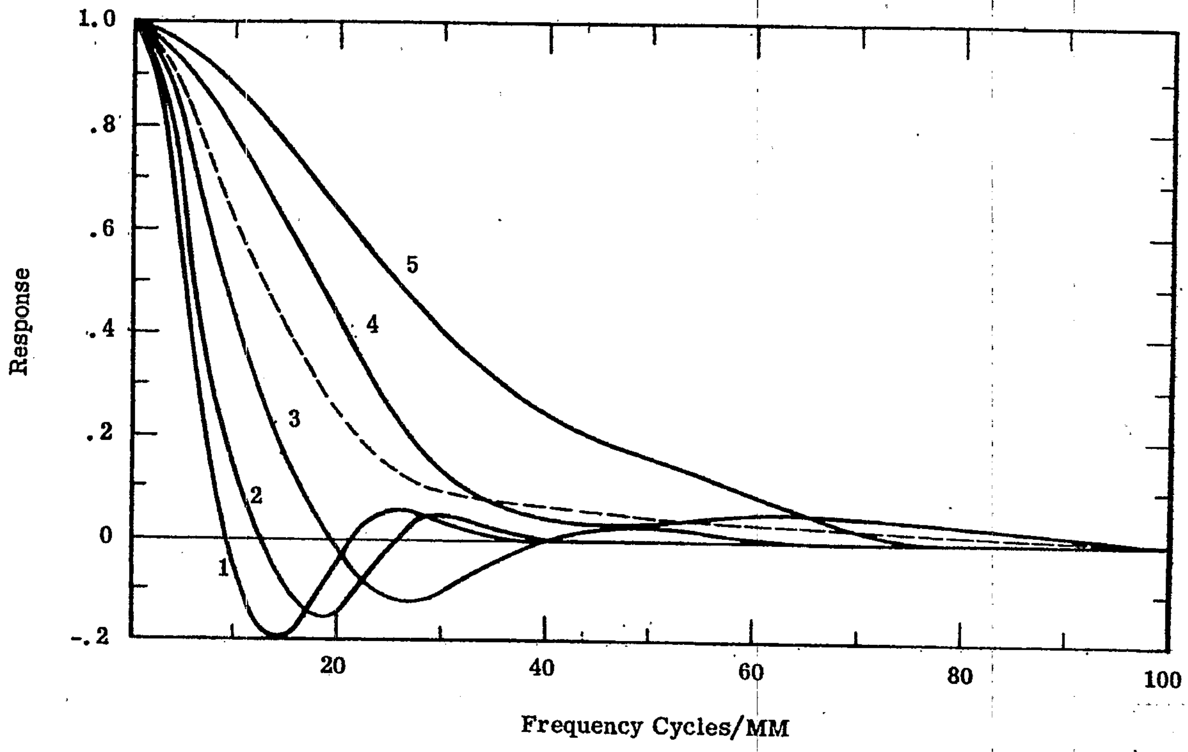

Figure 26.10 - Sine wave response factor vs line number (frequency) of lens A, .4 mm inside focus. In this and in following figures, curves numbered 1, 2, 3, 4 and 5 were obtained with Wratten filters 29, 25, 90, 16 + 60, and 45 respectively. The dashed curve was obtained with no filter. (Extracted from National Bureau of Standards Report No. 5483, Investigations into the Correlation between Photographic and Photoelectric Image Evaluation, R. Shack, under Air Force Contract Number 33(616)56-16)

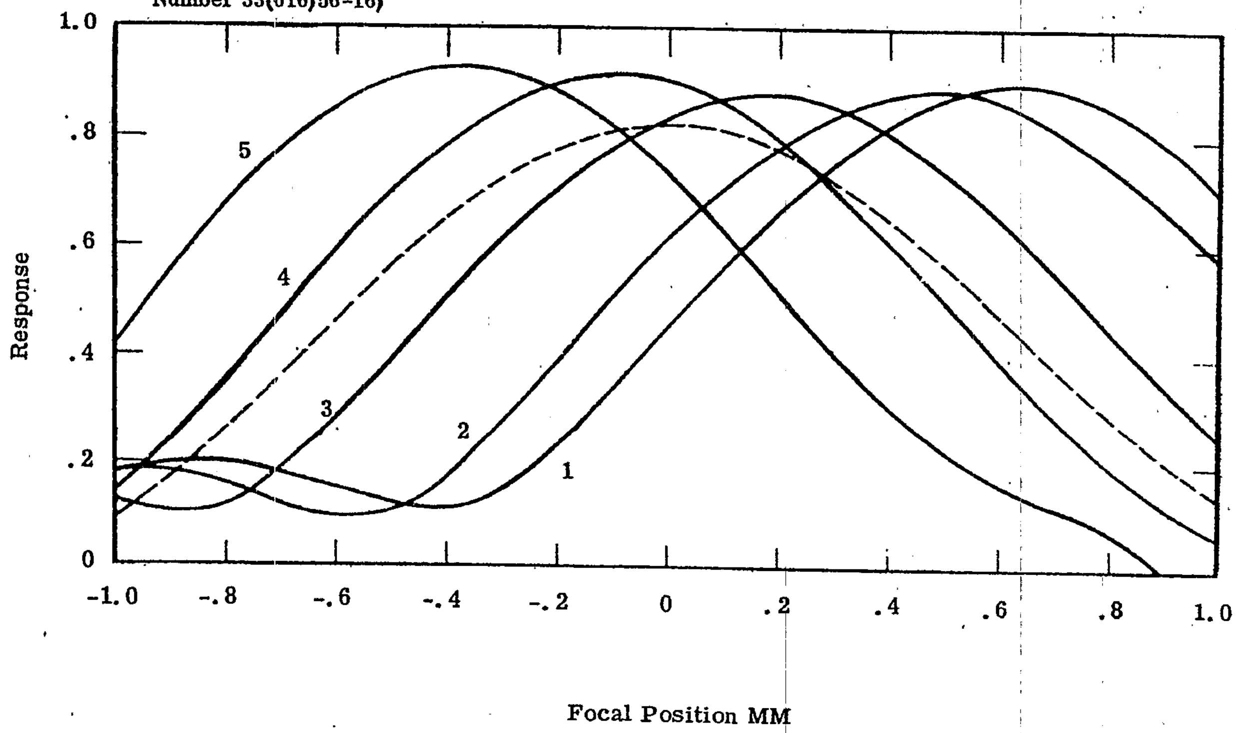

Figure 26.11 - Variation in response with focal position for lens A for different colors at a fixed frequency. The frequency chosen was 8 cycles per mm. (Extracted from National Bureau of Standards Report No. 5483, Investigations into the Correlation between Photographic and Photoelectric Image Evaluation, R. Shack, under Air Force Contract Number 33(616)56-16)

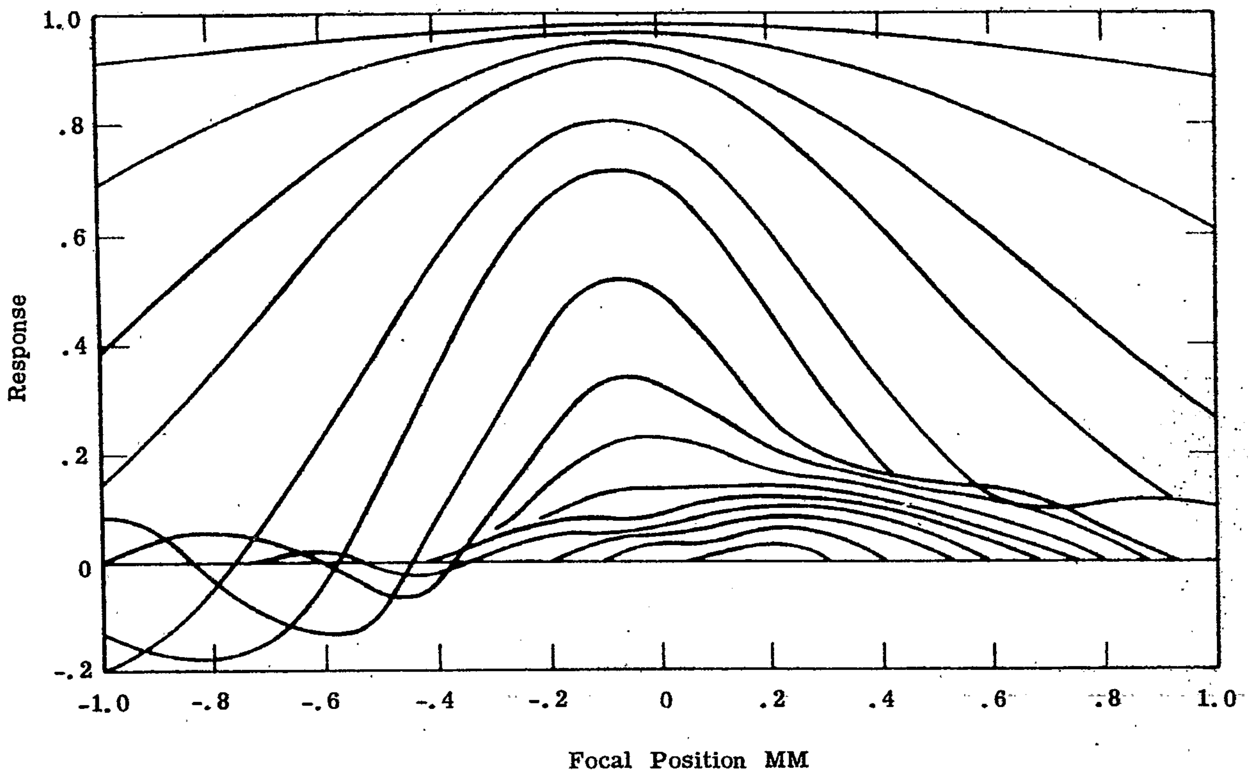

Figure 26.12- Through-focus response curves for lens A with filter 16 + 60.
(Extracted from National Bureau of Standards Report No. 5483, Investigations into the Correlation between Photographic and Photoelectric Image Evaluation, R. Shack, under Air Force Contract Number 33(616)56-16)

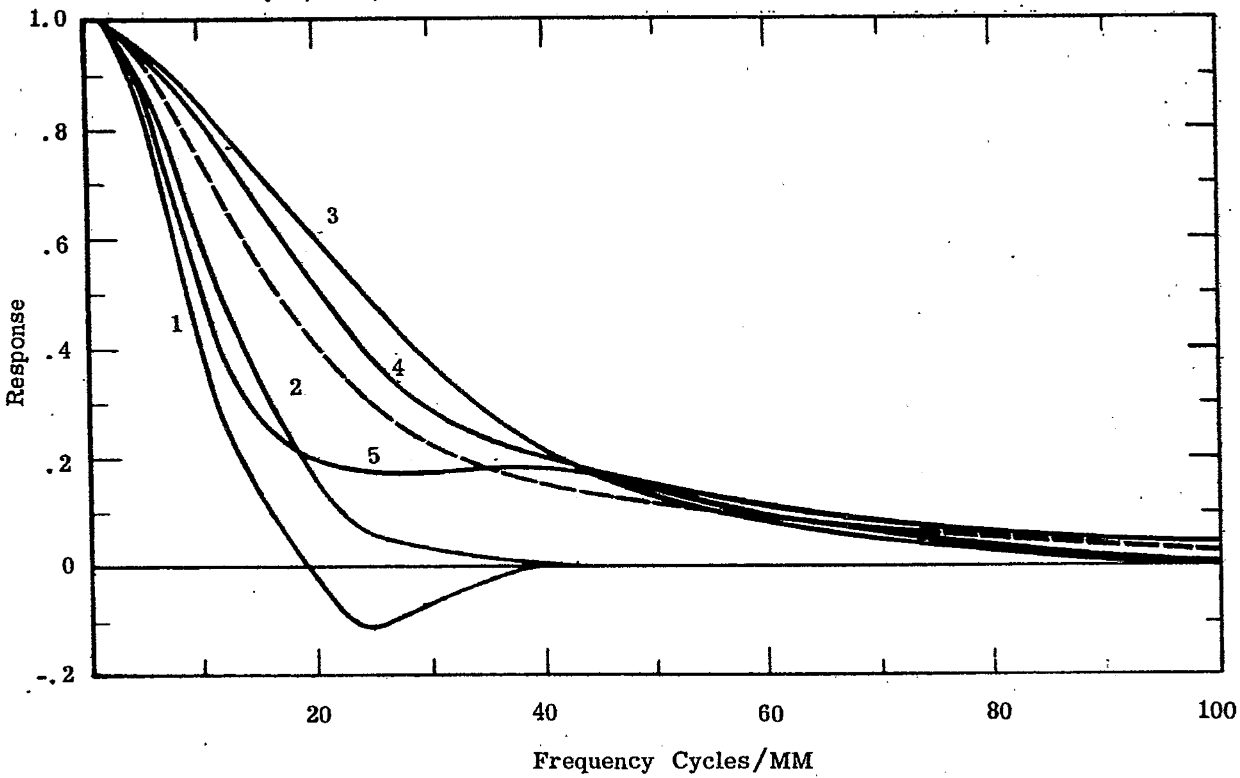

Figure 26.13- Frequency response of lens A at focus for various colors.
(Extracted from National Bureau of Standards Report No. 5483, Investigations into the Correlation between Photographic and Photoelectric Image Evaluation, R. Shack, under Air Force Contract Number 33(616)56-16)

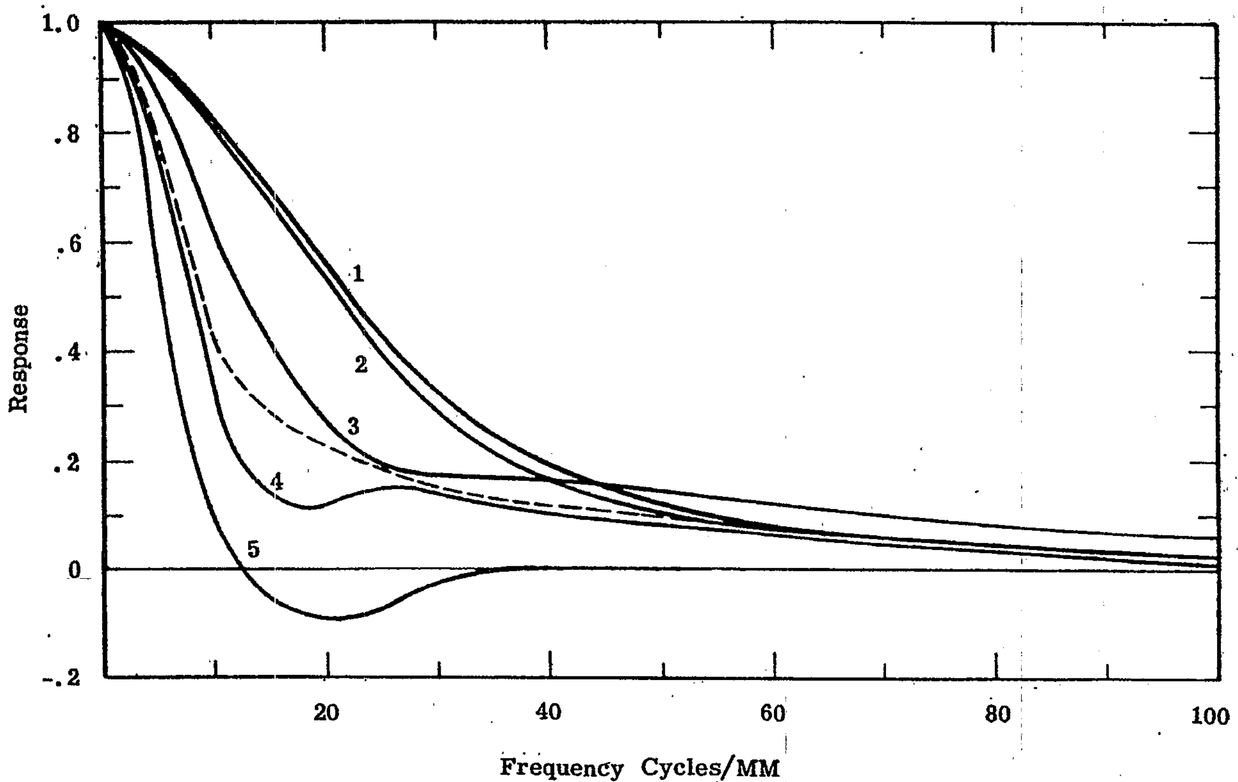

Figure 26.14- Frequency response of lens A .4 mm outside focus for various colors.
(Extracted from National Bureau of Standards Report No. 5483, Investigations into the Correlation between Photographic and Photoelectric Image Evaluation, R. Shack, under Air Force Contract Number 33(616)56-16)

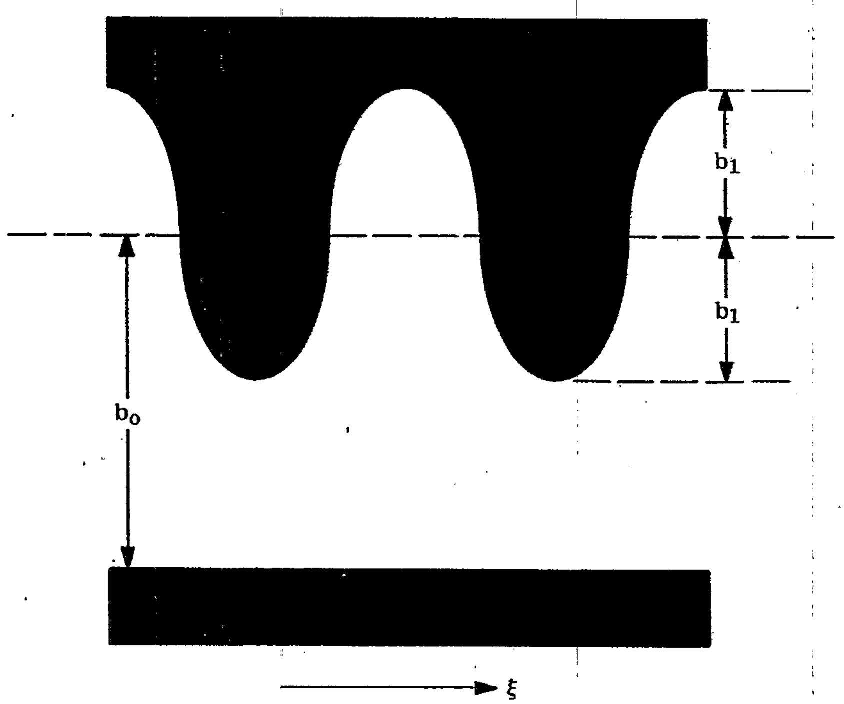

Figure 26.15- The Lambert's test object for measuring sine wave response.
(Extracted from National Bureau of Standards Report No. 5483, Investigations into the Correlation between Photographic and Photoelectric Image Evaluation, R. Shack, under Air Force Contract Number 33(616)56-16)

of the target. ϕ is the spatial phase angle between object and image and is something not covered specifically in Schade's original work. A* is the sine wave response previously defined. The lens bench used in the experiments set up to confirm the theory is shown schematically in Figure 26.16. TO is the test object, which for this work was either a slit (used to determine the spread function) or the target shown in Figure 26.9. L is the lens under test, with SS being the scanning slit, and P the photomultiplier and recorder ensemble. T is a tangent bar arranged to tilt the object and lens, L, when studying off-axis response.

26.3.2.3 The action of the system is similar to that of the basic method, and the reader may refer to the original article for further details. The reader should pay particular attention to the excellent discussion of the significance of the spatial phase angle, and the symmetric and asymmetric spread functions. Attention is also called to the discussion of the derivation of the spread function from the sine wave response. This is important when one remembers that in the introduction to this section the spread function was defined first, with the sine wave response introduced subsequently as a dependent variable. The fact that the one may be calculated from an experimental determination of the other bears out the statement made earlier about their relationship.

26.3.2.4 The significance of phase angle is pointed up in discussions of objects that represent coherent, incoherent, or partially coherent sources. Even with the simple systems checked by Lamberts the phase angle was a strong function of spatial frequency. Figure 26.17 shows both the normalized amplitude in percent (directly relatable to sine wave response via equation 7) and the phase angle as a function of spatial frequency in lines/mm for a certain lens.

26.3.2.5 Stephens (31) has recently indicated an interesting way of determining experimentally not only the cosine of the phase angle but also the sine of the phase angle. The advantage is that of increased precision for angles up to 45°.

26.3.3 The recording electronic lens bench of Herriott.

26.3.3.1 The recording lens bench we are about to describe is a long way from the first exploratory efforts in this field. Actually this lens bench is similar in purpose to the K.D.C. apparatus in that each was designed not so much to do research work as to check out large number of lenses routinely by their respective techniques. The target for this apparatus was first made by W. Herriott (32) and is shown in Figure 26.18. Note carefully that the spatial frequency varies continuously on the actual target with samples taken discontinuously along the length of the film to show the variation in the spatial frequency. The scanning slit is oriented vertically with respect this page. The target is on a 36 in. strip of 35mm film with 50 parallel opague tracks on 0.010 in. centers. The slit is a few microns wide and long enough to span most of the width of the 50 tracks.

26.3.3.2 In use the target film is wound around a drum inside of which is the light source and appropriate motors and clutches. Attention is called to the fact that the target does not directly present a sinusoidal variation of intensity to the optical system under test. The scanning slit, however, integrates the image over its length and the result is effectively the same as with the Schade system. The complete schematic layout of the system is shown in Figure 26.19.

26.3.3.3 In this method the sine wave response is measured by the contrast rendition which is defined as $\frac{\text{"image max - image min"}}{\text{object max - object min}}$. Defined in this way, the result is independent of the contrast in the object, a point about which there was much discussion in connection with resolving power targets. The contrast rendition is plotted automatically as a function of spatial frequency. A typical recording showing the result of a through focus test is shown in Figure 26.20. (33)

26.4 SINE WAVE TESTING WITH SQUARE WAVE TARGETS

26.4.1 General discussion.

26.4.1.1 One of the problems involved in sine wave testing is the actual production of the sine wave targets themselves. This has proved to be a major problem, particularly so as the demands of the theorists got tighter and tighter. One method has already been outlined above Other techniques have been developed (34 - 36) but the fact remains that it is still easier to make a square wave target than a sine wave target. The question has naturally arisen "can we not utilize the known Fourier sine wave content of a square wave to produce the equivalent of a pure multiple frequency sine wave target?" The answer is "yes" with some restrictions. If

(31) Stephens, Computation of Achromatic Objectives, NBS, (1954).
(32) Herriott, W., JOSA 37, 472 (1947)
(33) Herriott, D., JOSA 48, 968 (1958)
(34) Kapany and Pike, JOSA, 46, 867 (1956)
(35) Kapany, Eyer, and Shannon, JOSA 47, 103 (1957)
(36) Kelly, Lynch, and Ross, JOSA 48, 858, (1958)

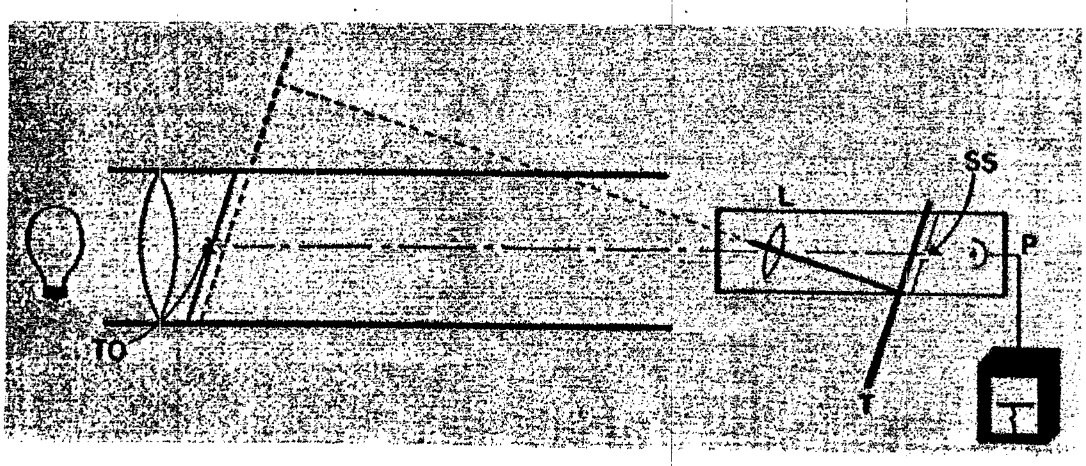

Figure 26.16 - Lambert's lens bench for determining sine wave response factors.

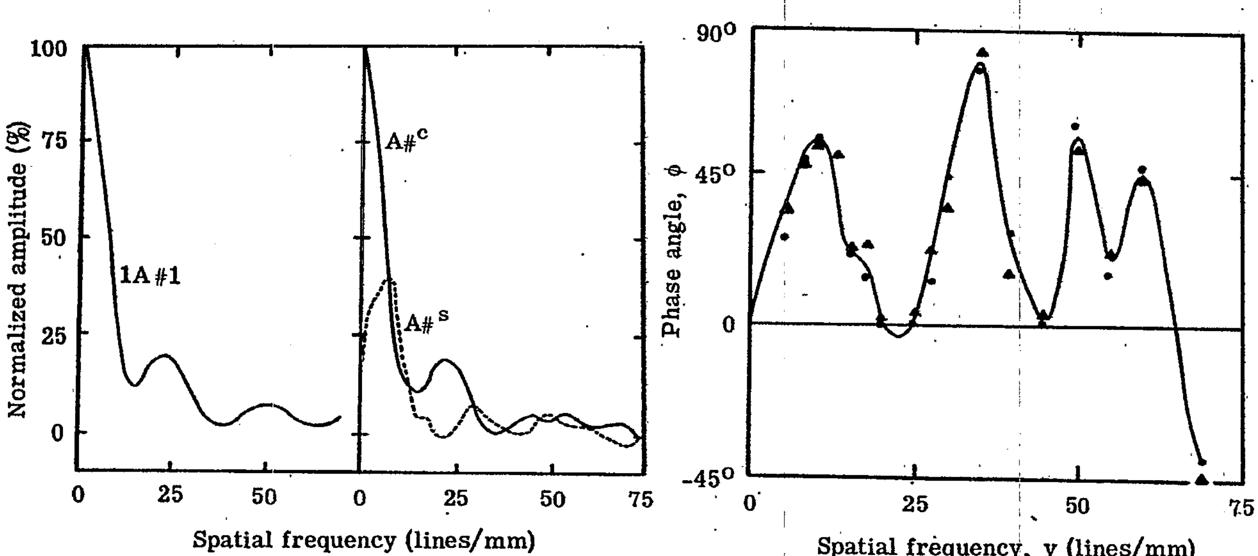

(a) Sine-wave response |A#| (left) and Fourier transfoms of it $A\#^c$ and $A\#^s$ (right) for a certain lens. A single sinusoidal test object was used to obtain |A#| and a double test object for $A\#^c$; $A\#^s$ was computed from the other two.

(b) Phase angle as a function of frequency for the lens of fig. (a). The curve represents the mean of the two determinations ● and ▲.

Figure 26.17 - Normalized amplitude and phase angle as a function of spatial frequency.
(From Jour. Optical Soc. America, Lamberts 89, 1958)

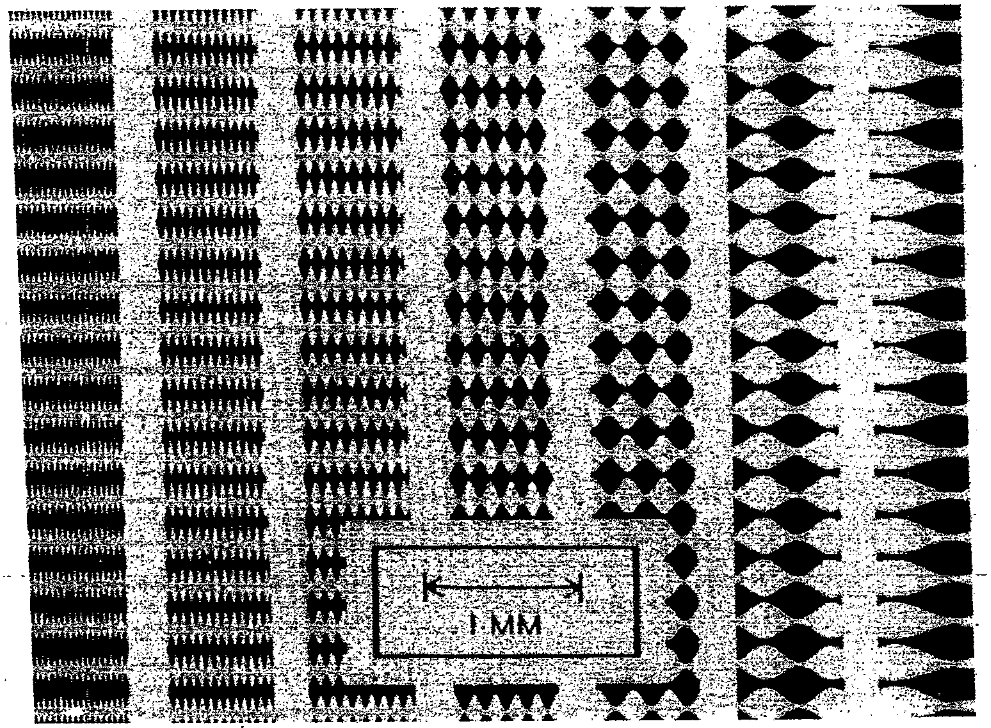

Enlarged photographs at intervals along a sinusoidal target on which the frequency change is continuous.

Figure 26.18 - The Herriott continuous spatial frequency target for determining sine wave response. (From Jour. Optical Soc. America, W. Herriott 37; 472, 1947)

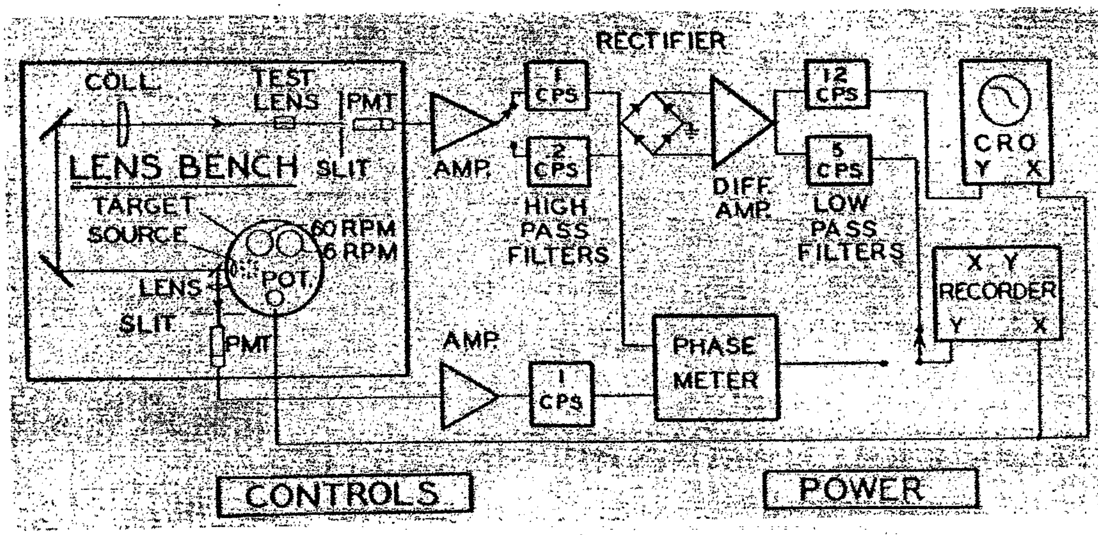

Figure 26.19 - Schematic diagram of the electronic system of the Herriott recording electronic lens bench. (From Jour. Optical Soc. America, W. Herriott 37; 472, 1947)

we suppose the optical system to accurately image a spatial frequency square wave such as a series of alternate dark and bright bars equally spaced, then the image may be represented as a spatial frequency series as,

$$F(x) = B_1 + \Delta B_1 \frac{4}{\pi} \left[\cos (2\pi n \frac{x}{\delta}) - \frac{1}{3} \cos 3(2\pi n \frac{x}{\delta}) + \frac{1}{5} \cos 5(2\pi n \frac{x}{\delta}) \ldots \right] \quad (8)$$

Where x is the lateral coordinate and is defined as the width of a rectangle with the same area and height as the aperture flux distribution as shown in Figure 26.21 taken from Coltman (37). The square wave response factor is defined then as

$$r(n) = \frac{\Delta B_2/\Delta B_1}{B_2/B_1} \quad (9)$$

and the sine wave response factor is defined as

$$R(n) = \frac{\Delta B_2/\Delta B_1}{B_2/B_1} \quad (10)$$

26.4.1.2 It should be noted that there is a variation in the definition of response factors from author to author. This is clear if the reader will go back and check the definition of similar terms by Schade and D. Herriott. The end result in each case is essentially the same and one definition can be converted into another with no basic change in principle.

26.4.1.3 Coltman (38) shows that r(n) may be expressed in terms of the sine wave responses R(n) as given in equation (11).

$$r(n) = \frac{4}{\pi} \left[R(n) - \frac{R(3n)}{3} + \frac{R(5n)}{5} - \frac{R(7n)}{7} \ldots\ldots \right] \quad (11)$$

solving for R(n) by successively subtracting series for $\frac{r(Kn)}{K}$ we can get,

$$R(n) = \frac{\pi}{4} \left[r(n) + \frac{r(3n)}{3} - \frac{r(5n)}{5} + \frac{r(7n)}{7} \ldots\ldots \right] \quad (12)$$

The reader should see Coltman for the details. Suffice it to say that we have now expressed the sine wave response at a spatial frequency of n, the number of cycles in some unit distance. There are basically two ways of determining R(n). These will now be discussed.

26.4.2 The Coltman variable frequency square wave method.

26.4.2.1 The Coltman technique is similar in principle to the corresponding technique used in testing electrical amplifiers (39) with variable frequency square waves. Others such as Rosberry have also studied the method. It is usually found to be more trouble than it is worth to test electrical amplifiers this way, since if you have to vary the frequency of square wave, you might just as well vary the frequency of a sine wave and be done with it. In the optical case it is easier to vary the frequency of the square wave because spatial square waves can be made more easily than can spatial sine waves.

26.4.2.2 Coltman's method is similar, then, in principle to that discussed in Schade and Herriott's paper except for an analysis (40) that allows him to measure the sine wave response of the system by use of the more easily manufactured square waves. Not only is Coltman's article highly informative but it also gives an excellent discussion of the basis of the method and a specific example in the field of X-ray fluoroscopic work. Here the relative ease of studying systems in cascade by the sine wave method is shown and a discussion as to why sine wave targets are not used is given.

26.4.3 The fixed frequency square wave method.

26.4.3.1 Suppose that instead of variable spatial frequency square wave, we used a fixed spatial fequency square wave and get the higher frequency components by wave analysis of the electrical output of the photomultiplier tube. We now assume that the combination of scanning pinhole and associated photomultiplier circuit that transduces the spatial frequency to a temporal frequency spectrum in the image can be directly

(37) Coltman, JOSA 44, 468, (1954)
(38) ibid.
(39) Rosberry, A Correlation Investigation Between Photoelectric and Image Analysis, NBS Report No. 5799
(40) Loc. cit.,

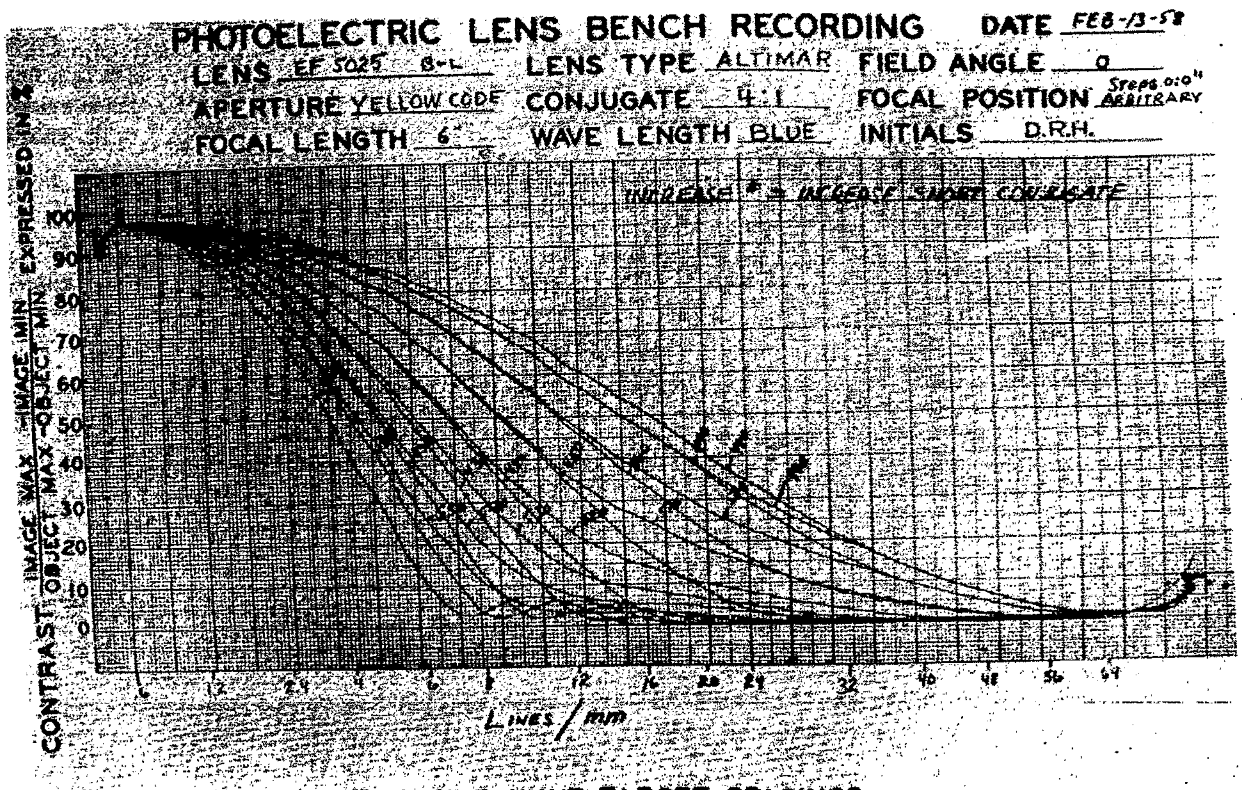

Curves of contrast rendition measured through focus and recorded directly on preprinted paper.

Figure 26.20- Sample contrast rendition vs spatial frequency recording taken with the Herriott system.
(From Jour. Optical Soc. America, D. Herriott 48; 968, 1958)

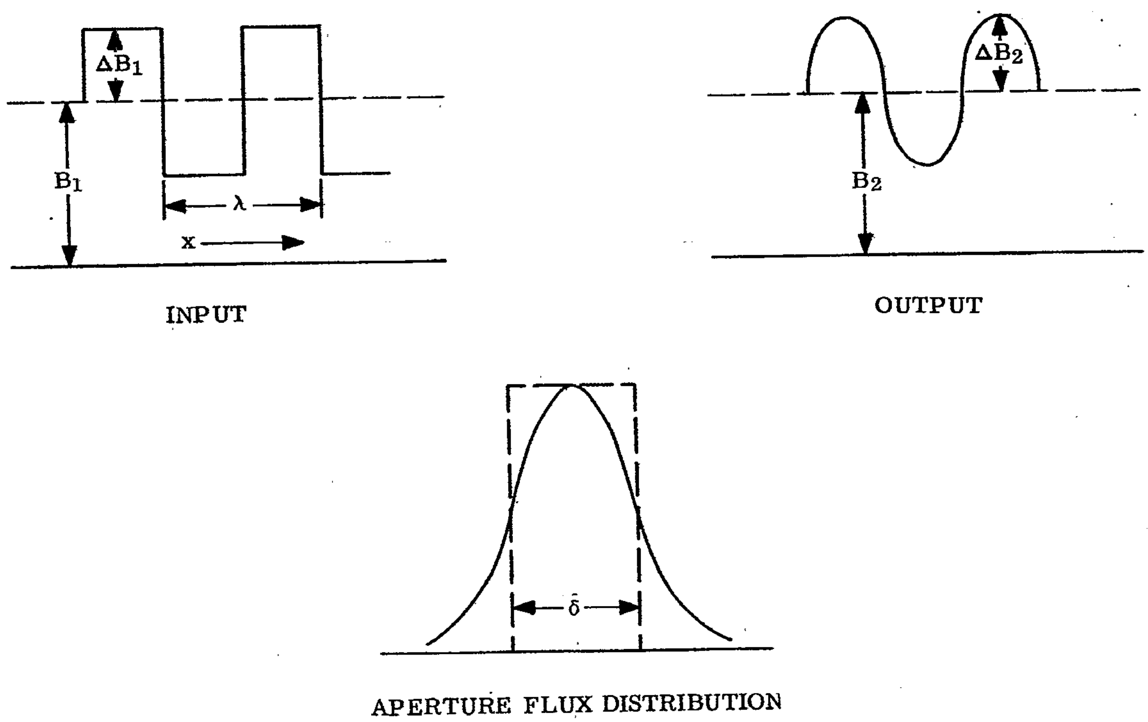

Figure 26.21- Quantities used in the Coltman definition of response factors.
(From Jour. Optical Soc. America, Coltman 44; 468, 1958)

related to the spatial frequency. Furthermore electrical tunable narrow band temporal frequency filters are standard items and have been for years. Therefore by feeding the output of the transducing element to a temporal frequency filter tuned to the fundamental of the square wave we can determine the sine wave response at that frequency. We then retune the filter to the next harmonic, record the output, etc. Account must be taken of the reduction in amplitude of the harmonics as given by the coefficients in equation (8).

26.4.3.2 It might occur to those versed in Fourier analysis that some other wave shape might be chosen such as a triangular wave that has all harmonics and not just the odd harmonics as in the case of the square wave. Such a wave could be used, but again the problem of production is such that it probably would be undesirable. Actually a single square wave target can suffice to cover almost any desired spatial frequency band - provided it is used with a minifying or magnifying system whose quality is far superior to that of the system being tested.

26.4.3.3 The difficulty involved with this method of square wave testing is that there is a phase shift associated with the tunable electrical filter. While there are ways to take this into account, they are rather complicated. Furthermore, it was assumed above that the percentage reduction of the amplitude as a function of frequency in the ideal image was known. This is true providing the detecting system is completely linear. For some systems, notably photographic ones, this may well not be so. Hence while we can get the sine wave response at any frequency, it may be difficult to relate it numerically to the response at other frequencies.

26.4.4 Automatic determination of power of an opthalmic lens by sine wave response.

26.4.4.1 In 1953 Gunter and Panetta (41) developed a method of applying the sine wave response criteria to the problem of automatically maintaining large aerial cameras in focus. The aerial camera aspects of the technique are of not so much interest to us here as is Gunter's definition of best focus used in connection with their analysis of the problem viz, "best focus is that point in image space where the spatial frequency response is an optimum within the bandwidth of information in which the observer is most interested." This definition is certainly a far cry from that usually found in optics and photography. It stems from the work of Schade rather than from that of the traditional treatments of Conrady etc.

26.4.4.2 Shortly thereafter Gunter (42), (43), (44) applied these same principles and this same definition of focus to the automatic determination of the power of opthalmic lenses. This was a research problem to see if the human factor could be removed in the routine inspection of opthalmic lenses. The women who customarily do this work are wont to get tired and their judgment varies. The first target was a square wave made by rotating a square cut gear as shown in Figure 26.22.

26.4.4.3 In the initial study the combination of SS and PM was moved along a lathe bed until the meter showed a maximum, the bandwidth of information having been selected by trial. Specifically this meant that a lens of say 2 diopters as judged by the eye was selected. This lens was placed in the test device and the temporal frequency filter adjusted until the meter output was maximum at a distance of exactly 50 cm. By checking with other standard lenses the variation of focal point as judged by the maximum meter response and the eye were shown to be well within commercial tolerances. A plot of meter response vs. focal position looked essentially the same as Figure 26.12.

26.4.4.4 The technique having been proved, the quest was now how to change the system so that a lens could be snapped into place and have the SS-PM unit automatically move so as to maximize the meter response i.e. move to the position of best focus. Important in the final system was a novel "square wave target" suggested by Hayes. The original square cut gear (seen from above) was modified as shown by the dotted lines in Figure 26.23 the hatched part of the gear remaining. The lens under test sees sequentially now edge a, b, a', b', a", b" etc. This is the equivalent of a square wave tipped at an angle of 45° in so far as L_X is concerned. The light from the source S was focussed midway between a and b so that the edges a and b appeared equally sharp to L_X. The action is simple. Referring to Figure 26.12 we see that near the peak the response curve as a function of focal length is quite symmetrical. An electronic circuit separated the responses from edges a and b and ordered a motor to adjust the position of the SS-PM unit until the responses were equal. The motor then stopped and the power of the lens was read directly from the scale. The system was easily more than sufficiently accurate. Modifications of the system were developed for specific purposes but the basic technique was unchanged.

---

(41) Gunter and Panetta, An Automatic Electronic Focussing Device for Aerial Cameras, Boston University Optical Research Laboratory Technical Note 113, June, 1954

(42) Gunter, Whitney, Hayes. U. S. Patent 2897722, Electronic Lensometer.

(43) Gunter, Whitney, Hayes. U. S. Patent 2803995, Special Frequency Centering Device.

(44) Wing, Whitney, Hayes. U. S. Patent 2792748, Pyramid Centering Device.

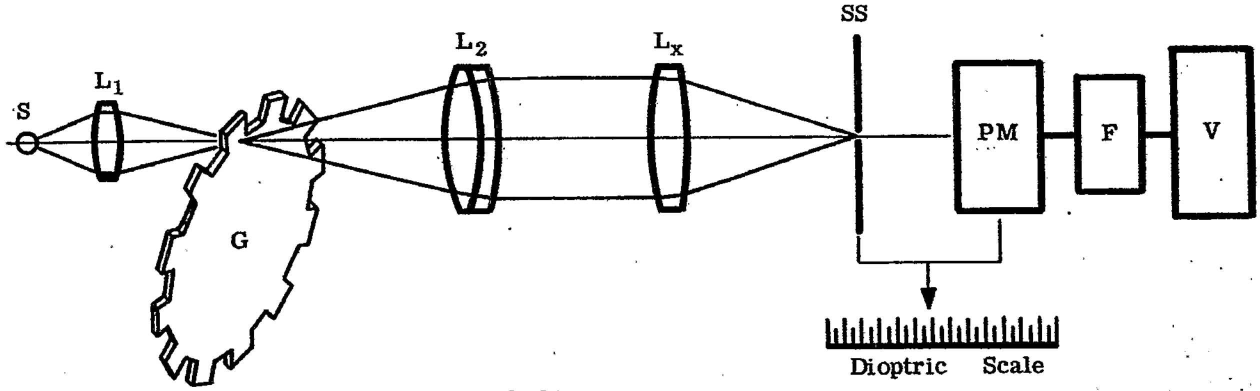

S = source of light

L_1 = lens to focus light from S onto the teeth of G.

G = square cut gear rotated at 1800 rpm.

L_2 = a collimating lens.

L_x = the opthalmic lens under test.

SS = pinhole scanning aperture.

PM = photomultiplier tube and associated circuits

F = a tunable electric filter

V = voltmeter

Figure 26.22 - Basic square wave system for studying Opthalmic lens power.

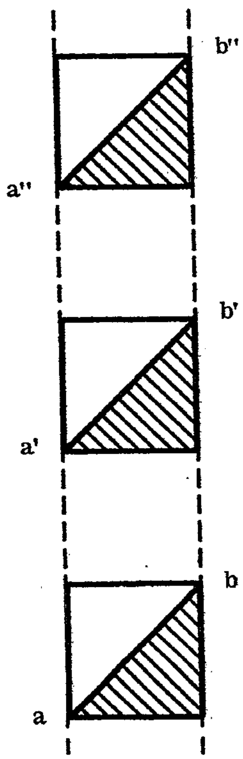

Figure 26.23 - The Hayes target for the American Optical automatic lens power measurement system.

Custodians:
Army - U.S. Army Munitions Command
Navy - Bureau of Ships
Air Force - Middletown Air Materiel Area

Preparing activity:
Army - U.S. Army Munitions Command

Sine	Angle	Interp. Constant	Sine	Angle	Interp. Constant	Sine	Angle	Interp. Constant	Sine	Angle	Interp. Constant
001	.001000	1.000	051	.051021	1.001	101	.101172	1.005	151	.151579	1.012
002	.002000	1.000	052	.052022	1.001	102	.102177	1.006	152	.152591	1.011
003	.003000	1.000	053	.053023	1.002	103	.103183	1.005	153	.153602	1.012
004	.004000	1.000	054	.054025	1.001	104	.104188	1.006	154	.154614	1.013
005	.005000	1.000	055	.055026	1.002	105	.105194	1.005	155	.155627	1.012
006	.006000	1.000	056	.056028	1.001	106	.106199	1.005	156	.156639	1.013
007	.007000	1.000	057	.057029	1.002	107	.107204	1.006	157	.157652	1.012
008	.008000	1.000	058	.058031	1.002	108	.108210	1.006	158	.158664	1.013
009	.009000	1.000	059	.059033	1.002	109	.109216	1.005	159	.159677	1.013
010	.010000	1.000	060	.060035	1.001	110	.110221	1.007	160	.160690	1.013
011	.011000	1.000	061	.061036	1.002	111	.111228	1.006	161	.161703	1.013
012	.012000	1.000	062	.062038	1.002	112	.112234	1.007	162	.162716	1.013
013	.013000	1.000	063	.063040	1.002	113	.113241	1.006	163	.163729	1.014
014	.014000	1.000	064	.064042	1.003	114	.114247	1.007	164	.164743	1.014
015	.015000	1.000	065	.065045	1.002	115	.115254	1.006	165	.165757	1.014
016	.016000	1.000	066	.066047	1.002	116	.116260	1.007	166	.166771	1.014
017	.017000	1.000	067	.067049	1.003	117	.117267	1.007	167	.167785	1.014
018	.018000	1.000	068	.068052	1.002	118	.118274	1.007	168	.168799	1.015
019	.019000	1.000	069	.069054	1.003	119	.119281	1.008	169	.169814	1.015
020	.020000	1.001	070	.070057	1.002	120	.120289	1.007	170	.170829	1.014
021	.021001	1.000	071	.071059	1.003	121	.121296	1.009	171	.171843	1.016
022	.022001	1.000	072	.072062	1.002	122	.122305	1.007	172	.172859	1.015
023	.023001	1.001	073	.073064	1.003	123	.123312	1.008	173	.173874	1.015
024	.024002	1.000	074	.074067	1.003	124	.124320	1.007	174	.174889	1.016
025	.025002	1.000	075	.075070	1.003	125	.125327	1.008	175	.175905	1.015
026	.026002	1.000	076	.076073	1.003	126	.126335	1.008	176	.176920	1.016
020	.027002	1.001	077	.077076	1.003	127	.127343	1.008	177	.177936	1.016
028	.028003	1.000	078	.078079	1.003	128	.128351	1.008	178	.178952	1.016
029	.029003	1.001	079	.079082	1.003	129	.129359	1.009	179	.179968	1.017
030	.030004	1.000	080	.080085	1.003	130	.130368	1.009	180	.180985	1.016
031	.031004	1.001	081	.081088	1.003	131	.131377	1.009	181	.182001	1.017
032	.032005	1.001	082	.082091	1.004	132	.132386	1.009	182	.183018	1.018
033	.033006	1.000	083	.083095	1.003	133	.133395	1.009	183	.184036	1.017
034	.034006	1.001	084	.084098	1.004	134	.134404	1.009	184	.185053	1.017
035	.035007	1.000	085	.085102	1.004	135	.135413	1.009	185	.186070	1.018
036	.036007	1.001	086	.086106	1.003	136	.136422	1.010	186	.187088	1.018
037	.037008	1.001	087	.087109	1.004	137	.137432	1.010	187	.188106	1.018
038	.038009	1.000	088	.088113	1.004	138	.138442	1.009	188	.189124	1.018
039	.039009	1.001	089	.089117	1.004	139	.139451	1.010	189	.190142	1.019
040	.040010	1.001	090	.090121	1.004	140	.140461	1.010	190	.191161	1.019
041	.041011	1.001	091	.091125	1.004	141	.141471	1.010	191	.192180	1.019
042	.042012	1.001	092	.092129	1.005	142	.142481	1.010	192	.193199	1.019
043	.043013	1.001	093	.093134	1.004	143	.143491	1.011	193	.194218	1.019
044	.044014	1.001	094	.094138	1.004	144	.144502	1.010	194	.195237	1.020
045	.045015	1.001	095	.095142	1.005	145	.145512	1.011	195	.196257	1.019
046	.046016	1.001	096	.096147	1.005	146	.146523	1.011	196	.197276	1.020
047	.047017	1.001	097	.097152	1.005	147	.147534	1.011	197	.198296	1.020
048	.048018	1.001	098	.098157	1.004	148	.148545	1.011	198	.199316	1.021
049	.049019	1.001	099	.099161	1.006	149	.149556	1.012	199	.200337	1.020
050	.050020	1.001	100	.100167	1.005	150	.150568	1.011	200	.201357	1.021

Table 1 - Sine - Angle Conversion Table (Sheet 1 of 5)

Sine	Angle	Interp. Constant	Sine	Angle	Interp. Constant	Sine	Angle	Interp. Constant	Sine	Angle	Interp. Constant
201	.202378	1.021	251	.253717	1.033	301	.305741	1.049	351	.358638	1.068
202	.203399	1.021	252	.254746	1.033	302	.306790	1.049	352	.359706	1.068
203	.204420	1.021	253	.255779	1.035	303	.307839	1.049	353	.360774	1.069
204	.205441	1.022	254	.256814	1.034	304	.308888	1.050	354	.361843	1.070
205	.206463	1.022	255	.257848	1.034	305	.309938	1.050	355	.362913	1.070
206	.207485	1.022	256	.258882	1.035	306	.310988	1.051	356	.363983	1.070
207	.208507	1.022	257	.259917	1.034	307	.312039	1.051	357	.365053	1.071
208	.209529	1.022	258	.260951	1.035	308	.313090	1.051	358	.366124	1.072
209	.210551	1.023	259	.261986	1.035	309	.314141	1.052	359	.367196	1.072
210	.211574	1.023	260	.263021	1.036	310	.315193	1.052	360	.368268	1.071
211	.212597	1.023	261	.264057	1.036	311	.316245	1.052	361	.369339	1.073
212	.213620	1.023	262	.265093	1.037	312	.317297	1.053	362	.370412	1.073
213	.214643	1.024	263	.266130	1.036	313	.318350	1.053	363	.371485	1.074
214	.215667	1.024	264	.267166	1.037	314	.319403	1.053	364	.372559	1.074
215	.216691	1.024	265	.268203	1.038	315	.320456	1.054	365	.373633	1.074
216	.217715	1.024	266	.269241	1.037	316	.321510	1.054	366	.374707	1.075
217	.218739	1.025	267	.270278	1.038	317	.322564	1.054	367	.375782	1.075
218	.219764	1.024	268	.271316	1.038	318	.323618	1.055	368	.376857	1.076
219	.220788	1.025	269	.272354	1.039	319	.324673	1.056	369	.377933	1.076
220	.221813	1.026	270	.273393	1.038	320	.325729	1.056	370	.379009	1.076
221	.222839	1.025	271	.274431	1.039	321	.326785	1.056	371	.380085	1.077
222	.223864	1.026	272	.275470	1.039	322	.327841	1.056	372	.381162	1.078
223	.224890	1.026	273	.276509	1.040	323	.328897	1.057	373	.382240	1.078
224	.225916	1.026	274	.277549	1.040	324	.329954	1.058	374	.383318	1.078
225	.226942	1.027	275	.278589	1.040	325	.331012	1.057	375	.384396	1.079
226	.227969	1.026	276	.279629	1.041	326	.332069	1.058	376	.385475	1.079
227	.228995	1.027	277	.280670	1.041	327	.333127	1.058	377	.386554	1.081
228	.230022	1.027	278	.281711	1.041	328	.334185	1.059	378	.387635	1.080
229	.231049	1.028	279	.282752	1.041	329	.335244	1.059	379	.388715	1.081
230	.232077	1.027	280	.283793	1.042	330	.336303	1.060	380	.389796	1.082
231	.233104	1.028	281	.284835	1.042	331	.337363	1.060	381	.390878	1.081
232	.234132	1.029	282	.285877	1.043	332	.338423	1.060	382	.391959	1.082
233	.235161	1.028	283	.286920	1.043	333	.339483	1.061	383	.383041	1.083
234	.236189	1.029	284	.287963	1.043	334	.340544	1.061	384	.394124	1.083
235	.237218	1.028	285	.289006	1.043	335	.341605	1.061	385	.395207	1.084
236	.238246	1.030	286	.290049	1.044	336	.342666	1.062	386	.396291	1.084
237	.239276	1.029	287	.291093	1.044	337	.343728	1.063	387	.397375	1.085
238	.240305	1.030	288	.292137	1.044	338	.344791	1.062	388	.398460	1.085
239	.241335	1.030	289	.293181	1.045	339	.345853	1.063	389	.399545	1.086
240	.242365	1.030	290	.294226	1.045	340	.346916	1.064	390	.400631	1.086
241	.243395	1.031	291	.295271	1.045	341	.347980	1.064	391	.401717	1.087
242	.244426	1.031	292	.296316	1.047	342	.349044	1.064	392	.402804	1.087
243	.245457	1.031	293	.297363	1.046	343	.350108	1.065	393	.403891	1.088
244	.246488	1.031	294	.298409	1.046	344	.351173	1.065	394	.404979	1.088
245	.247519	1.032	295	.299455	1.047	345	.352238	1.065	395	.406067	1.088
246	.248551	1.032	296	.300502	1.047	346	.353303	1.067	396	.407155	1.090
247	.249583	1.032	297	.301549	1.048	348	.354370	1.067	397	.408245	1.090
248	.250615	1.032	298	.302597	1.048	348	.355437	1.066	398	.409335	1.090
249	.251647	1.033	299	.303645	1.047	349	.356503	1.067	399	.410425	1.091
250	.252680	1.033	300	.304692	1.049	350	.357570	1.068	400	.411516	1.091

Table 1 - Sine - Angle Conversion Table (Sheet 2 of 5)

Sine	Angle	Interp. Constant	Sine	Angle	Interp. Constant	Sine	Angle	Interp. Constant	Sine	Angle	Interp. Constant
401	.412607	1.092	451	.467885	1.121	501	.524754	1.156	551	.583562	1.199
402	.413699	1.092	452	.469006	1.121	502	.525910	1.156	552	.584761	1.200
403	.414791	1.093	453	.470127	1.122	503	.527066	1.158	553	.585961	1.200
404	.415884	1.094	454	.471249	1.123	504	.528224	1.158	554	.587161	1.202
405	.416978	1.094	455	.472372	1.123	505	.529382	1.159	555	.588363	1.203
406	.418072	1.095	456	.473495	1.124	506	.530541	1.160	556	.589566	1.203
407	.419167	1.095	457	.474619	1.125	507	.531701	1.160	557	.590769	1.205
408	.420262	1.096	458	.475744	1.125	508	.532861	1.162	558	.591974	1.205
409	.421358	1.096	459	.476869	1.126	509	.534023	1.162	559	.593179	1.207
410	.422454	1.096	460	.477995	1.127	510	.535185	1.163	560	.594386	1.207
411	.423550	1.097	461	.479122	1.127	511	.536348	1.163	561	.595593	1.209
412	.424647	1.098	462	.480249	1.128	512	.537511	1.165	562	.596802	1.209
413	.425745	1.099	463	.481377	1.128	513	.538676	1.165	563	.598011	1.211
414	.426844	1.099	464	.482505	1.130	514	.539841	1.167	564	.599222	1.211
415	.427943	1.100	465	.483635	1.130	515	.541008	1.167	565	.600433	1.213
416	.429043	1.099	466	.484765	1.130	516	.542175	1.167	566	.601646	1.213
417	.430142	1.101	467	.485895	1.131	517	.543342	1.169	567	.602859	1.215
418	.431243	1.101	468	.487026	1.132	518	.544511	1.170	568	.604074	1.215
419	.432344	1.101	469	.488158	1.133	519	.545681	1.170	569	.605289	1.217
420	.433445	1.103	470	.489291	1.133	520	.546851	1.171	570	.606506	1.217
421	.434548	1.102	471	.490424	1.134	521	.548022	1.172	571	.607723	1.219
422	.435650	1.103	472	.491558	1.135	522	.549194	1.173	572	.608942	1.220
423	.436753	1.104	473	.492693	1.135	523	.550367	1.173	573	.610162	1.220
424	.437857	1.104	474	.493828	1.136	524	.551540	1.175	574	.611382	1.222
425	.438961	1.105	475	.494964	1.137	525	.552715	1.175	575	.612604	1.223
426	.440066	1.106	476	.496101	1.137	526	.553890	1.177	576	.613827	1.224
427	.441172	1.106	477	.497238	1.138	527	.555067	1.177	577	.615051	1.225
428	.442278	1.107	478	.498376	1.139	528	.556244	1.178	578	.616276	1.226
429	.443385	1.107	479	.499515	1.140	529	.557422	1.179	579	.617502	1.227
430	.444492	1.108	480	.500655	1.140	530	.558601	1.179	580	.618729	1.228
431	.445600	1.109	481	.501795	1.141	531	.559780	1.181	581	.619957	1.229
432	.446709	1.108	482	.502936	1.142	532	.560961	1.181	582	.621186	1.230
433	.447817	1.110	483	.504078	1.142	533	.562142	1.182	583	.622416	1.232
434	.448927	1.111	484	.505220	1.143	534	.563324	1.184	584	.623648	1.232
435	.450038	1.110	485	.506363	1.144	535	.564508	1.184	585	.624880	1.234
436	.451148	1.112	486	.507507	1.145	536	.565692	1.185	586	.626114	1.234
437	.452260	1.112	487	.508652	1.145	537	.566877	1.186	587	.627348	1.236
438	.453372	1.113	488	.509797	1.146	538	.568063	1.186	588	.628584	1.237
439	.454485	1.113	489	.510943	1.147	539	.569249	1.188	589	.629821	1.238
440	.455598	1.113	490	.512090	1.147	540	.570437	1.189	590	.631059	1.239
441	.456711	1.115	491	.513237	1.148	541	.571626	1.189	591	.632298	1.240
442	.457826	1.115	492	.514385	1.149	542	.572815	1.191	592	.633538	1.242
443	.458941	1.116	493	.515534	1.150	543	.574006	1.191	593	.634780	1.242
444	.460057	1.116	494	.516684	1.151	544	.575197	1.192	594	.636022	1.244
445	.461173	1.117	495	.517835	1.151	545	.576389	1.193	595	.637266	1.245
446	.462290	1.113	496	.518986	1.152	546	.577582	1.194	596	.638511	1.245
447	.463408	1.119	497	.520138	1.153	547	.578776	1.195	597	.639756	1.247
448	.464527	1.118	498	.521291	1.153	548	.579971	1.196	598	.641003	1.249
449	.465645	1.120	499	.522444	1.155	549	.581167	1.197	599	.642252	1.249
450	.466765	1.120	500	.523599	1.155	550	.582364	1.198	600	.643501	1.251

Table 1 - Sine - Angle Conversion Table (Sheet 3 of 5)

Sine	Angle	Interp. Constant	Sine	Angle	Interp. Constant	Sine	Angle	Interp. Constant	Sine	Angle	Interp. Constant
601	.644752	1.251	651	.708901	1.318	701	.776799	1.403	751	.849575	1.516
602	.646003	1.253	652	.710219	1.320	702	.778202	1.405	752	.851091	1.518
603	.647256	1.255	653	.711539	1.321	703	.779607	1.407	753	.852609	1.521
604	.648511	1.256	654	.712860	1.323	704	.781014	1.409	754	.854130	1.524
605	.649766	1.256	655	.714183	1.324	705	.782423	1.411	755	.855654	1.526
606	.651022	1.258	656	.715507	1.325	706	.783334	1.413	756	.857180	1.529
607	.652280	1.259	657	.716832	1.328	707	.785247	1.415	757	.858709	1.532
608	.653539	1.260	658	.718160	1.329	708	.786662	1.417	758	.860241	1.535
609	.654799	1.262	659	.719489	1.330	709	.788079	1.419	759	.861776	1.537
610	.656061	1.262	660	.720819	1.332	710	.789498	1.421	760	.863313	1.540
611	.657323	1.264	661	.722151	1.333	711	.790919	1.423	761	.864853	1.543
612	.658587	1.265	662	.723484	1.335	712	.792342	1.426	762	.866396	1.546
613	.659852	1.266	663	.724819	1.337	713	.793768	1.427	763	.867942	1.548
614	.661118	1.268	664	.726156	1.338	714	.795195	1.429	764	.869490	1.551
615	.662386	1.269	665	.727494	1.340	715	.796624	1.432	765	.871041	1.555
616	.663655	1.270	666	.728834	1.341	716	.798056	1.433	766	.872596	1.557
617	.664925	1.271	667	.730175	1.343	717	.799489	1.436	767	.874153	1.559
618	.666196	1.273	668	.731518	1.345	718	.800925	1.438	768	.875712	1.563
619	.667469	1.274	669	.732863	1.346	719	.802363	1.439	769	.877275	1.566
620	.668743	1.275	670	.734209	1.348	720	.803802	1.442	770	.878841	1.569
621	.670018	1.276	671	.735557	1.349	721	.805244	1.445	771	.880410	1.572
622	.671294	1.278	672	.736906	1.351	722	.806689	1.446	772	.881982	1.574
623	.672572	1.279	673	.738257	1.353	723	.808135	1.449	773	.883556	1.578
624	.673851	1.281	674	.739610	1.355	724	.809584	1.450	774	.885134	1.581
625	.675132	1.281	675	.740965	1.356	725	.811034	1.453	775	.886715	1.584
626	.676413	1.283	676	.742321	1.358	726	.812487	1.456	776	.888299	1.587
627	.677696	1.284	677	.743679	1.359	727	.813943	1.457	777	.889886	1.590
628	.678980	1.286	678	.745038	1.362	728	.815400	1.460	778	.891476	1.593
629	.680266	1.287	679	.746400	1.363	729	.816860	1.462	779	.893069	1.597
630	.681553	1.289	680	.747763	1.364	730	.818322	1.464	780	.894666	1.599
631	.682842	1.289	681	.749127	1.367	731	.819786	1.467	781	.896265	1.603
632	.684131	1.291	682	.750494	1.368	732	.821253	1.469	782	.897868	1.606
633	.685422	1.293	683	.751862	1.370	733	.822722	1.471	783	.899474	1.610
634	.686715	1.293	684	.753232	1.372	734	.824693	1.474	784	.901084	1.612
635	.688008	1.296	685	.754604	1.373	735	.825667	1.476	785	.902696	1.616
636	.689304	1.296	686	.755977	1.376	736	.827143	1.478	786	.904312	1.619
637	.690600	1.298	687	.757353	1.377	737	.828621	1.481	787	.905931	1.623
638	.691898	1.299	688	.758730	1.378	738	.830102	1.483	788	.907554	1.626
639	.693197	1.301	689	.760108	1.381	739	.831585	1.485	789	.909180	1.629
640	.694498	1.302	690	.761489	1.383	740	.833070	1.488	790	.910809	1.633
641	.695800	1.304	691	.762872	1.384	741	.834558	1.491	791	.912442	1.636
642	.697104	1.305	692	.764256	1.386	742	.836049	1.493	792	.914078	1.640
643	.698409	1.306	693	.765642	1.388	743	.837542	1.495	793	.915718	1.643
644	.699715	1.308	694	.767030	1.390	744	.839037	1.498	794	.917361	1.647
645	.701023	1.310	695	.768420	1.392	745	.840535	1.500	795	.919008	1.650
646	.702333	1.310	696	.769812	1.393	746	.842035	1.503	796	.920658	1.654
647	.703643	1.313	697	.771205	1.396	747	.843538	1.505	797	.922312	1.657
648	.704956	1.313	698	.772601	1.397	748	.845043	1.509	798	.923969	1.661
649	.706269	1.315	699	.773998	1.400	749	.846552	1.510	799	.925630	1.665
650	.707584	1.317	700	.775398	1.401	750	.848062	1.513	800	.927295	1.669

Table 1 - Sine - Angle Conversion Table (Sheet,4 of 5)

Sine	Angle	Interp. Constant	Sine	Angle	Interp. Constant	Sine	Angle	Interp. Constant	Sine	Angle	Interp. Constant
801	.928964	1.672	851	1.017887	1.907	901	1.122069	2.311	951	1.256454	3.251
802	.930636	1.676	852	1.019794	1.913	902	1.124380	2.322	952	1.259705	3.284
803	.932312	1.680	853	1.021707	1.919	903	1.126702	2.333	953	1.262989	3.317
804	.933992	1.683	854	1.023626	1.925	904	1.129035	2.345	954	1.266306	3.354
805	.935675	1.688	855	1.025551	1.931	905	1.131380	2.356	955	1.269660	3.390
806	.937363	1.691	856	1.027482	1.938	906	1.133736	2.368	956	1.273050	3.428
807	.939054	1.696	857	1.029420	1.943	907	1.136104	2.381	957	1.276478	3.467
808	.940750	1.699	858	1.031363	1.950	908	1.138485	2.393	958	1.279945	3.508
809	.942449	1.703	859	1.033313	1.957	909	1.140878	2.406	959	1.283453	3.550
810	.944152	1.707	860	1.035270	1.963	910	1.143282	2.419	960	1.287003	3.593
811	.945859	1.712	861	1.037233	1.969	911	1.145703	2.431	961	1.290596	3.639
812	.947571	1.715	862	1.039202	1.976	912	1.148134	2.444	962	1.294235	3.686
813	.949286	1.720	863	1.041178	1.983	913	1.150578	2.458	963	1.297921	3.736
814	.951006	1.723	864	1.043161	1.989	914	1.153036	2.472	964	1.301657	3.787
815	.952729	1.728	865	1.045150	1.997	915	1.155508	2.486	965	1.305444	3.840
816	.954457	1.732	866	1.047147	2.003	916	1.157994	2.500	966	1.309284	3.896
817	.956189	1.736	867	1.049150	2.010	917	1.160494	2.514	967	1.313180	3.955
818	.957925	1.741	868	1.051160	2.018	918	1.163008	2.529	968	1.317135	4.016
819	.959666	1.745	869	1.053178	2.024	919	1.165537	2.544	969	1.321151	4.080
820	.961411	1.749	870	1.055202	2.032	920	1.168081	2.559	970	1.325231	4.148
821	.963160	1.754	871	1.057234	2.039	921	1.168081	2.575	971	1.329379	4.219
822	.964914	1.758	872	1.059273	2.047	922	1.173215	2.591	972	1.333598	4.294
823	.966672	1.763	873	1.061320	2.054	923	1.175806	2.607	973	1.337892	4.373
824	.968435	1.767	874	1.063374	2.062	924	1.178413	2.623	974	1.342265	4.457
825	.970202	1.772	875	1.065436	2.069	925	1.181036	2.640	975	1.346722	4.545
826	.971974	1.776	876	1.067505	2.078	926	1.183676	2.658	976	1.351267	4.640
827	.973750	1.782	877	1.069583	2.085	927	1.186334	2.675	977	1.355907	4.742
828	.975532	1.785	878	1.071668	2.093	928	1.189009	2.693	978	1.360649	4.849
829	.977317	1.791	879	1.073761	2.101	929	1.191702	2.711	979	1.365498	4.964
830	.979108	1.795	880	1.075862	2.110	930	1.194413	2.730	980	1.370462	5.089
831	.980903	1.800	881	1.077972	2.117	931	1.197143	2.749	981	1.375551	5.223
832	.982703	1.805	882	1.080089	2.127	932	1.199892	2.769	982	1.380774	5.370
833	.984508	1.810	883	1.082216	2.135	933	1.202661	2.789	983	1.386144	5.529
834	.986318	1.815	884	1.084351	2.143	934	1.205450	2.809	984	1.391673	5.702
835	.988133	1.820	885	1.086494	2.152	935	1.208259	2.831	985	1.397375	5.894
836	.989953	1.825	886	1.088646	2.161	936	1.211090	2.852	986	1.403269	6.108
837	.991778	1.830	887	1.090807	2.170	937	1.213942	2.874	987	1.409377	6.345
838	.993608	1.835	888	1.092977	2.180	938	1.216816	2.896	988	1.415722	6.614
839	.995443	1.840	889	1.095157	2.188	939	1.219712	2.919	989	1.422336	6.921
840	.997283	1.846	890	1.097345	2.198	940	1.222631	2.943	990	1.429257	7.275
841	.999129	1.851	891	1.099543	2.207	941	1.225574	2.967	991	1.436532	7.689
842	1.000980	1.856	892	1.101750	2.218	942	1.228541	2.992	992	1.444221	8.186
843	1.002862	1.862	893	1.103968	2.226	943	1.231533	3.018	993	1.452407	8.791
844	1.004698	1.867	894	1.106194	2.238	944	1.234551	3.044	994	1.461198	9.557
845	1.006565	1.873	895	1.108432	2.246	945	1.237595	3.071	995	1.470755	10.569
846	1.008438	1.878	896	1.110678	2.257	946	1.240666	3.099	996	1.481324	11.993
847	1.010316	1.884	897	1.112935	2.268	947	1.243765	3.127	997	1.493317	14.225
848	1.012200	1.890	898	1.115203	2.278	948	1.246892	3.157	998	1.507542	18.529
849	1.014090	1.895	899	1.117481	2.289	949	1.250049	3.187	999	1.526071	44.725
850	1.015985	1.902	900	1.119770	2.299	950	1.253236	3.218	1000	1.570796	

Table 1 - Sine - Angle Conversion Table (Sheet 5 of 5)

Angle	Sine	Interp. Constant	Angle	Sine	Interp. Constant	Angle	Sine	Interp. Constant	Angle	Sine	Interp. Constant
001	.001000	1.000	051	.050978	.999	101	.100828	.995	151	.150427	.988
002	.002000	1.000	052	.051977	.998	102	.101823	.995	152	.151415	.989
003	.003000	1.000	053	.052975	.999	103	.102818	.995	153	.152404	.988
004	.004000	1.000	054	.053974	.998	104	.103813	.994	154	.153392	.988
005	.005000	1.000	055	.054972	.999	105	.104807	.995	155	.154380	.988
006	.006000	1.000	056	.055971	.998	106	.105802	.994	156	.155368	.988
007	.007000	1.000	057	.056969	.998	107	.106796	.994	157	.156356	.987
008	.008000	1.000	058	.057967	.999	108	.107790	.994	158	.157343	.988
009	.009000	1.000	059	.058966	.998	109	.108784	.994	159	.158331	.987
010	.010000	1.000	060	.059964	.998	110	.109778	.994	160	.159318	.987
011	.011000	1.000	061	.060962	.998	111	.110772	.994	161	.160305	.987
012	.012000	1.000	062	.061960	.998	112	.111766	.994	162	.161292	.987
013	.013000	1.000	063	.062958	.998	113	.112760	.993	163	.162279	.987
014	.014000	.999	064	.063956	.998	114	.113753	.994	164	.163266	.986
015	.014999	1.000	065	.064954	.998	115	.114747	.993	165	.164252	.987
016	.015999	1.000	066	.065952	.998	116	.115740	.993	166	.165239	.986
017	.016999	1.000	067	.066950	.998	117	.116733	.993	167	.166225	.986
018	.017999	1.000	068	.067948	.997	118	.117726	.993	168	.167211	.986
019	.018999	1.000	069	.068945	.998	119	.118719	.993	169	.168197	.985
020	.019999	.999	070	.069943	.997	120	.119712	.993	170	.169182	.985
021	.020998	1.000	071	.070940	.998	121	.120705	.993	171	.170167	.986
022	.021998	1.000	072	.071938	.997	122	.121698	.992	172	.171153	.985
023	.022998	1.000	073	.072935	.997	123	.122690	.992	173	.172138	.985
024	.023998	.999	074	.073932	.998	124	.123682	.993	174	.173123	.985
025	.024997	1.000	075	.074930	.997	125	.124675	.992	175	.174108	.985
026	.025997	1.000	076	.075927	.997	126	.125667	.992	176	.175093	.984
027	.026997	.999	077	.076924	.997	127	.126659	.992	177	.176077	.985
028	.027996	1.000	078	.077921	.997	128	.127651	.992	178	.177062	.984
029	.028996	1.000	079	.078918	.997	129	.128643	.991	179	.178046	.984
030	.029996	.999	080	.079915	.996	130	.129634	.992	180	.179030	.983
031	.030995	1.000	081	.080911	.997	131	.130626	.991	181	.180013	.984
032	.031995	.999	082	.081908	.997	132	.131617	.991	182	.180997	.983
033	.032994	.999	083	.082905	.996	133	.132608	.991	183	.181980	.984
034	.033993	1.000	084	.083901	.997	134	.133599	.991	184	.182964	.982
035	.034993	.999	085	.084898	.996	135	.134590	.991	185	.183946	.983
036	.035992	1.000	086	.085894	.996	136	.135581	.991	186	.184929	.983
037	.036992	.999	087	.086890	.996	137	.136572	.990	187	.185912	.983
038	.037991	.999	088	.087886	.997	138	.137562	.991	188	.186895	.982
039	.038990	.999	089	.088883	.996	139	.138553	.990	189	.187877	.982
040	.039989	1.000	090	.089879	.995	140	.139543	.990	190	.188859	.982
041	.040989	.999	091	.090874	.996	141	.140533	.990	191	.189841	.982
042	.041988	.999	092	.091870	.996	142	.141523	.990	192	.190823	.981
043	.042987	.999	093	.092866	.996	143	.142513	.990	193	.191804	.981
044	.043986	.999	094	.093862	.995	144	.143503	.989	194	.192785	.982
045	.044985	.999	095	.094857	.996	145	.144492	.990	195	.193767	.980
046	.045984	.999	096	.095853	.995	146	.145482	.989	196	.194747	.981
047	.046983	.999	097	.096848	.995	147	.146471	.989	197	.195728	.981
048	.047982	.998	098	.097843	.995	148	.147460	.989	198	.196709	.980
049	.048980	.999	099	.098838	.995	149	.148449	.989	199	.197689	.980
050	.049979	.999	100	.099833	.995	150	.149438	.989	200	.198669	.980

Table 2 - Angle - Sine Conversion Table (Sheet 1 of 5)

Angle	Sine	Interp. Constant	Angle	Sine	Interp. Constant	Angle	Sine	Interp. Constant	Angle	Sine	Interp. Constant
201	.199649	.980	251	.248373	.968	301	.296475	.955	351	.343837	.939
202	.200629	.979	252	.249341	.969	302	.297430	.955	352	.344776	.938
203	.201608	.980	253	.250310	.968	303	.298385	.954	353	.345714	.939
204	.202588	.979	254	.251278	.967	304	.299339	.954	354	.346653	.937
205	.203567	.978	255	.252245	.968	305	.300293	.954	355	.347590	.938
206	.204546	.979	256	.253213	.967	306	.301247	.953	356	.348528	.937
207	.205525	.978	257	.254180	.967	307	.302200	.953	357	.349465	.937
208	.206503	.979	258	.255147	.967	308	.303153	.953	358	.350402	.936
209	.207482	.978	259	.256114	.967	309	.304106	.953	359	.351338	.936
210	.208460	.978	260	.257081	.966	310	.305059	.952	360	.352274	.936
211	.209438	.978	261	.258047	.966	311	.306011	.952	361	.353210	.935
212	.210416	.977	262	.259013	.966	312	.306963	.951	362	.354145	.935
213	.211393	.977	263	.259979	.965	313	.307914	.952	363	.355080	.935
214	.212370	.977	264	.260944	.965	314	.308866	.950	364	.356015	.934
215	.213347	.977	265	.261909	.965	315	.309816	.951	365	.356949	.934
216	.214324	.977	266	.262874	.965	316	.310767	.950	366	.357883	.934
217	.215301	.976	267	.263839	.964	317	.311717	.950	367	.358817	.933
218	.216277	.977	268	.264803	.965	318	.312667	.950	368	.359750	.933
219	.217254	.976	269	.265768	.963	319	.313617	.950	369	.360683	.932
220	.218230	.975	270	.266731	.964	320	.314567	.949	370	.361615	.933
221	.219205	.976	271	.267695	.963	321	.315516	.948	371	.362548	.931
222	.220181	.975	272	.268658	.964	322	.316464	.949	372	.363479	.932
223	.221156	.975	273	.269622	.962	323	.317413	.948	373	.364411	.931
224	.222131	.975	274	.270584	.963	324	.318361	.948	374	.365342	.931
225	.223106	.975	275	.271547	.962	325	.319309	.947	375	.366273	.930
226	.224081	.975	276	.272509	.962	326	.320256	.947	376	.367203	.930
227	.225056	.974	277	.273471	.962	327	.321203	.947	377	.368133	.929
228	.226030	.974	278	.274433	.961	328	.322150	.947	378	.369062	.930
229	.227004	.974	279	.275394	.962	329	.323097	.946	379	.369992	.928
230	.227978	.973	280	.276356	.961	330	.324043	.946	380	.370920	.929
231	.228951	.973	281	.277317	.960	331	.324989	.945	381	.371849	.928
232	.229924	.973	282	.278277	.961	332	.325934	.946	382	.372777	.928
233	.230897	.973	283	.279238	.960	333	.326880	.945	383	.373705	.927
234	.231870	.973	284	.280198	.959	334	.327825	.944	384	.374632	.927
235	.232843	.972	285	.281157	.960	335	.328769	.944	385	.375559	.927
236	.233815	.973	286	.282117	.959	336	.329713	.944	386	.376486	.926
237	.234788	.971	287	.283076	.959	337	.330657	.944	387	.377412	.926
238	.235759	.972	288	.284035	.959	338	.331601	.943	388	.378338	.925
239	.236731	.972	289	.284994	.958	339	.332544	.943	389	.379263	.925
240	.237703	.971	290	.285952	.958	340	.333487	.943	390	.380188	.925
241	.238674	.971	291	.286910	.958	341	.334430	.942	391	.381113	.924
242	.239645	.971	292	.287868	.958	342	.335372	.942	392	.382037	.924
243	.240616	.970	293	.288826	.957	343	.336314	.941	393	.382961	.924
244	.241586	.970	294	.289783	.957	344	.337255	.942	394	.383885	.923
245	.242556	.970	295	.290740	.957	345	.338197	.941	395	.384808	.923
246	.243526	.970	296	.291697	.956	346	.339138	.940	396	.385731	.922
247	.244496	.970	297	.292653	.956	347	.340078	.940	397	.386653	.922
248	.245466	.969	298	.293609	.956	348	.341018	.940	398	.387575	.922
249	.246435	.969	299	.294565	.955	349	.341958	.940	399	.388497	.921
250	.247404	.969	300	.295520	.955	350	.342898	.939	400	.389418	.921

Table 2 - Angle - Sine Conversion Table (Sheet 2 of 5)

Angle	Sine	Interp. Constant	Angle	Sine	Interp. Constant	Angle	Sine	Interp. Constant	Angle	Sine	Interp. Constant
401	.390339	.921	451	.435866	.900	501	.480303	.877	551	.523539	.852
402	.391260	.920	452	.436766	.899	502	.481180	.876	552	.524391	.851
403	.392180	.919	453	.437665	.899	503	.482056	.876	553	.525342	.851
404	.393099	.920	454	.438564	.898	504	.482932	.875	554	.526093	.850
405	.394019	.919	455	.439462	.898	505	.483807	.875	555	.526943	.850
406	.394938	.918	456	.440360	.898	506	.484682	.875	556	.527793	.849
407	.395856	.918	457	.441258	.897	507	.485557	.874	557	.528642	.849
408	.396774	.918	458	.442155	.897	508	.486431	.873	558	.529491	.848
409	.397692	.917	459	.443052	.896	509	.487304	.873	559	.530339	.847
410	.398609	.917	460	.443948	.896	510	.488177	.873	560	.531186	.847
411	.399526	.917	461	.444844	.895	511	.489050	.872	561	.532033	.847
412	.400443	.916	462	.445739	.895	512	.489922	.871	562	.532880	.846
413	.401359	.916	463	.446634	.895	513	.490793	.871	563	.533726	.845
414	.402275	.915	464	.447529	.894	514	.491664	.871	564	.534571	.845
415	.403190	.915	465	.448423	.893	515	.492535	.870	565	.535416	.844
416	.404105	.914	466	.449316	.894	516	.493405	.869	566	.536260	.844
417	.405019	.914	467	.450210	.892	517	.494274	.870	567	.537104	.843
418	.405933	.914	468	.451102	.892	518	.495144	.868	568	.537947	.843
419	.406847	.913	469	.451994	.892	519	.496012	.868	569	.538790	.842
420	.407760	.913	470	.452886	.892	520	.496880	.868	570	.539632	.842
421	.408673	.913	471	.453778	.891	521	.497748	.867	571	.540474	.841
422	.409586	.912	472	.454669	.890	522	.498615	.866	572	.541315	.840
423	.410498	.912	473	.455559	.890	523	.499481	.866	573	.542155	.840
424	.411410	.911	474	.456449	.889	524	.500347	.866	574	.542995	.840
425	.412321	.911	475	.457338	.890	525	.501213	.865	575	.543835	.839
426	.413232	.910	476	.458228	.888	526	.502078	.865	576	.544674	.838
427	.414142	.910	477	.459116	.888	527	.502943	.864	577	.545512	.838
428	.415052	.910	478	.460004	.888	528	.503807	.863	578	.546350	.837
429	.415962	.909	479	.460892	.887	529	.504670	.863	579	.547187	.837
430	.416871	.909	480	.461779	.887	530	.505533	.863	580	.548024	.836
431	.417780	.908	481	.462666	.886	531	.506396	.862	581	.548860	.836
432	.418688	.908	482	.463552	.886	532	.507258	.861	582	.549696	.835
433	.419596	.907	483	.464438	.885	533	.508119	.862	583	.550531	.834
434	.420503	.907	484	.465323	.885	534	.508981	.860	584	.551365	.834
435	.421410	.907	485	.466208	.885	535	.509841	.860	585	.552199	.834
436	.422317	.906	486	.467093	.884	536	.510701	.860	586	.553033	.833
437	.423223	.906	487	.467977	.883	537	.511561	.859	587	.553866	.832
438	.424129	.906	488	.468860	.883	538	.512420	.858	588	.554698	.832
439	.425035	.904	489	.469743	.883	539	.513278	.858	589	.555530	.831
440	.425939	.905	490	.470626	.882	540	.514136	.857	590	.556361	.831
441	.426844	.904	491	.471508	.882	541	.514993	.857	591	.557192	.830
442	.427748	.904	492	.472390	.881	542	.515850	.857	592	.558022	.829
443	.428652	.903	493	.473271	.880	543	.516707	.856	593	.558851	.829
444	.429555	.903	494	.474151	.881	544	.517563	.855	594	.559680	.829
445	.430458	.902	495	.475032	.879	545	.518418	.855	595	.560509	.828
446	.431360	.902	496	.475911	.880	546	.519273	.854	596	.561337	.827
447	.432262	.902	497	.476791	.878	547	.520127	.854	597	.562164	.827
448	.433164	.901	498	.477669	.879	548	.520981	.853	598	.562991	.826
449	.434065	.901	499	.478548	.878	549	.521834	.853	599	.563817	.825
450	.434966	.900	500	.479426	.877	550	.522687	.852	600	.564642	.826

Table 2 - Angle - Sine Conversion Table (Sheet 3 of 5)

Angle	Sine	Interp. Constant	Angle	Sine	Interp. Constant	Angle	Sine	Interp. Constant	Angle	Sine	Interp. Constant
601	.565468	.824	651	.605982	.795	701	.644982	.764	751	.682370	.731
602	.566292	.824	652	.606777	.795	702	.645746	.763	752	.683101	.730
603	.567116	.823	653	.607572	.794	703	.646509	.763	753	.683831	.729
604	.567939	.823	654	.608366	.793	704	.647272	.762	754	.684560	.729
605	.568762	.822	655	.609159	.793	705	.648034	.761	755	.685289	.728
606	.569584	.822	656	.609952	.792	706	.648795	.761	756	.686017	.727
607	.570406	.821	657	.610744	.792	707	.649556	.760	757	.686744	.726
608	.571227	.821	658	.611536	.791	708	.650316	.759	758	.687470	.726
609	.572048	.819	659	.612327	.790	709	.651075	.759	759	.688196	.725
610	.572867	.820	660	.613117	.790	710	.651834	.758	760	.688921	.725
611	.573687	.819	661	.613907	.789	711	.652592	.757	761	.689646	.724
612	.574506	.818	662	.614696	.788	712	.653349	.757	762	.690370	.723
613	.575324	.817	663	.615484	.788	713	.654106	.756	763	.691093	.722
614	.576141	.818	664	.616272	.787	714	.654862	.755	764	.691815	.722
615	.576959	.816	665	.617059	.787	715	.655617	.755	765	.692537	.721
616	.577775	.816	666	.617846	.786	716	.656372	.754	766	.693258	.720
617	.578591	.815	667	.618632	.785	717	.657126	.754	767	.693978	.720
618	.579406	.815	668	.619417	.785	718	.657880	.753	768	.694698	.719
619	.580221	.814	669	.620202	.784	719	.658633	.752	769	.695417	.718
620	.581035	.814	670	.620986	.784	720	.659385	.751	770	.696135	.718
621	.581849	.813	671	.621770	.782	721	.660136	.751	771	.696853	.717
622	.582662	.812	672	.622552	.783	722	.660887	.750	772	.697570	.716
623	.583474	.812	673	.623335	.781	723	.661637	.750	773	.698286	.715
624	.584286	.811	674	.624116	.781	724	.662387	.748	774	.699001	.715
625	.585097	.811	675	.624897	.781	725	.663135	.749	775	.699716	.714
626	.585908	.810	676	.625678	.779	726	.663884	.747	776	.700430	.714
627	.586718	.810	677	.626457	.780	727	.664631	.747	777	.701144	.712
628	.587528	.808	678	.627237	.778	728	.665378	.746	778	.701856	.712
629	.588336	.809	679	.628015	.778	729	.666124	.746	779	.702568	.711
630	.589145	.807	680	.628793	.777	730	.666870	.744	780	.703279	.711
631	.589952	.808	681	.629570	.777	731	.667614	.745	781	.703990	.710
632	.590760	.806	582	.630347	.776	732	.668359	.743	782	.704700	.709
633	.591566	.806	383	.631123	.775	733	.669102	.743	783	.705409	.708
634	.592372	.806	684	.631898	.775	734	.669845	.742	784	.706117	.708
635	.593178	.804	685	.632673	.774	735	.670587	.742	785	.706825	.707
636	.593982	.804	686	.633447	.774	736	.671329	.740	786	.707532	.707
637	.594786	.804	687	.634221	.773	737	.672069	.741	787	.708239	.705
638	.595590	.803	688	.634994	.772	738	.672810	.739	788	.708944	.705
639	.596393	.802	689	.635766	.771	739	.673549	.739	789	.709649	.704
640	.597195	.802	690	.636537	.771	740	.674288	.738	790	.710353	.704
641	.597997	.801	691	.637308	.770	741	.675026	.738	791	.711057	.703
642	.598798	.801	692	.638078	.770	742	.675764	.736	792	.711760	.702
643	.599599	.800	693	.638848	.769	743	.676500	.736	793	.712462	.701
644	.600399	.799	694	.639617	.768	744	.677236	.736	794	.713163	.701
645	.601198	.799	695	.640385	.768	745	.677972	.735	795	.713864	.700
646	.601997	.798	696	.641153	.767	746	.678707	.733	796	.714564	.699
647	.602795	.798	697	.641920	.767	747	.679440	.734	797	.715263	.698
648	.603593	.797	698	.642687	.766	748	.680174	.733	798	.715961	.698
649	.604390	.796	699	.643453	.765	749	.680907	.732	799	.716659	.697
650	.605186	.796	700	.644218	.764	750	.681639	.731	800	.717356	.696

Table 2 - Angle - Sine Conversion Table (Sheet 4 of 5)

Angle	Sine	Interp. Constant	Angle	Sine	Interp. Constant	Angle	Sine	Interp. Constant	Angle	Sine	Interp. Constant
801	.718052	.696	851	.751940	.659	901	.783948	.621	951	.813997	.580
802	.718748	.695	852	.752599	.658	902	.784569	.619	952	.814577	.580
803	.719443	.694	853	.753257	.657	903	.785188	.619	953	.815157	.579
804	.720137	.694	854	.753914	.657	904	.785807	.618	954	.815736	.578
805	.720831	.692	855	.754571	.656	905	.786425	.617	955	.816314	.577
806	.721523	.692	856	.755227	.655	906	.787042	.617	956	.816891	.576
807	.722215	.692	857	.755882	.654	907	.787659	.616	957	.817467	.576
808	.722907	.690	858	.756536	.654	908	.788275	.615	958	.818043	.575
809	.723597	.690	859	.757190	.653	909	.788890	.614	959	.818618	.574
810	.724287	.689	860	.757843	.652	910	.789504	.613	960	.819192	.573
811	.724976	.689	861	.758495	.651	911	.790117	.613	961	.819765	.572
812	.725665	.687	862	.759146	.650	912	.790730	.611	962	.820337	.571
813	.726352	.687	863	.759796	.650	913	.791341	.611	963	.820908	.571
814	.727039	.687	864	.760446	.649	914	.791952	.611	964	.821479	.570
815	.727726	.685	865	.761095	.649	915	.792563	.609	965	.822049	.569
816	.728411	.685	866	.761744	.647	916	.793172	.609	966	.822618	.568
817	.729096	.684	867	.762391	.647	917	.793781	.607	967	.823186	.567
818	.729780	.683	868	.763038	.646	918	.794388	.607	968	.823753	.567
819	.730463	.683	869	.763684	.645	919	.794995	.607	969	.824320	.566
820	.731146	.682	870	.764329	.644	920	.795602	.605	970	.824886	.565
821	.731828	.681	871	.764973	.644	921	.796207	.605	971	.825451	.564
822	.732509	.680	872	.765617	.643	922	.796812	.604	972	.826015	.563
823	.733189	.680	873	.766260	.642	923	.797416	.603	973	.826578	.562
824	.733869	.679	874	.766902	.642	924	.798019	.602	974	.827140	.562
825	.734548	.678	875	.767544	.640	925	.798621	.601	975	.827702	.561
826	.735226	.677	876	.768184	.640	926	.799222	.601	976	.828263	.560
827	.735903	.677	877	.768824	.639	927	.799823	.600	977	.828823	.559
828	.736580	.676	878	.769463	.638	928	.800423	.599	978	.829382	.558
829	.737256	.675	879	.770101	.638	929	.801022	.598	979	.829940	.557
830	.737931	.675	880	.770739	.637	930	.801620	.597	980	.830497	.557
831	.738606	.674	881	.771376	.636	931	.802217	.597	981	.831054	.556
832	.739280	.673	882	.772012	.635	932	.802814	.596	982	.831610	.555
833	.739953	.672	883	.772647	.634	933	.803410	.595	983	.832165	.554
834	.740625	.672	884	.773281	.634	934	.804005	.594	984	.832719	.553
835	.741297	.670	885	.773915	.633	935	.804599	.593	985	.833272	.553
836	.741967	.670	886	.774548	.632	936	.805192	.593	986	.833825	.551
837	.742637	.670	887	.775180	.631	937	.805785	.592	987	.834376	.551
838	.743307	.668	888	.775811	.631	938	.806377	.591	988	.834927	.550
839	.743975	.668	889	.776442	.630	939	.806968	.590	989	.835477	.549
840	.744643	.667	890	.777072	.629	940	.807558	.589	990	.836026	.548
841	.745310	.667	891	.777701	.628	941	.808147	.589	991	.836574	.548
842	.745977	.665	892	.778329	.627	942	.808736	.588	992	.837122	.546
843	.746642	.665	893	.778956	.627	943	.809324	.587	993	.837668	.546
844	.747307	.664	894	.779583	.626	944	.809911	.586	994	.838214	.545
845	.747971	.663	895	.780209	.625	945	.810497	.585	995	.838759	.544
846	.748634	.663	896	.780834	.625	946	.811082	.585	996	.839303	.543
847	.749297	.662	897	.781459	.623	947	.811667	.584	997	.839846	.543
848	.749959	.661	898	.782082	.623	948	.812251	.582	998	.840389	.541
849	.750620	.660	899	.782705	.622	949	.812833	.583	999	.840930	.541
850	.751280	.660	900	.783327	.621	950	.813416	.581	1.000	.841471	.540

Table 2 - Angle - Sine Conversion Table (Sheet 5 of 5)

INDEX

☆ U.S. GOVERNMENT PRINTING OFFICE: 1963 O - 709-648